AGU PUBLICATIONS

Reviews of Geophysics

REVIEW ARTICLE
10.1002/2015RG000493

Key Points:
- Intra-annual AMOC variability is large and forced by the wind
- Decadal AMOC variability is associated with density variations on the ocean boundaries
- The subtropical-subpolar transition zone is a pacemaker for decadal AMOC variability

Correspondence to:
M. W. Buckley,
marthabuckley@gmail.com

Citation:
Buckley, M. W. and J. Marshall (2016), Observations, inferences, and mechanisms of Atlantic Meridional Overturning Circulation variability: A review, *Rev. Geophys.*, *54*, 5–63, doi:10.1002/2015RG000493.

Received 10 JUN 2015
Accepted 17 DEC 2015
Accepted article online 22 DEC 2015
Published online 26 JAN 2016
Corrected 23 FEB 2016

This article was corrected on 23 FEB 2016. See the end of the full text for details.

Observations, inferences, and mechanisms of the Atlantic Meridional Overturning Circulation: A review

Martha W. Buckley[1,2] and John Marshall[3]

[1]Department of Atmospheric, Oceanic, and Earth Sciences, George Mason University, Fairfax, Virginia, USA, [2]Oceanography Research Group, Atmospheric and Environmental Research, Lexington, Massachusetts, USA, [3]Department of Earth, Atmospheric and Planetary Sciences, Massachusetts Institute of Technology, Cambridge, Massachusetts, USA

Abstract This is a review about the Atlantic Meridional Overturning Circulation (AMOC), its mean structure, temporal variability, controlling mechanisms, and role in the coupled climate system. The AMOC plays a central role in climate through its heat and freshwater transports. Northward ocean heat transport achieved by the AMOC is responsible for the relative warmth of the Northern Hemisphere compared to the Southern Hemisphere and is thought to play a role in setting the mean position of the Intertropical Convergence Zone north of the equator. The AMOC is a key means by which heat anomalies are sequestered into the ocean's interior and thus modulates the trajectory of climate change. Fluctuations in the AMOC have been linked to low-frequency variability of Atlantic sea surface temperatures with a host of implications for climate variability over surrounding landmasses. On intra-annual timescales, variability in AMOC is large and primarily reflects the response to local wind forcing; meridional coherence of anomalies is limited to that of the wind field. On interannual to decadal timescales, AMOC changes are primarily geostrophic and related to buoyancy anomalies on the western boundary. A pacemaker region for decadal AMOC changes is located in a western "transition zone" along the boundary between the subtropical and subpolar gyres. Decadal AMOC anomalies are communicated meridionally from this region. AMOC observations, as well as the expanded ocean observational network provided by the Argo array and satellite altimetry, are inspiring efforts to develop decadal predictability systems using coupled atmosphere-ocean models initialized by ocean data.

1. Introduction

The troposphere is heated from below, principally in the tropics. Air rises in a near-equatorial quasi-contiguous band of intense convection with compensating downwelling occurring in subtropical latitudes. The resulting Hadley overturning circulation is a central part of the general circulation of the atmosphere [see, e.g., *Marshall and Plumb*, 2008]. In the ocean, by contrast, convection is driven by buoyancy loss at its upper surface, primarily at polar latitudes. Meridional overturning cells emanate from both poles. The cell emanating from the northern North Atlantic forms the "upper cell" of the ocean's Meridional Overturning Circulation (MOC). The upper cell of the AMOC (Atlantic MOC) ventilates the upper 2 km or so of the ocean. A deeper overturning cell, the "lower cell," originates from around Antarctica and supplies fluid to the abyssal ocean.

This is a review about the upper cell of the AMOC, its mean structure, temporal variability, controlling mechanisms, and role in the coupled climate system. Despite the sinking branch of the AMOC being confined to a tiny part of the globe, it plays an outsized role in climate, past, present, and (likely) future. As can be seen from the pattern of surface and middepth currents in the North Atlantic (Figure 1), warm near-surface waters move poleward to far northerly latitudes where they undergo buoyancy loss, sink, and return southward at depth. If one zonally averages this complex, three-dimensional circulation across the basin, one obtains a much simpler description, that of the meridional overturning cell shown in Figure 2a. The AMOC connects the two hemispheres and is a principal cause of interhemispheric asymmetries in climate. The AMOC carries order 0.5 PW of heat across the equator (Figure 3a) and, as we review here, is responsible for the Northern Hemisphere (NH) being slightly warmer than the Southern Hemisphere (SH) (Figure 3c) and for the mean position

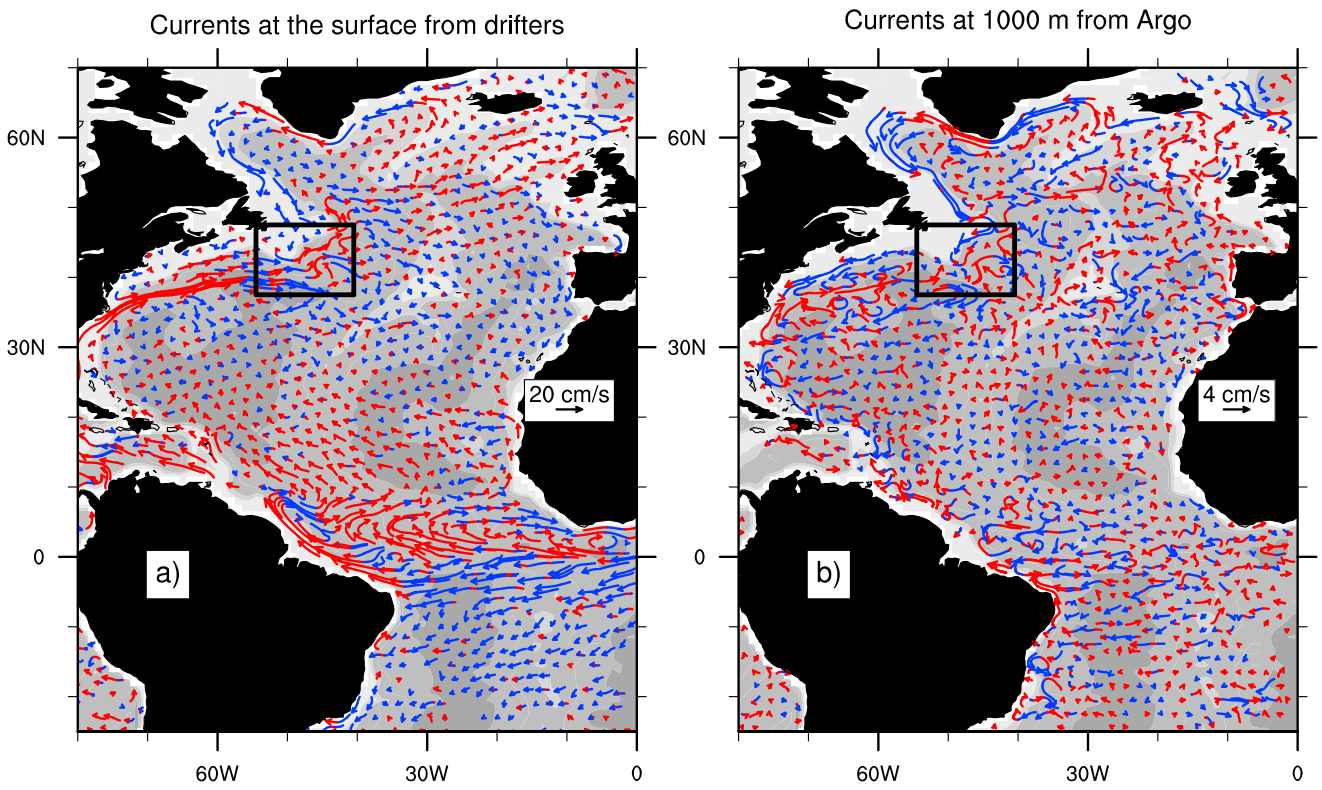

Figure 1. Mean currents at (a) the surface from the Global Drifter Program [*Lumpkin et al.*, 2013; *Lumpkin and Johnson*, 2013] and (b) a depth of 1000 m from the ANDRO data set [*Ollitrault and Rannou*, 2013; *Ollitrault and Colin de Verdiére*, 2014] derived from Argo float displacements. Vectors with northward velocities are shown in red, and vectors with southward velocities are shown in blue. Note the scale for the vectors located over Africa. Bathymetry is shaded in grey, with lighter (darker) colors indicating shallower (deeper) regions. The white contours are at levels of 1–4 km. The black box indicates the transition zone (TZ). Figure courtesy of Nicolas Barrier (OT-MED Labex).

of the zonal average Intertropical Convergence Zone (ITCZ) being just north of the equator [e.g., *Frierson et al.*, 2013; *Marshall et al.*, 2014a].

Upwelling of dense waters, which provide a return path to the surface, is essential in order to sustain the AMOC [*Wunsch*, 2002; *Wunsch and Ferrari*, 2004; *Kuhlbrodt et al.*, 2007; *Visbeck*, 2007]. Recent work suggests that upwelling of dense waters formed in the North Atlantic occurs primarily along isopycnals that outcrop in the Southern Ocean, drawn up to the surface by the strong winds blowing around Antarctica (see *Toggweiler and Samuels* [1995] and *Marshall and Speer* [2012] for a review). Thus, on long (centennial) timescales, the AMOC and the global ocean circulation are connected through the Southern Ocean.

Changes in the AMOC are frequently invoked as a player in paleoclimate shifts [*Broecker*, 1997, 2003]. A shutdown in the AMOC is hypothesized to lead to a colder Arctic, more extensive Arctic ice, an equatorward shift of the ITCZ, and weakened Indian and Asian summer monsoons; conversely, a stronger AMOC is associated with a warmer Arctic, less ice, and a northward shift of the ITCZ [*Vellinga and Wood*, 2002; *Chiang and Bitz*, 2005; *Cheng et al.*, 2007; *Zhang and Delworth*, 2005; *Stouffer et al.*, 2006; *Kang et al.*, 2008]. The AMOC is also invoked as a key player in the "bipolar seesaw," antiphase changes in Arctic and Antarctic climates thought to be caused by AMOC-related ocean heat transport variations [*Broecker*, 1998; *Stocker*, 1998; *Rahmstorf*, 2002; *Skinner et al.*, 2007; *Pedro et al.*, 2011].

On much shorter (decadal and centennial) timescales, variations in AMOC may be associated with changes in Atlantic sea surface temperatures (SSTs), such as the Atlantic Multidecadal Oscillation/Atlantic Multidecadal Variability (AMO/AMV) [see, e.g., *Schlesinger and Ramankutty*, 1994; *Knight et al.*, 2005; *Delworth et al.*, 2007; *Deser et al.*, 2010]. Decadal prediction systems are predicated on the hypothesis that at low frequencies SST anomalies are associated with slow ocean processes, such as the AMOC, which may have predictability. Indeed, this is one of the main reasons that AMOC observing systems, such as the Rapid Climate Change (RAPID) array [*Cunningham et al.*, 2007; *Kanzow et al.*, 2010; *Johns et al.*, 2011], have been set up in the Atlantic

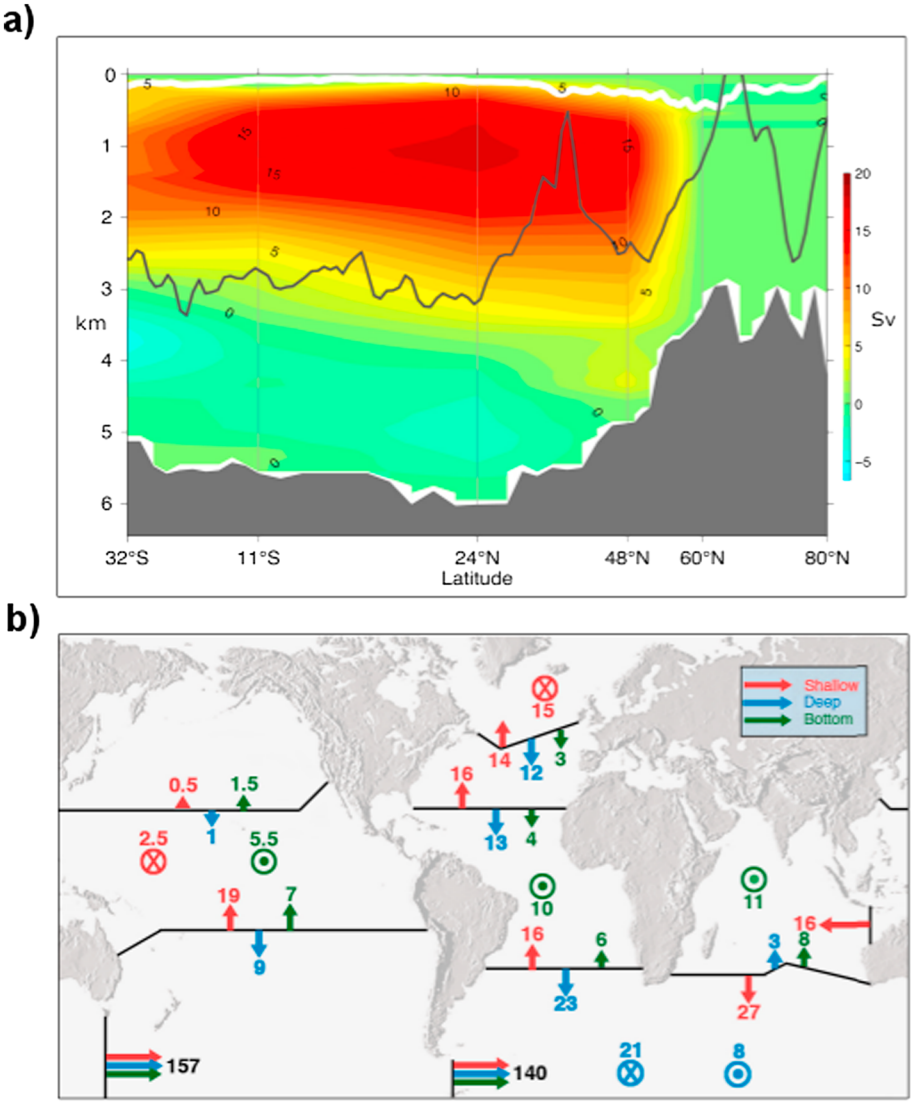

Figure 2. (a) Mean Atlantic Meridional Overturning stream function (AMOC) in depth coordinates estimated from tracer inversion by *Lumpkin and Speer* [2007]. Grey shading indicates the ocean bottom (maximum depth in the Atlantic at each latitude), and the black line indicates the crest of the Mid-Atlantic Ridge. The thick white line near the surface represents the deepest (climatological) mixed layer depth. (b) Estimate of global ocean circulation patterns based on the box model inversion of *Ganachaud and Wunsch* [2000]. The circulation is separated into three layers: shallow (red, <2 km), deep (blue, 2–4 km), and bottom (green, >4 km). Colored arrows across the sections (solid black lines) indicate the volume transport in Sverdrups. Circles represent the vertical transport out of the layer (open circle with dot for upwelling and open circle with cross for downwelling) [from *Marshall and Plumb*, 2008] (modified from *Alley et al.* [2002]).

and are now being expanded. The AMOC plays a central role in the response of the climate to anthropogenic forcing, as it is a primary means for transporting heat and carbon from the surface to the deep ocean [*Drijfhout et al.*, 2012; *Meehl et al.*, 2013; *Winton et al.*, 2013; *Marshall et al.*, 2014a, 2014b; *Kostov et al.*, 2014].

This review aims to synthesize what is known about AMOC and its variability on intra-annual to decadal timescales, focusing on processes local to the Atlantic. On longer timescales (centennial and beyond) the AMOC interacts with the global ocean, including, for example, interhemispheric connections between the Atlantic and the Southern Ocean. Although of great relevance to paleoclimate, we do not attempt to review these aspects here. Recent reviews focused on other aspects of the AMOC include (1) theoretical discussions of the mean strength of the AMOC and its driving processes [*Gnanadesikan et al.*, 2007; *Kuhlbrodt et al.*, 2007; *Marshall and Speer*, 2012]; (2) a review of historical estimates of the AMOC [*Longworth and Bryden*, 2007];

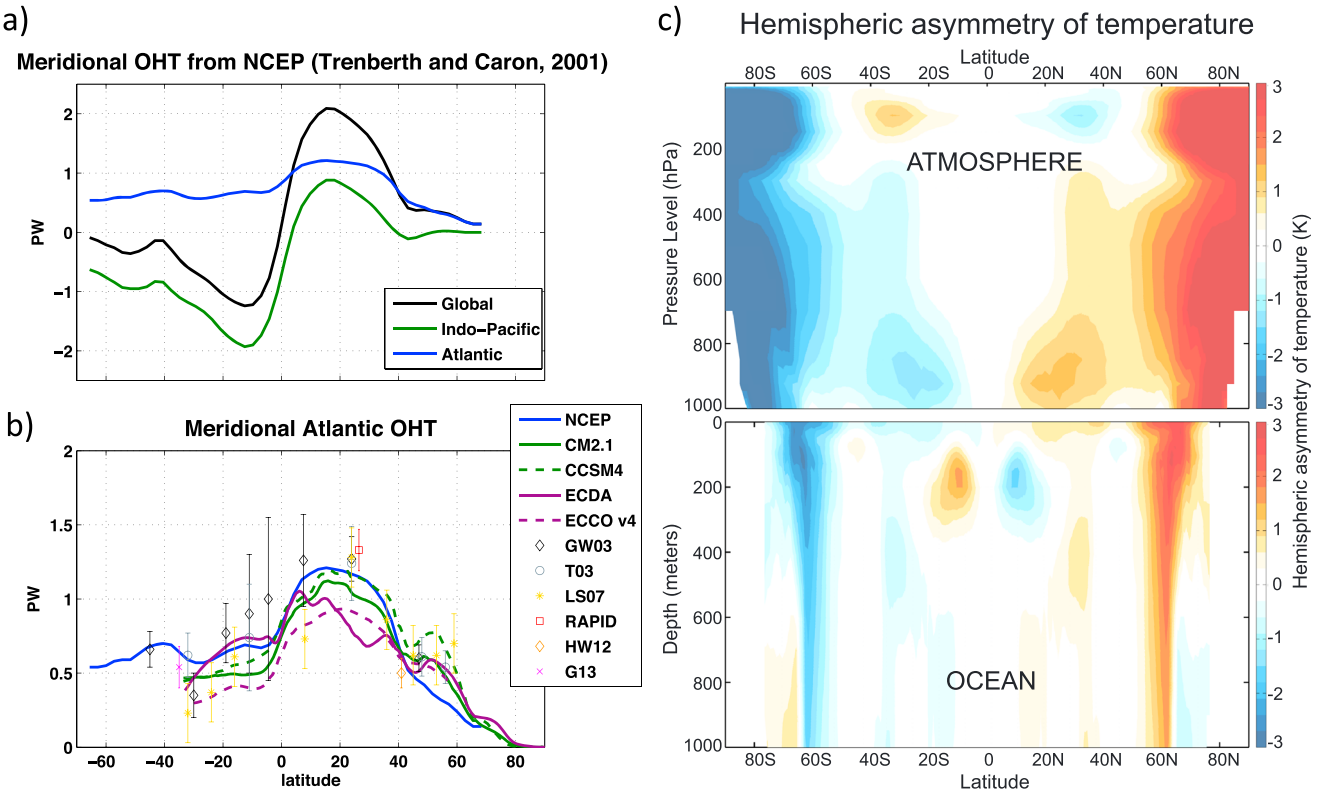

Figure 3. (a) Meridional ocean heat transports (OHT, positive northward) in PW (10^{15} W) for the global ocean (black), the Indo-Pacific (green), and the Atlantic (blue) from NCEP atmospheric reanalysis [*Trenberth and Caron*, 2001]. (b) Atlantic OHT from NCEP atmospheric reanalysis (blue) [*Trenberth and Caron*, 2001] is compared to several direct estimates: *Ganachaud and Wunsch* [2003] (black diamonds), *Talley* [2003] (grey circles), *Lumpkin and Speer* [2007] (yellow stars), the RAPID-MOCHA array at 26.5°N (red square) [*Johns et al.*, 2011], *Hobbs and Willis* [2012] (orange diamond), and *Garzoli et al.* [2013] (magenta cross). The vertical bars indicate the uncertainty range for the direct estimates. Also compared are the Atlantic OHT in CM2.1 (green solid) and CCSM4 (green dashed) preindustrial control simulations (modified from *Msadek et al.* [2013]) and the GFDL ECDA (1960–2010, solid purple) [*Chang et al.*, 2012] and ECCO v4 (1992–2012, dashed purple) [*Forget and Ponte*, 2015; *Forget et al.*, 2015] ocean state estimates. (c) Observed hemispheric asymmetry of temperature in the atmosphere and ocean (in °C) computed from the NCEP reanalysis and the World Ocean Atlas. The asymmetric component of a temperature field $T(\phi)$ is defined as $T_{as}(\phi) = (T(\phi) - T(-\phi))/2$ where ϕ is the latitude [from *Marshall et al.*, 2014a].

(3) reviews of observations of the AMOC [*Srokosz et al.*, 2012], with particular focus on observations and inferences from a decade of AMOC observations at 26.5°N [*Srokosz and Bryden*, 2015]; (4) a critical discussion of the linkages between deep convection and the AMOC [*Lozier*, 2012]; (5) a review of the surface and deep pathways of the AMOC [*Lozier*, 2010]; (6) a review on the importance of the South Atlantic to the AMOC [*Garzoli and Matano*, 2011]; (7) a brief review of the relationship between the AMOC and sea level, in particular sea level fluctuations on the east coast of the United States [*Srokosz and Bryden*, 2015]; and (8) reviews on connections between the AMOC and climate on paleoclimate timescales [*Broecker*, 2007] and abrupt climate change [*Clark et al.*, 2002; *Alley*, 2007].

Despite the interest and scrutiny of AMOC by the community, progress in understanding decadal climate variability and its connection to the AMOC has been hampered by a paucity of observations, the formidable challenge of representing key processes in models, and our somewhat limited knowledge of underlying mechanisms. Controlling mechanisms are a function of timescale. On short (intra-annual to interannual) timescales, AMOC variability is primarily the response to local wind forcing. On longer (decadal) timescales, AMOC variability involves a complex interplay between wind-driven and thermohaline processes. A coordinating theme running through this review is the critical role played by buoyancy anomalies in the region east of the Grand Banks, where the separated Gulf Stream, the North Atlantic Current, and Labrador Currents interact at the western confluence of the subtropical and subpolar gyres. We shall call this region (marked by a box in Figures 1 and 4) the "transition zone" and use simple dynamical considerations to argue that it is central to our understanding of decadal and multidecadal AMOC variability.

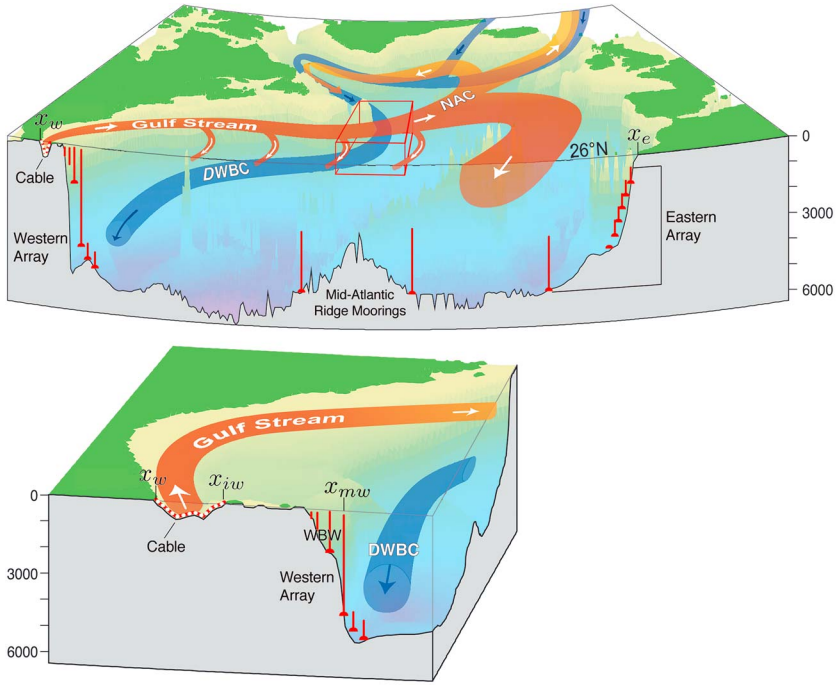

Figure 4. A schematic of the North Atlantic Ocean circulation (modified from *Church* [2007]): (top) the entire basin and (bottom) a close-up of the western boundary region. Surface currents, including the Gulf Stream, the North Atlantic Current (NAC), and Labrador Current, are shown in red, and the deep western boundary current (DWBC) is shown in blue. The TZ is marked by a red box, corresponding to the same region indicated by the black box in Figure 1. The southern face of the schematic is at 26°N. The components of the RAPID array are indicated: the western, eastern, and Mid-Atlantic Ridge arrays; the western boundary wedge (WBW), where currents are directly measured via current meters and upward looking acoustic doppler profilers; and the cable measuring the Florida Current transport. Variables x_w, x_e, x_{iw}, and x_{mw} refer to longitude limits in equation (10).

Our review is set out as follows. In section 2, we discuss the role of the AMOC in climate, including its role in ocean heat transport (section 2.3), decadal climate variability (section 2.4), and modulating the trajectory of anthropogenic climate change (section 2.5). Key definitions of AMOC and its dynamical components are introduced in section 3, and the importance of the AMOC in ocean heat and freshwater transports is discussed. In section 4 we review what is known about the AMOC from direct observations, ocean state estimates, and models. In section 5, we attempt a critical review of mechanisms of decadal AMOC variability, drawing attention to the importance of the transition zone in this variability. The impact of the AMOC on the atmosphere and on intra-annual to decadal climate predictions is discussed in section 6. Conclusions and future outlook are presented in section 7.

2. The AMOC and Its Role in Climate

The AMOC is commonly defined as the zonally and vertically integrated northward volume transport; thus, the AMOC is defined as a function of latitude and depth and has units of $m^3\ s^{-1}$, which is almost universally expressed in terms of Sverdrups ($1\ Sv \equiv 10^6\ m^3\ s^{-1}$). The AMOC strength as a function of latitude is typically defined as the maximum over depth. In this section we discuss the geometry of the AMOC, the reason for the confinement of the AMOC to the Atlantic sector, and the role of the AMOC in the coupled climate system.

2.1. Phenomenology of the AMOC

The simplicity of the zonally integrated circulation in the Atlantic, with northward flow near the surface and southward flow at depth (Figure 2a and idealized schematic Figure 4), masks the more complex circulation patterns evident in Figure 1. In the South Atlantic, northward near-surface flow occurs in the Benguela Current. A portion of these waters flows toward the western boundary in the southern equatorial current and then travels northward across the equator in the North Brazil Current (see *Stramma and England* [1999] and *Garzoli and Matano* [2011] for more details on the circulation of the South Atlantic). Northward surface flow in the NH subtropical gyre is carried by the Gulf Stream, which separates from the coast at Cape Hatteras and becomes

a freely meandering jet to the northeast. At the Tail of the Grand Banks (black box in Figure 1), the warm northward flowing waters of the Gulf Stream meet the cold southward flowing waters of the Labrador Current, the western boundary current of the cyclonic subpolar gyre. The majority of the near-surface waters from the Labrador Current join the Gulf Stream to form the North Atlantic Current (NAC) east of the Grand Banks [e.g., *Rossby*, 1999]. As the NAC travels northward, it exhibits meanders that are locked in place by topography, the most prevalent of which is the anticyclonic Mann Eddy (centered at 42°N, 44°W, near the center of the box in Figures 1 and 4). The NAC continues past the Flemish Cap and then retroflects to the east and begins its course across the North Atlantic as a broad baroclinic transport between 48° and 52°N. The NAC then splits into several branches which enter the subpolar gyre, including one branch that passes through the Iceland Basin and another through Rockall Trough [*Rossby*, 1996; *Fratantoni*, 2001]. A more detailed summary of the subpolar Atlantic circulation can be found in *Schott and Brandt* [2007].

Estimates of the magnitude of the subtropical to subpolar throughput range from 13 to 20 Sv [*Hall and Bryden*, 1982; *Roemmich and Wunsch*, 1985; *Ganachaud and Wunsch*, 2003; *Willis*, 2010], which is roughly 20–25% of the overall transport by the upper layers of the Gulf Stream [*Brambilla and Talley*, 2006]. However, Lagrangian studies demonstrate that there is little surface transport between the subtropical and subpolar gyres due to the transport barrier of the Gulf Stream/NAC core [*Bower et al.*, 1985; *Bower and Lozier*, 1994; *Rypina et al.*, 2011; *Burkholder and Lozier*, 2011a] and to a lesser extent southward Ekman velocities [*Brambilla and Talley*, 2006]. Instead, subtropical waters primarily enter the subpolar gyre through subsurface pathways [*Burkholder and Lozier*, 2011a, 2014].

Intense buoyancy loss and mixing in the marginal seas of the North Atlantic, both in the open ocean [*Marshall and Schott*, 1999] and around the rims of the basins [*Spall and Pickart*, 2001], cause these surface waters to become dense and sink to great depth. These dense waters are generally referred to as North Atlantic Deep Water (NADW). NADW can be separated into several constituent water masses based on its place or origin and properties [e.g., *Smethie and Fine*, 2001]: Labrador Sea Water (LSW) is formed in the Labrador Sea, while Overflow Waters are denser than LSW and are formed via convective activity in the Nordic Seas and delivered to the North Atlantic across the Greenland-Iceland-Scotland Ridge [e.g., *Quadfasel and Käse*, 2007].

NADW is exported from convective regions through the Deep Western Boundary Current (DWBC) and complex interior pathways. *Stommel* [1958] first postulated that the DWBC is the primarily export pathway for deep waters. Assuming that dense water formation at high latitudes is balanced by uniform upwelling, he used a first-order vorticity balance to argue that the interior flow must be poleward, and hence, equatorward flow must occur in a DWBC. Decades later, direct velocity measurements demonstrated that velocities in the deep ocean near the western boundary are equatorward and are generally greater than interior velocities [*Fischer et al.*, 2004; *Schott et al.*, 2004; *Dengler et al.*, 2006], confirming the existence of the DWBC. Passive tracers, such as chlorofluorocarbons (CFCs), have also been utilized to understand the pathways of NADW, as these tracers are injected at the surface when water masses form through deep convection and are then transported via the ocean circulation. CFC concentrations can be used to calculate both water mass formation rates and the downstream age of water masses, where the age is the time elapsed since the water mass was in contact with the surface. Tracer concentrations are higher, and tracer ages are younger in the DWBC than in the ocean interior (Figure 5) [*Smethie et al.*, 2000; *Fine et al.*, 2002; *Smethie et al.*, 2007; *Rhein et al.*, 2015], which supports the role of the DWBC as a primarily export pathway. However, significant tracer concentrations are also found in the ocean interior, and tracer ages exceed the advective timescales for transit down the DWBC (Figure 5) [*Watts*, 1991; *Rhein*, 1994; *Lozier*, 1999; *LeBel et al.*, 2008; *Rhein et al.*, 2015]. Despite this, the dominance of the DWBC as the conduit for the lower limb of the overturning was not called into question until a series of studies showed that most of the floats released in the DWBC near the exit of the Labrador Sea were detrained from the DWBC and recirculated within the Labrador Sea [*Lavender et al.*, 2000; *Fischer and Schott*, 2002; *Bower et al.*, 2009, 2011; *Gary et al.*, 2011]; of the floats that did reach the subtropical gyre, most did so by interior pathways [*Bower et al.*, 2009, 2011; *Gary et al.*, 2011]. Modeling studies have confirmed the presence of interior pathways for both LSW and Overflow Waters [*Bower et al.*, 2009; *Gary et al.*, 2011; *Lozier et al.*, 2013], although the recirculation of Overflow Waters in the subpolar basin is markedly less than that for LSW [*Lozier et al.*, 2013]. These interior pathways, as well as the older-than-expected tracer ages in the DWBC, are signatures of eddy-driven recirculation gyres generated by the instabilities of the Gulf Stream/NAC system [*Lozier et al.*, 1997; *Lozier*, 1999; *Gary et al.*, 2011].

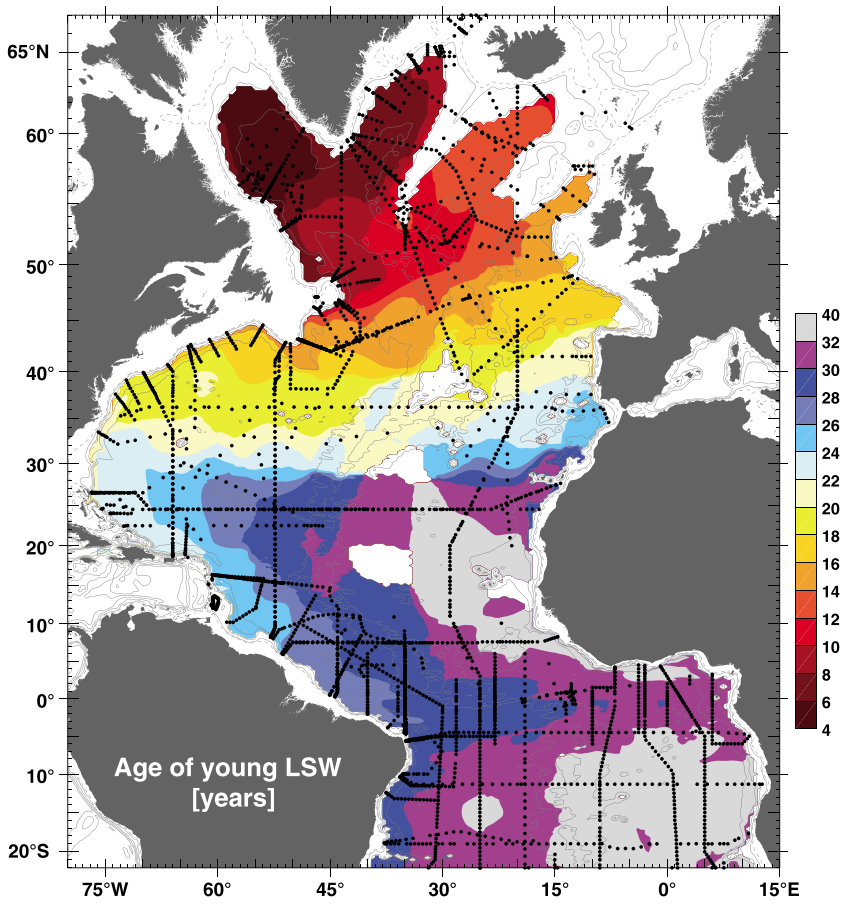

Figure 5. Map of tracer age of the Labrador Sea Water (LSW) layer (defined based on density classes) calculated from CFC concentrations for LSW younger than 40 years. LSW in the subpolar gyre is young, there are strong gradients in age in the TZ, and a tongue of relatively young water extends southward in the western basin of the subtropical gyre [from *Rhein et al.*, 2015].

Near 26°N the majority of southward flowing deep waters rejoin the DWBC [*Bower et al.*, 2009] and cross 5°S as a narrow western boundary current [*Garzoli et al.*, 2015]. However, at 8°S the DWBC breaks up into eddies; southward of this latitude, the transport of NADW is accomplished by migrating eddies [*Dengler et al.*, 2004; *Garzoli et al.*, 2015]. Deep waters are exported from the South Atlantic, and the upwelling of dense waters occurs primarily along isopycnals that outcrop in the Southern Ocean, drawn up to the surface by the strong winds blowing around Antarctica [*Toggweiler and Samuels*, 1995; *Marshall and Speer*, 2012]. Inflow of near-surface waters into the South Atlantic is needed to balance the export of NADW; waters from the Pacific enter through Drake Passage (cold route), and waters from the Indian Ocean enter through the Agulhas leakage (warm route) [see *Garzoli and Matano*, 2011, and references therein].

In summary, the AMOC involves the interaction between surface currents, deep currents, and eddy-driven circulations and involves a number of regions of strong water mass transformation. Here we highlight the region east of the Grand Banks as an important region for the North Atlantic circulation. This region is a place not only where the Gulf Stream and Labrador Current interact but also where the southward flowing DWBC abuts, and ultimately crosses underneath, the northward flowing Gulf Stream. Furthermore, the DWBC undergoes significant modifications in this region, as it interacts with the NAC, and a significant portion of waters from the DWBC enter the interior. Some of the key elements of this complex circulation are presented in the schematic diagram in Figure 4 (modified from *Church* [2007]). This schematic draws out, in an idealized way, the confluence region of the subtropical and subpolar gyres on the western margin of the basin. We will henceforth refer to this region (marked by a box in Figures 1 and 4) as the transition zone (TZ).

2.2. Localization of a Deep Meridional Overturning Cell to the Atlantic Basin

One wonders why a deep overturning cell is observed in the Atlantic—why not also in the Pacific? Experiments with coupled aqua-planet models [see, e.g., *Ferreira et al.*, 2010] suggest that two geometrical asymmetries in the continental configurations of the present climate play a key role: an interhemispheric asymmetry due to the presence of the Drake Passage and a zonal asymmetry due to the presence of a small basin (the Atlantic) and a large basin (the Pacific).

The zonal mean climate is profoundly affected by the interhemispheric asymmetry. The lack of meridional boundaries in the Southern Ocean permits a circumpolar current around Antarctica, the Antarctic Circumpolar Current. The resulting marked reduction in ocean heat transport (OHT) leads to Antarctica being thermally isolated and covered with a substantial ice cap over its land mass. In contrast, OHT in the NH is sustained to high latitudes, resulting in large air-sea temperature differences in marginal seas, heat loss to the atmosphere, and deep-reaching ocean convection [e.g., *Marshall and Schott*, 1999]. Deep water formation feeds the DWBC and an interhemispheric MOC. Moreover, the presence of a circumpolar channel around Antarctica at the latitude of strong westerlies enables dense waters to upwell adiabatically, drawn up to the surface by the winds [*Toggweiler and Samuels*, 1995; *Marshall and Speer*, 2012]. Consequently, the winds over the Southern Ocean provide much of the energy needed to sustain a deep overturning circulation [*Kuhlbrodt et al.*, 2007].

The difference in the size of the Atlantic relative to the Pacific ultimately results in a more saline Atlantic, the restriction of deep convection to the North Atlantic, and the localization of the MOC to the Atlantic Basin. The higher salinity of the Atlantic is due to a deficit of freshwater supply to the basin. The fetch of the rain and the zonal transport of moisture in the atmosphere, as well as the small width of the Atlantic Basin and the configuration of the river networks over the continents, combine to create an anomalous transfer of freshwater out of the Atlantic Basin into, ultimately, the Pacific. The midlatitude westerlies and the trade winds are a major contributor to the freshwater export from the Atlantic in both observations [*Zaucker and Broecker*, 1992] and models [*Czaja*, 2009; *Ferreira et al.*, 2010]. *Warren* [1983] attributes the freshwater import to the Pacific to low evaporation rates over cold surface waters, which result from a weak import of warm subtropical water into the northern Pacific. However, calculations presented in *Ferreira et al.* [2010] suggest that precipitation rather than evaporation is the key element. Moreover, revisiting Warren's study using recent data sets, *Emile-Geay et al.* [2003] attribute the freshness of the North Pacific to an excess of precipitation due to the atmospheric moisture transport associated with the Asian monsoon.

As a result of their high salinity, North Atlantic surface waters become extremely dense when subjected to wintertime cooling, enabling them to sink to great depths. In contrast, the low salinity of the North Pacific surface waters prevents them from sinking to depth even in the presence of intense wintertime cooling [*Warren*, 1983]. Furthermore, in order to sustain a vigorous adiabatic overturning circulation, isopycnals must outcrop in both high northern latitudes and in the circumpolar channel at high southern latitudes [*Wolfe and Cessi*, 2010, 2014]. Due to the lower salinity of the Pacific, the isopycnals in the North Pacific are too light to outcrop in the channel around Antarctica, and thus, a deep overturning circulation fed from the Pacific cannot be sustained.

2.3. Role of the AMOC in Ocean Heat Transport

The ocean contributes substantially to the meridional heat transport, with the strongest contribution in the tropics and about 30% contribution to the peak transport at 30°N [*Trenberth and Caron*, 2001; *Held*, 2001; *Wunsch*, 2005; *Czaja and Marshall*, 2006] (see section 3.2 for equations used to calculate OHT). As shown in Figure 3a, the major ocean basins (Atlantic and Indo-Pacific) play fundamentally different roles. In the Indo-Pacific the heat flux is asymmetric about the equator and directed poleward in both hemispheres, resulting from ocean heat uptake in the tropics and heat loss in the subpolar and polar latitudes. In the Atlantic, however, OHT is northward everywhere, peaking at about 1 PW at 20°N. Thus, in the South Atlantic heat is transported up the large-scale temperature gradient. Notably, there is a cross-equatorial heat transport of about 0.5 PW and convergence of heat into the North Atlantic. As a result, poleward of 40°N the Atlantic thermocline is much warmer (by as much as 3°C) than the Pacific. Northward OHT in the Atlantic is commonly attributed to the AMOC, the result of warm, near-surface water flowing northward across the equator, cooling, sinking, and then flowing southward as NADW (see Figure 2a). In contrast, the Pacific Ocean does not support a significant deep-reaching overturning cell, and thus, heat transports are solely due to near-surface subtropical overturning cells and gyre circulations.

The significant heat transport achieved by the Atlantic Ocean imprints itself on global climate, not just in the Atlantic sector. For example, recent studies suggest the fundamental role that northward cross-equatorial Atlantic OHT plays in setting the mean position of the ITCZ north of the equator. The hemispheric net top-of-the-atmosphere radiative forcing of the climate is nearly symmetric about the equator [*Trenberth and Caron*, 2001; *Voigt et al.*, 2013; *Marshall et al.*, 2014a]; thus, the total (atmosphere plus ocean) heat transport across the equator is small, about 0.2 PW northward. Therefore, to compensate for significant northward OHT, the ITCZ is displaced north of the equator and atmospheric heat transport is southward across the equator [*Kang et al.*, 2008, 2009; *Frierson et al.*, 2013; *Marshall et al.*, 2014a]. As a result of the northward cross-equatorial OHT, the atmosphere and ocean are slightly warmer (by $\approx$2°C) in the NH than in the SH [*Feulner et al.*, 2013; *Marshall et al.*, 2014a] (Figure 3b). By virtue of its relative warmth, the NH emits slightly more outgoing longwave radiation than the SH, leading to the slight asymmetry in top-of-the-atmosphere radiation and supporting the small northward heat transport by the coupled system across the equator [*Kang et al.*, 2014; *Marshall et al.*, 2014a].

There is an ongoing debate about the relative roles of the ocean and atmosphere in sustaining Europe's mild winters compared to similar latitudes in North America [e.g., *Seager et al.*, 2002; *Rhines et al.*, 2008; *Palter*, 2014; *Yamamoto et al.*, 2015]. It is agreed that differences in the climate between the east coast of North America and western Europe result from the former having a continental climate and the latter having a maritime climate due to the prevailing westerly winds, as well as orography-induced stationary wave patterns which result in cold northwesterly flow over the eastern United States and warm southwesterly flow over Europe [*Seager et al.*, 2002]. However, there is considerable debate about whether the ocean is merely a reservoir for seasonally stored heat [*Seager et al.*, 2002] or whether ocean heat transport convergences play a significant role [*Rhines et al.*, 2008], although both studies agree that ocean heat transport convergences are important in maintaining ice-free regions. Variability in European climate appears to be controlled primarily by atmospheric pathways on interannual timescales [*Yamamoto et al.*, 2015], but ocean dynamics play a role on decadal timescales [*Palter*, 2014; *Yamamoto et al.*, 2015].

2.4. The AMOC and Atlantic Multidecadal Variability (AMV)

The role of the AMOC in ocean heat transport suggests that variability in the AMOC leads to ocean heat content anomalies and potentially impacts SST. In this section we review observations of low-frequency Atlantic SST variability and studies that address the origin of these SST anomalies.

The instrumental record [*Schlesinger and Ramankutty*, 1994; *Kushnir*, 1994; *Delworth et al.*, 2007; *Deser et al.*, 2010] and proxy data [*Mann and Park*, 1994; *Delworth and Mann*, 2000; *Gray et al.*, 2004; *Svendsen et al.*, 2014] indicate that Atlantic SSTs exhibit significant interannual to decadal variability. An important observed mode of SST variability is a warming/cooling of the North Atlantic on decadal timescales [*Schlesinger and Ramankutty*, 1994; *Kerr*, 2000; *Knight et al.*, 2005; *Delworth et al.*, 2007; *Deser et al.*, 2010], known as the Atlantic Multidecadal Oscillation/Atlantic Multidecadal Variability (AMO/AMV, AMV hereafter). For example, Figure 6a shows the AMV index, defined as the basin average (0–60°N) SST over the North Atlantic from the Hadley Centre Sea Ice and Sea Surface Temperature data set (HadISST) [*Rayner et al.*, 2003]; the global mean SST has been removed (as in *Trenberth and Shea* [2006]), as an approximation of the externally forced response (see discussion of various methods for removing the forced response below). The AMV time series has significant low-frequency variability; its power spectrum (Figure 6b) has the characteristics of red noise, with power increasing with timescale. While previous studies of instrumental record and proxy data have suggested both decadal (~20 years) [e.g., *Mann et al.*, 1995; *Frankcombe et al.*, 2010; *Chylek et al.*, 2011, 2012] and multidecadal peaks (~40–70 years) [e.g., *Frankcombe et al.*, 2010] in the power spectra of the AMV index, the present analysis has only a hint of a broad, statistically significant peak at a timescale of 70 years, which is not fully resolved by the 143 year time series. The spatial pattern of SST anomalies associated with the AMV is a basin-wide warming of the North Atlantic, with the largest anomalies occurring in subpolar regions. The AMV has both regional and global impacts [see, e.g., *Delworth et al.*, 2007]; it is capable of explaining the observed low-frequency variations in NH mean temperatures [*Zhang et al.*, 2007] and is thought to control low-frequency variations in the position of the ITCZ (see sections 2.3 and 6.1).

The AMV is widely believed to be a mode of variability associated with slow ocean processes, the most invoked being variability of the AMOC. Yet as pointed out by *Lozier* [2010], no observational study to date has successfully linked SST changes to AMOC variability. Modeling results linking the AMV to the AMOC are often based on statistical analyses (e.g., lagged correlations), and the SST patterns associated with the AMOC differ

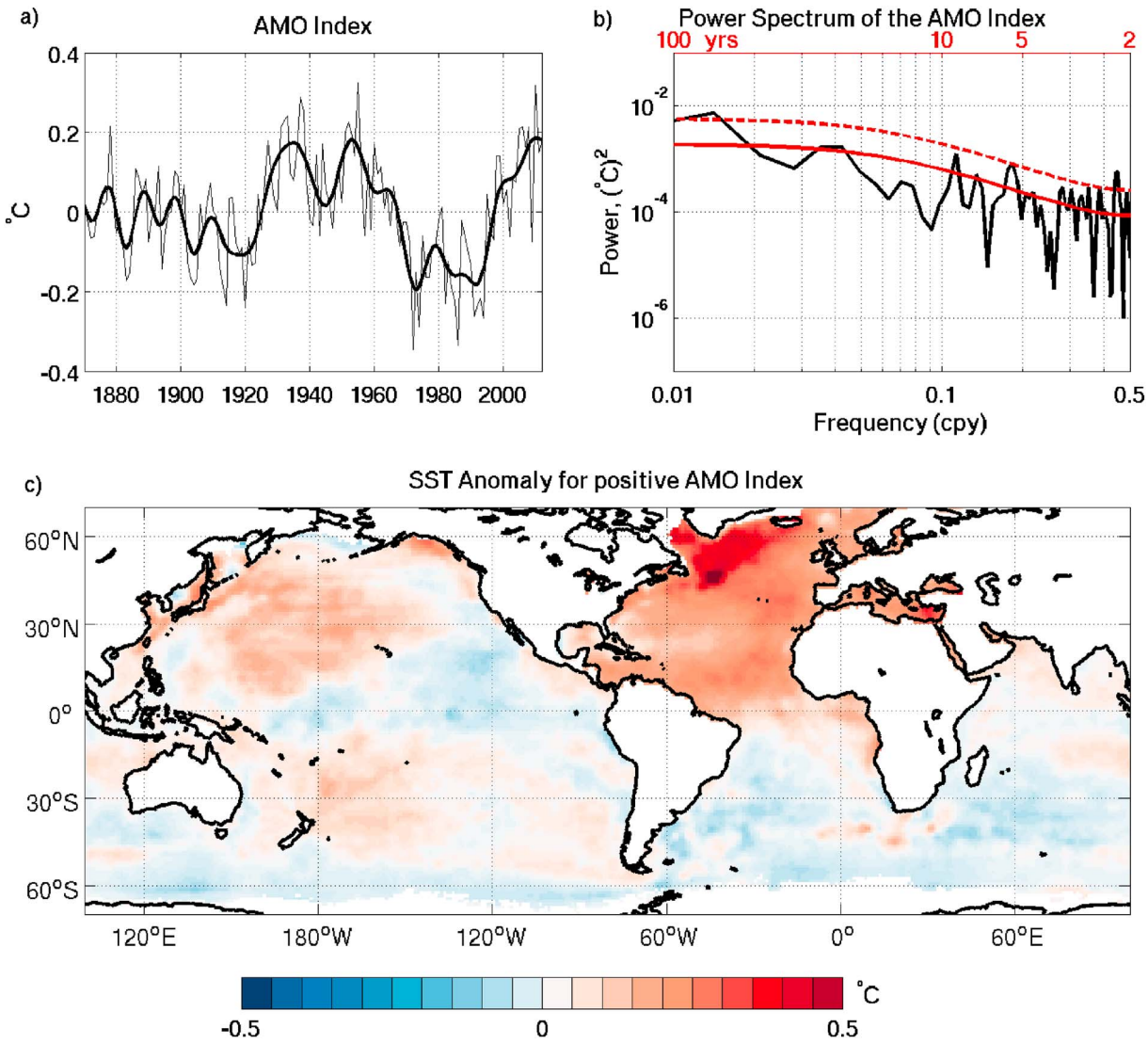

Figure 6. Low-frequency North Atlantic SST variability from annual mean SST over the period 1870–2012. SST data are from HadISST [*Rayner et al.*, 2003]. (a) The AMV index is defined as the average SST in the North Atlantic over the domain 0°N to 60°N. The global mean SST is removed (as in *Trenberth and Shea* [2006]), to extract the externally forced response. The thin line indicates yearly values; the thick line shows the low-pass-filtered time series using a cutoff period of 10 years. (b) Power spectrum of AMV time series. The solid black line denotes the spectral estimate, the solid red line is the spectrum of a first-order Markov process (red noise) derived from the time series, and the dashed line is the 95% confidence limit about that red noise spectrum. The power spectrum is calculated by detrending the time series and applying a Hanning tapering window and then using the fast Fourier transform algorithm. (c) The spatial pattern of low-pass-filtered SST regressed against the low-pass-filtered AMV index, with magnitude 1σ of the yearly AMV index (+0.14°C). Figure provided by Brian Green, MIT (personal communication, 2014).

between models. The relative roles of external (e.g., greenhouse gas and aerosol) forcing, ocean processes, and atmospheric forcing in creating decadal SST anomalies remain to be quantified, as we now review.

Quantifying the externally forced SST signal in the North Atlantic from observations is a difficult task. Methods include identifying a linear trend [*Enfield et al.*, 2001; *Sutton and Hodson*, 2005; *Knight et al.*, 2006], regressing onto global mean sea surface temperature [*Trenberth and Shea*, 2006; *Mann and Emanuel*, 2006], and signal-to-noise maximizing empirical orthogonal function analysis [*Ting et al.*, 2009]. Each method produces somewhat different estimates of the separation into externally and internally forced components, indicating uncertainties in the assumptions used to estimate the externally forced signal [*Delworth et al.*, 2007; *Ting et al.*, 2009; *Deser et al.*, 2010; *Mann et al.*, 2014] and potentially nonlinearities in the system.

Model ensembles, formed by perturbing initial conditions in order to create multiple realizations of climate with the same external forcing, are a powerful tool for partitioning climate signals into externally forced

components and internal variability. If sufficient ensemble members are available, internal variability will be averaged out in the ensemble mean, and thus, it will approximate the response of the climate to external forcing [*Knight*, 2009; *Terray*, 2012; *Mann et al.*, 2014]. In general, neither the mean of single model ensembles nor of multimodel ensembles show decadal SST variability resembling observations [*Knight*, 2009], indicating that Atlantic decadal SST variability is a consequence of internal atmospheric and oceanic processes, the phasing of which are not set by external forcing. However, *Booth et al.* [2012] use the HadGEM2-ES (Hadley Centre Global Environmental Model version 2 Earth System configuration) coupled model to argue that most of the Atlantic multidecadal SST variability can be explained by aerosol emissions and periods of volcanic activity [see also *Otterå et al.*, 2010] and claim that the failure of previous multimodel ensemble means to capture multidecadal Atlantic SST variability is due to the models' failure to include aerosol-cloud microphysical effects. *Zhang et al.* [2013] challenge these conclusions, arguing that there are significant discrepancies between North Atlantic Ocean heat content anomalies in HadGEM2-ES and observations [*Zhang*, 2007]. *Terray* [2012] focuses on the regional variations in the contributions of forced and internal variability to North Atlantic SST, finding that external forcing dominates in the tropics and subtropics, while internal variability dominates in subpolar regions.

Internal SST variability can be further partitioned into portions forced directly by the atmosphere and those resulting from variability of the ocean circulation. A common statistical technique for assessing the relative roles of atmospheric forcing and ocean dynamics is to compute correlations between winds/air-sea heat fluxes and SST as a function of timescale. *Kushnir* [1994] utilizes SST and sea level pressure data to argue that while the atmosphere forces SST anomalies on interannual timescales [*Hasselmann*, 1976; *Cayan*, 1992a, 1992b; *Barsugli and Battisti*, 1998], ocean dynamics plays a role in setting SST on decadal timescales. He suggests that AMOC variability is a likely mechanism for creating the observed decadal SST anomalies. *Gulev et al.* [2013] show that correlations between an AMV-like index and the surface heat flux are positive on decadal timescales and negative on interannual timescales, implying that surface turbulent heat fluxes are driven by the ocean and may force the atmosphere on timescales longer than 10 years. In contrast, in an earlier study, *Deser and Blackmon* [1993] do not find such a transition and argue that SST is the passive response to atmospheric forcing on all timescales in their study, which used 90 years of data. As further evidence of an active ocean circulation, *Czaja and Marshall* [2001] use SST and sea level pressure observations to show that the spectral characteristics of SST anomalies in the North Atlantic can be explained by changes in the ocean circulation, specifically the wind-driven gyres. *McCarthy et al.* [2015] use an index of sea level along the North American coast as a proxy for the ocean circulation and show that these circulation changes impact the AMV on decadal timescales.

A complementary technique for understanding the relative roles of atmospheric forcing and ocean dynamics in setting SST is to compare the SST variability in an ocean mixed layer model to that of a fully coupled general circulation model (GCM). Using this technique, *Seager et al.* [2000] argue that the majority of wintertime SST variability observed during the last four decades can be explained as a (local) passive response to atmospheric forcing. However, this study primarily focuses on the ability of the mixed layer model to simulate tripole SST anomalies associated with the North Atlantic Oscillation (NAO), rather than basin-wide SST anomalies (e.g., the AMV). Additionally, as atmospheric winds are prescribed, the origin of low-frequency atmospheric variability is not addressed, leaving open the potential that the ocean circulation is important in creating low-frequency atmospheric variability. Using interactive ensemble coupled GCMs, *Fan and Schneider* [2011] and *Chen et al.* [2015] show that the feedbacks to the extratropical atmosphere from North Atlantic SST anomalies are small compared with the weather noise and tend to act as a damping term. These results suggest that variability in atmospheric forcing over the extratropical North Atlantic is primarily the result of atmospheric noise.

Budget analyses can also be used to assess the roles of local (air-sea heat flux and Ekman transport) variability versus geostrophic ocean dynamics in setting SST/upper ocean heat content (UOHC). *Buckley et al.* [2014a, 2014b, 2015] find that local air-sea heat fluxes and Ekman transport variability explain the majority of UOHC variability in the interior of the subtropical gyre over their 19 year study period. In contrast, in the Gulf Stream region and the subpolar gyre ocean dynamics are important in setting interannual UOHC anomalies (see Figure 7a, described in detail in section 5.2.1), which are then damped by air-sea heat fluxes [*Dong and Kelly*, 2004; *Dong et al.*, 2007; *Zhai and Sheldon*, 2012; *Buckley et al.*, 2014a]. *Buckley et al.* [2014a] estimate the damping timescale of UOHC anomalies to be 3–4 years in the Gulf Stream region and 5–6 years in the subpolar gyre. *Marsh et al.* [2008] and *Grist et al.* [2010] use eddy-permitting models to show that advection plays a substantial role in the depth-integrated heat budget in the middle and high latitudes and significantly impacts

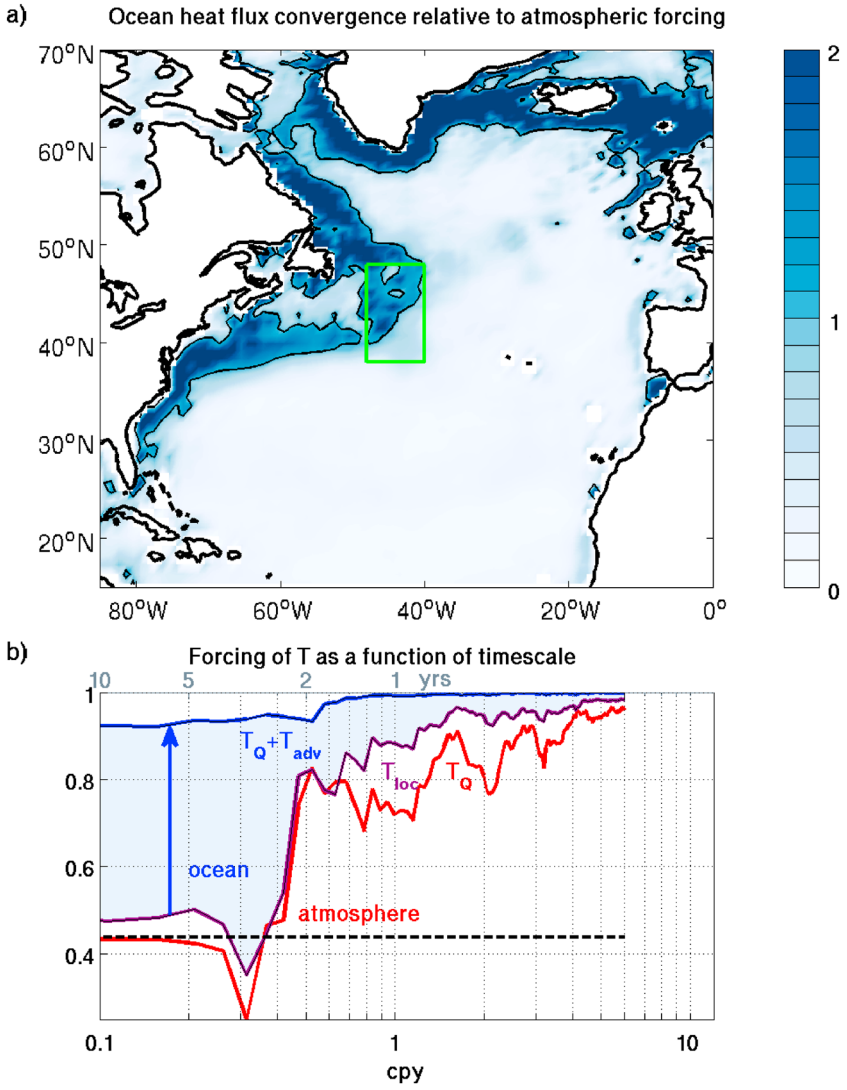

Figure 7. A heat budget analysis over the maximum climatological mixed layer depth using the ECCO v4 state estimate (1992–2010). (a) Map shows the ratio of the variance of heat transport convergences due to dynamical ocean processes, including geostrophic, bolus, and diffusive convergences, to the variance of convergences due to local atmospheric forcing, including air-sea heat fluxes and convergences due to Ekman mass transport variability. The ratio is small over the gyre interiors but large over boundary currents and the TZ region. (b) The relative importance of various terms in the heat budget over the region 40°–48°W, 38°–48°N (green box in panel (a)) at the heart of the TZ as a function of timescale. Plotted are the magnitude of the coherence between temperature relative to the initial temperature ($T - T_o$) and integrated air-sea heat fluxes (T_Q), integrated local (air-sea heat fluxes and Ekman) atmospheric forcing (T_{loc}), and the sum of T_Q and integrated advective heat transport convergences (T_{adv}). It is apparent that T_{loc} explains the majority of the variability of $T - T_o$ on intra-annual timescales, but on timescales longer than a couple of years, heat transport convergences due to ocean dynamics become increasingly important.

SST on interannual to decadal timescales. These results highlight the fact that the timescale at which ocean dynamics becomes important in setting SST/UOHC depends strongly on the region considered.

The hypothesis that ocean dynamics, in particular the AMOC, are important in creating decadal SST anomalies has led to numerous GCM studies exploring the relationships between decadal AMOC and SST variability (e.g., the AMV). While these studies generally find significant lagged correlations between low-frequency variability of the AMOC and SST, it is not clear whether AMOC variability plays a dominant role in creating these SST patterns. Some studies argue that SST anomalies are the result of AMOC variability and resulting OHT convergence variability [*Häkkinen*, 1999; *Delworth and Mann*, 2000; *Knight et al.*, 2005; *Latif et al.*, 2007; *Msadek and Frankignoul*, 2009; *Zhang*, 2010a; *Delworth and Zeng*, 2012; *Roberts et al.*, 2013a]. Other studies suggest that

SST anomalies are the result of other processes (local atmospheric forcing, Rossby waves, and shifts in fronts), and when upper ocean temperature anomalies reach the western boundary, they lead to AMOC variability in accord with the thermal wind relation [*Danabasoglu*, 2008; *Frankcombe et al.*, 2008; *Buckley et al.*, 2012; *Zanna et al.*, 2012]. Still other studies suggest a two-way feedback loop in which SST and the AMOC exert a significant influence on each other [*Delworth et al.*, 1993; *Delworth and Greatbatch*, 2000; *Dong and Sutton*, 2005; *Msadek and Frankignoul*, 2009]; a theoretical framework for considering such coupling is given in *Marshall et al.* [2001a]. Relationships between the AMOC and SST are expected to depend strongly on timescale, with the AMOC playing a more active role on longer timescales. For example, *Schmith et al.* [2014] argue that the AMOC contributed significantly to North Atlantic SST trends since the midnineteenth century.

The AMV has also been related to changes in the subtropical and subpolar gyre circulations. A weakening of the subtropical and subpolar gyres driven by changes in the wind stress curl allows greater penetration of warm subtropical waters into the subpolar gyre [*Häkkinen and Rhines*, 2004; *Hátún et al.*, 2005; *Häkkinen and Rhines*, 2009; *Häkkinen et al.*, 2011a] and thus a positive phase of the AMV [*Häkkinen et al.*, 2011b, 2013]. *Häkkinen et al.* [2011b] argue that the weakening of the gyres is due to a mode of wind stress curl variability associated with more frequent blocking between Greenland and western Europe. *Schneider and Fan* [2012] show that changes in the strength of the mean gyre circulations are required to explain observed Atlantic SST variability, in particular an index of the NAO tripole.

In summary, while it is clear that on intra-annual to interannual timescales, Atlantic SST variability primarily reflects the passive response to stochastic atmospheric forcing, on interannual to decadal timescales the origin of Atlantic SST variability is less certain. Local atmospheric forcing, ocean dynamics (including changes in the AMOC), and external forcing all likely play a role. Furthermore, the degree to which ocean dynamics are important in setting SST depends strongly on region as well as timescale, with ocean dynamics playing a larger role in regions of strong currents/fronts and less of a role in gyre interiors.

2.5. The AMOC and Its Role in Climate Change

Forced with greenhouse gases, the climate system adjusts toward a new equilibrium on various timescales: ultrafast responses in the stratosphere and troposphere (days to weeks), fast responses of the land surface and the ocean's mixed layer (months to years), and a long-term adjustment of the deeper ocean (decades to millennia) [e.g., *Gregory*, 2000; *Stouffer*, 2004; *Gregory and Webb*, 2008; *Held et al.*, 2010; *Andrews et al.*, 2012]. The ocean's response timescales depend not only on the rate at which energy is absorbed at the sea surface (the net ocean heat uptake) but also on the efficiency with which that energy is transported away from the surface and into the ocean interior [e.g., *Hansen et al.*, 1985]. In addition to setting the adjustment timescale to equilibrium, ocean heat uptake (see summary of observational estimates of ocean heat uptake in *Abraham et al.* [2013]) plays a central role in transient climate change, essentially setting the pace of global warming well into the 22nd century [*Boé et al.*, 2009]. Moreover, analyses suggest that differences in ocean heat uptake may explain a significant portion of the large intermodel spread in simulated warming [*Raper et al.*, 2002; *Boé et al.*, 2009; *Hansen et al.*, 2011; *Kuhlbrodt and Gregory*, 2012; *Geoffroy et al.*, 2013a, 2013b].

The AMOC is a key means by which excess heat and carbon can be transported from the surface to the deep ocean. *Kostov et al.* [2014] show that the AMOC is central to transporting and redistributing anthropogenic temperature to depth, thus regulating the effective heat capacity of the ocean under global warming. Moreover, they show that coupled models used for climate change predictions differ substantially in their representation of the strength and depth of the AMOC and that this diversity largely accounts for the variability in the vertical distribution of ocean heat storage seen in the models. *Marshall et al.* [2014b, 2014c] also study the role of the AMOC in setting the patterns and timescale of the transient response of the climate to anthropogenic greenhouse gas forcing. They draw out the importance of the upper cell in delaying warming signals in the Southern Ocean and northern North Atlantic and in amplifying the warming signal in the Arctic.

In addition to mediating the transport of anthropogenic heat and carbon signals from the surface to the deep ocean, the AMOC itself may respond to climate change [*Broecker*, 1997]. In response to increasing greenhouse gases, the AMOC is projected to decline between 0% to more than 50% over the 21st century [*Gregory et al.*, 2005; *Solomon et al.*, 2007; *Cheng et al.*, 2013; *Meehl et al.*, 2013; *Kirtman et al.*, 2013], but no GCM included in the recent Coupled Model Intercomparison Project (CMIP5) exhibits a complete collapse of the AMOC [*Gregory et al.*, 2005; *Rugenstein et al.*, 2013]. *Drijfhout and Hazeleger* [2007] and *Drijfhout et al.* [2008] use an ensemble of climate model runs to separate AMOC variability due to greenhouse gas forcing and internal variability.

They find that the greenhouse forced signal consists of an overall decrease and shoaling of the AMOC, with a maximum amplitude of 10 Sv per century. In addition to the effects of greenhouse gases, the AMOC may be influenced by anthropogenic aerosols [*Delworth and Dixon*, 2006; *Stenchikov et al.*, 2009; *Gregory*, 2010; *Cowan and Cai*, 2013; *Ding et al.*, 2014]. *Delworth and Dixon* [2006] show that the greenhouse gas-induced AMOC weakening is partially offset by increasing anthropogenic aerosols, which tend to strengthen the AMOC.

Weakening of the AMOC under greenhouse gas forcing results from both reduced heat loss to the atmosphere and increasing freshwater fluxes at high latitudes, both leading to lighter surface waters [e.g., *Thorpe et al.*, 2001]. Although much research has focused on changes in freshwater fluxes [e.g., *Manabe and Stouffer*, 1994; *Stouffer et al.*, 2006], recent work suggests that weakening of the AMOC is primarily due to changes in air-sea heat fluxes and ocean temperatures [*Gregory et al.*, 2005; *Weaver et al.*, 2007; *Marshall et al.*, 2014c]. Lighter surface waters may lead to a reduction or collapse of deep convection in sinking regions and thus impact the strength of the AMOC [e.g., *Rahmstorf*, 1999; *Zhang*, 2010a]. Furthermore, if isopycnals in the North Atlantic become too light to outcrop in the Southern Ocean, where intense upwelling along isopycnals occurs, a vigorous adiabatic overturning circulation cannot be sustained [*Wolfe and Cessi*, 2010, 2014].

AMOC changes can imprint themselves onto regional and global climate. Temperature trends over the twentieth century and climate change projections show a conspicuous region of cooling over the Atlantic subpolar gyre, which has been termed the "warming hole." A number of studies have explored whether the warming hole can be attributed to changes in the ocean circulation. *Marshall et al.* [2014c] suggest that the warming hole can be understood in terms of anomalous advection of heat by the ocean circulation, and *Winton et al.* [2013] focus on the role of changing currents in determining the spatial patterns of anthropogenic ocean heat uptake. *Rahmstorf et al.* [2015] argue that the warming hole may be due to a reduction of the AMOC over the twentieth century, particularly after 1970 [see *Dima and Lohmann*, 2010; *Thompson et al.*, 2010]. Modeling studies suggest that the warming hole is associated with an AMOC decline in historical runs and climate change projection scenarios [*Drijfhout et al.*, 2012; *Woollings et al.*, 2012]; however, the warming hole cannot be fully attributed to changes in the AMOC in historical runs, in which AMOC changes are modest.

The warming hole in the North Atlantic potentially impacts global climate. Uptake of anthropogenic heat by the ocean occurs preferentially in regions of delayed warming [*Winton et al.*, 2013; *Marshall et al.*, 2014c]. Thus, *Winton et al.* [2013] argue that the presence of the warming hole (which they attribute to ocean circulation changes) shifts the uptake of anthropogenic heat from low latitudes to high latitudes. Because the atmosphere is more sensitive to forcing at high latitudes due to ice-albedo feedbacks and more stable lapse rates [*Hansen et al.*, 1997; *Winton et al.*, 2010; *Rugenstein et al.*, 2013], global surface warming is significantly reduced by ocean circulation changes.

The potential for abrupt AMOC collapse due to greenhouse gas forcing remains controversial. The basis for this risk is the potential existence of two stable regimes of the AMOC ("on" and "off"). Bistable behavior of the AMOC has been identified in a range of idealized climate models [*Stommel*, 1961; *Manabe and Stouffer*, 1988; *Rahmstorf*, 1995; *Kuhlbrodt et al.*, 2001; *Gregory et al.*, 2003; *Johnson et al.*, 2007; *Lenton et al.*, 2009], including Earth system models of intermediate complexity (EMICs) [*Rahmstorf et al.*, 2005]. However, unstable behavior has not been observed in state-of-the-art coupled GCMs, leading to the interpretation that the AMOC is more stable than simple models indicate. A possible explanation for this increased stability is that the presence of a dynamical atmosphere in coupled GCMs, missing in many EMICs, is crucial to capture the correct stability behavior of the AMOC [*Schiller et al.*, 1997; *Monahan*, 2002; *Yin et al.*, 2006]. As a result, both the Intergovernmental Panel on Climate Change (IPCC) Fourth and Fifth Assessment Reports (AR4, AR5) conclude that it is extremely unlikely that the AMOC will collapse in the 21st century [*Solomon et al.*, 2007; *Meehl et al.*, 2013; *Kirtman et al.*, 2013].

However, the stability of the AMOC in state-of-the-art GCMs has recently come into question due to indications that some of these models do not accurately represent ocean freshwater transports. Recent studies find that the freshwater budget over the Atlantic Basin is a key factor for bistable AMOC behavior; if the AMOC exports freshwater from the Atlantic Basin (see more on ocean freshwater transport in section 3.3), then the AMOC is in the bistable regime [*Rahmstorf*, 1996; *Schaeffer et al.*, 2002; *de Vries and Weber*, 2005; *Dijkstra*, 2007; *Huisman et al.*, 2010; *Hawkins et al.*, 2011; *Drijfhout et al.*, 2011; *Weaver et al.*, 2012; *Deshayes et al.*, 2013; *Liu and Liu*, 2014]. While it is difficult to observationally determine the freshwater input due to the AMOC, observations indicate that it is negative [*Weijer et al.*, 1999; *Bryden et al.*, 2011], suggesting that the AMOC is indeed in the

bistable regime. In many IPCC class GCMs, the AMOC imports freshwater into the Atlantic, contrary to observations, and thus, the AMOC may be artificially stable in these models [*Rahmstorf*, 1996; *Drijfhout et al.*, 2011]. However, recent work by *Weaver et al.* [2012] demonstrates that no CMIP5 model exhibits a rapid collapse of the AMOC, despite 40% of them being in the bistable regime.

In summary, the AMOC modulates the trajectory of global warming by controlling the rate at which heat and carbon are sequestered in the deep ocean. Furthermore, the AMOC is projected to decline as a response to climate change, and this decline has the potential to impact regional and global climate, leading to, for example, the warming hole over the North Atlantic subpolar gyre. While it appears that in the current climate the AMOC is in a bistable regime, state-of-the-art GCMs have not found evidence of AMOC collapse under typical global warming scenarios. Whether this apparent stability is a robust feature of future climate projections or due to model deficiencies remains to be determined.

3. AMOC Mass, Heat, and Freshwater Transports

Before going on to discuss direct observations of the AMOC, we take some care to precisely define it. We focus first on defining the overturning stream function and its associated heat and freshwater transports and then go on to describe a dynamical decomposition that has informed strategies to measure the AMOC from observations. This dynamical decomposition will guide our subsequent discussion of underlying mechanisms.

3.1. AMOC Definitions

We define the AMOC as the stream function for the zonally integrated meridional volume transport in depth coordinates:

$$\Psi(y,z) = \int_z^{\eta} \int_{x_w}^{x_e} v \, \mathrm{d}x \, \mathrm{d}z, \tag{1}$$

where v is the meridional velocity, z is a vertical coordinate increasing upward, η is the height of the free surface, and $x_w(z)$ and $x_e(z)$ are the westward and eastward positions of the bathymetry at a particular depth (see the diagram in Figure 4). With this standard sign convention, a positive stream function is a clockwise circulation, with northward flow at the surface and southward flow at depth. The AMOC can also be defined using density or temperature as a vertical coordinate [e.g., *Zhang*, 2010a, 2010b].

The strength of the AMOC at each latitude is defined as the maximum of the stream function over the water column:

$$\Psi_{\max}(y,t) = \max_z \Psi(y,z,t), \tag{2}$$

which occurs at the depth $z_{\max}(y,t)$. This simple scalar field has received an enormous amount of attention, both in models and in observations. According to the observational inversion in Figure 2a, $\Psi_{\max}$ reaches a magnitude of order +15 Sv in the North Atlantic. For comparison, the flow of the Amazon, the largest river on Earth, has a transport of order 0.2 Sv and the Antarctic Circumpolar Current has a transport of about 130 Sv.

3.2. Heat Transport

As discussed in section 2.3, due to the deep overturning circulation in the Atlantic, the Atlantic Ocean transports heat northward in both hemispheres (Figure 3a). The meridional Atlantic OHT can be expressed in terms of the stream function Ψ as

$$\mathcal{H} = \rho_o C_p \int_{-H}^{\eta} \int_{x_w}^{x_e} v \, \theta \, \mathrm{d}x \, \mathrm{d}z = -\rho_o C_p \int_{-H}^{\eta} \frac{\partial \Psi}{\partial z} \, \theta \, \mathrm{d}z, \tag{3}$$

where θ is potential temperature, ρ_o is the reference density, C_p is the heat capacity at constant pressure, and H is the ocean depth.

OHT can be expressed most concisely through overturning stream functions in temperature coordinates. Applying the quotient rule, the above equation can be written as

$$\mathcal{H} = \rho_o C_p \int_{-H}^{\eta} \Psi \frac{\partial \theta}{\partial z} \, \mathrm{d}z = \rho_o C_p \int_{\theta_{\text{bottom}}}^{\theta_{\text{top}}} \Psi \, \mathrm{d}\theta, \tag{4}$$

where θ_{top} is SST and θ_{bottom} is the temperature at the bottom of the ocean. In deriving the above we have assumed that Ψ is constant at the top and bottom of the ocean because there is no flow through these boundaries (see the discussion in *Czaja and Marshall* [2006] and *Marshall and Plumb* [2008]). The above tells us that the heat transport can be expressed in terms of the volume transport in temperature layers, or more generally, noting the multiplying factor $\rho_o C_p$, the mass transport in energy layers. Overturning stream functions in potential temperature coordinates [e.g., *Czaja and Marshall*, 2006; *Saenko and Merryfield*, 2006; *Ferrari and Ferreira*, 2011] clearly show the differing nature of the circulations responsible for OHT in the Atlantic and Indo-Pacific. In the Indo-Pacific, the stream function is dominated by shallow cells associated with wind-driven gyres and subtropical overturning cells. In contrast, the Atlantic also includes a cell that spans the surface and deep ocean, which is related to NADW formation, southward flow at cold temperatures, upwelling in the Southern Ocean, and a gradual warming as surface waters flow northward.

At the level of a scaling argument, it is then useful to write down $\mathcal{H}$ in the approximate form:

$$\mathcal{H} \simeq \rho_o \, C_p \, \Delta\theta \, \Psi_{\max} \tag{5}$$

where $\Delta\theta$ is the difference in potential temperature between the poleward and equatorward branches. So, for example, if the vertical temperature difference across the AMOC is 15°C, typical of the temperature drop across the thermocline, then equation (5) yields a heat transport in the Atlantic of 0.9 PW if the AMOC has a strength of 15 Sv, roughly in accord with Figure 3a.

Despite the central role that the AMOC plays in the asymmetry of OHT between the Atlantic and the Indo-Pacific, it is difficult to attribute precisely what fraction of the Atlantic OHT is a direct result of the deep overturning. Several studies have attempted to isolate the portion of Atlantic OHT due to the AMOC by separating the heat transport due to the zonal mean circulation and deviations from the zonal mean (the horizontal gyre component) [see, e.g., *Bryan*, 1962; *Hall and Bryden*, 1982; *Roemmich and Wunsch*, 1985; *Bryden*, 1993; *Marsh et al.*, 2008; *McDonagh et al.*, 2010]. This leads to the conclusion that OHT is dominated by the zonal mean overturning circulation, except in the subpolar gyre where the gyre circulation and eddy fluxes play substantial roles [*Marsh et al.*, 2008]. However, this decomposition cannot attribute the portion of OHT that is due to surface and deep processes because all circulations have a horizontal and vertical component. *Talley* [2003] uses hydrographic data to estimate the OHT due to shallow, intermediate, and deep circulations and demonstrates that NADW water formation and the upper cell of the AMOC carry a significant portion of northward heat transport. Model-based heat transport stream functions [*Boccaletti et al.*, 2005; *Ferrari and Ferreira*, 2011] demonstrate that OHT in the Indo-Pacific is the result of wind-driven gyres and overturning cells confined to the thermocline, but in the Atlantic the majority of the OHT is associated with a circulation that spans the thermocline and the deep ocean.

3.3. Freshwater Transport

In the mean, the patterns of precipitation (P), evaporation (E), and runoff (R) at the sea surface must be balanced by convergences of freshwater by the ocean. The ocean must converge freshwater in the subtropics where $E>P+R$ and diverge freshwater in along the equator and in subpolar regions where $E<P+R$. Since the Atlantic is a net evaporative basin, the ocean must also converge freshwater into the Atlantic Basin.

The meridional freshwater transport (FWT) is defined as

$$\mathcal{F}(y) = \int_{-H}^{\eta} \int_{x_w}^{x_e} v \left(1 - \frac{S}{S_o}\right) \mathrm{d}x \, \mathrm{d}z, \tag{6}$$

where S is salinity and S_o is a reference salinity. The FWT is approximately $-S_o$ times the salinity transport, with exact equality holding when there is no mass transport across the section. The salinity transport can be defined in a manner analogous to equations (3) and (4) by replacing θ with S, although interpretation of equation (4) is a little trickier because S is not monotonic in the vertical.

Since diffusive transports of salt can be neglected [*Schiller*, 1995], conservation of mass and salt requires that in steady state

$$\mathcal{F}(y_2) - \mathcal{F}(y_1) = \int_{y_1}^{y_2} \int_{x_w}^{x_e} (P + R - E) \, \mathrm{d}x \, \mathrm{d}y.$$

The relationship between atmospheric and oceanic FWT suggests that atmospheric FWT and its associated latent heat transport is a coupled ocean-atmosphere process. *Rhines et al.* [2008] emphasize that half of the atmospheric energy transport is due to latent heat transport and that the ocean circulation provides the return circuit for atmospheric vapor transport, without which freshwater would accumulate at the high latitudes. However, as discussed in *Ferreira et al.* [2010] and *Ferreira and Marshall* [2015], atmospheric FWT transport is essentially independent of the ocean state: the ocean circulation and salinity distribution adjust to achieve a return freshwater pathway demanded of them by the atmosphere. Nevertheless, changes in ocean FWT, the hydrological cycle, and changes in ice distributions can modulate the high-latitude convective and mixing processes involved in the sinking branch of the AMOC. We return to this in section 5.2.6.

Does the AMOC transport freshwater out of the Atlantic, contributing to the salinization of the basin, or into the basin, balancing the loss of freshwater to the atmosphere? *Broecker* [1991] and *Zaucker and Broecker* [1992] argue that freshwater loss along the path of the upper limb of the AMOC drives NADW formation and ultimately the overturning circulation. In this case, NADW must be saltier than the northward return flow, and the AMOC transports freshwater into the Atlantic Basin. From this perspective, the AMOC is stable, as a slowing of the AMOC will lead to a reduction of the northward FWT, a salinification of the Atlantic, and an increase in NADW formation. However, observations suggest that NADW is fresher than the surface return flow of salty subtropical water, indicating that the circulation of NADW transports freshwater out of the Atlantic Basin [*Weijer et al.*, 1999; *Talley*, 2008]. Furthermore, separating the ocean FWT into portions due to the overturning and gyre circulations indicates that the overturning circulation transports freshwater southward at most latitudes in the Atlantic, including at 30°S [*Rahmstorf*, 1996; *Weijer et al.*, 1999; *de Vries and Weber*, 2005; *Drijfhout et al.*, 2011; *Valdivieso et al.*, 2014]. From this perspective, the AMOC is potentially unstable, as a reduction of the AMOC leads to a reduction in salinity in the North Atlantic and further reductions in NADW formation (see section 2.5 for a discussion on the potential instability of the AMOC under climate change). The combination of a net surface freshwater loss over the Atlantic Basin and a southward freshwater export by the AMOC requires that the South Atlantic subtropical gyre carries a large amount of freshwater northward into the basin to satisfy the freshwater budget.

In summary, the atmosphere transports freshwater out of the Atlantic Basin, and thus, the ocean circulation must transport freshwater into the Atlantic. However, recent work suggests that while the gyre circulation is responsible for transporting freshwater into the basin to satisfy the freshwater budget, the overturning circulation transports freshwater out of the Atlantic Basin. Hence, the AMOC is potentially unstable since a reduction in its strength is expected to decrease the salinity of the North Atlantic and potentially further decrease NADW formation. However, such arguments assume that the gyre circulation does not adjust to changes in the AMOC, an assumption that is questionable given that the mean gyre circulation currently transports freshwater into the Atlantic Basin, compensating for the freshwater export by the atmosphere and the AMOC.

3.4. Dynamical Decomposition of the AMOC

The AMOC can be decomposed into Ekman and thermal wind/geostrophic components by separating the meridional velocity; thus, $v = v_g + v_{ek}$ [*Lee and Marotzke*, 1998; *Hirschi and Marotzke*, 2007]. The Ekman component is related to the wind stress, and the thermal wind component is related to buoyancy anomalies on the ocean boundaries. In more detail, v_g can be calculated from the buoyancy field b using the vertically integrated thermal wind relation:

$$v_g(z) = \frac{1}{f}\int_{-H}^{z} \frac{\partial b}{\partial x}\, \mathrm{d}z + v_b, \tag{7}$$

where f is the Coriolis parameter and v_b is the meridional bottom velocity. Assuming that the Ekman mass transport is uniformly distributed within an Ekman layer of thickness D_{ek} and zero below this layer, the Ekman velocity for $-D_{ek} \le z \le \eta$ is

$$v_{ek}(z) = -\frac{\tau^x}{\rho_o f D_{ek}}, \tag{8}$$

where τ_x is the zonal wind stress. The mass conservation constraint can be used to solve for the zonal average bottom velocity $\bar{v}_b$. We find

$$\bar{v}_b = -\frac{1}{A}\int_{-H}^{\eta} \frac{1}{f}\int_{-H}^{z} (b(x_e) - b(x_w))\, \mathrm{d}z\, \mathrm{d}z + \frac{1}{A}\int_{x_w}^{x_e} \frac{\tau^x}{\rho_o f}\, \mathrm{d}x,$$

where $A = \int_{-H}^{\eta}\int_{x_w}^{x_e} dx\, dz$ is the area of the longitude-depth section. A stream function can then be computed by integrating v zonally and vertically (see equation (1)):

$$\tilde{\Psi}(z) = \underbrace{\int_z^{\eta} \frac{1}{f}\int_{-H}^{z} (b(x_e) - b(x_w))\, dz\, dz}_{\Psi_{tw}(z)} + \underbrace{\int_z^{\eta}\int_{x_w}^{x_e} v_{ek}\, dx\, dz}_{\Psi_{ek}(z)} + \underbrace{A(z)\,\overline{v}_b}_{\Psi_{ext}(z)}, \quad (9)$$

where $A(z) = \int_z^{\eta}\int_{x_w}^{x_e} dx\, dz$. The stream function is thus separated into (1) the thermal wind component Ψ_{tw} which is related to buoyancy anomalies on the ocean boundaries, (2) the Ekman component Ψ_{ek} which is related to the zonal wind stress integrated over the basin, and (3) the external mode Ψ_{ext} which is related to bottom flows impinging over nonuniform topography.

Such a decomposition helps shed light on the origin of AMOC variability because each term has a different physical origin and is important on different timescales. For example, the Ekman component plays a substantial role on short timescales, whereas the geostrophic component dominates on longer (interannual to decadal) timescales. Moreover, the ability to estimate the strength of the AMOC from buoyancy anomalies on the ocean boundaries and the zonal wind stress is the basis of historical AMOC estimates from hydrographic sections and the AMOC and OHT estimates at 26.5°N from the RAPID and Meridional Overturning and Heatflux Array (MOCHA) programs, as will be outlined in section 4.1.2. Before proceeding, we stress that equation (9) indicates that we should have a keen interest in the buoyancy anomalies on meridional boundaries.

4. The AMOC in Observations, State Estimates, and Models

Here we review attempts that have been made to estimate the AMOC and Atlantic OHT (i) directly from observations at chosen lines across the Atlantic (ii) by constraining ocean models with observations and (iii) from ocean models and coupled climate models. The former yield "direct" estimates but at very few latitudes. The model-based estimates yield more complete description in space and time but are compromised by model imperfections.

4.1. Direct Inferences From Observations

4.1.1. Estimates From Hydrographic Sections and Inverse Methods

Early observational estimates of the AMOC and Atlantic OHT utilize trans-Atlantic hydrographic sections at a few selected latitudes, primarily 24.5°N, 36°N, and 48°N [*Bryan*, 1962; *Bryden and Hall*, 1980; *Hall and Bryden*, 1982; *Talley*, 1999, 2003; *Talley et al.*, 2003; *McDonagh et al.*, 2010; *Atkinson et al.*, 2012]. Despite sparser sampling in the South Atlantic, several studies have estimated the AMOC and OHT (see review by *Garzoli and Matano*, 2011 [2011]), primarily at 24°S [*Bryden et al.*, 2011] and 34°S [*Baringer and Garzoli*, 2007; *Garzoli and Baringer*, 2007; *Dong et al.*, 2009; *Garzoli et al.*, 2013; *Dong et al.*, 2014]. These studies focus on the mean strength of the AMOC and Atlantic OHT and assume that both quantities are stable so that snapshots are representative of climatological values. Geostrophic transports are computed from hydrography and Ekman transports from observations of zonal wind stress. As large mass and heat transports occur in narrow western boundary currents (see Figures 1 and 4), which are difficult to resolve using hydrographic sections, boundary current transports are often estimated separately. For example, the Gulf Stream transport through Florida Straits has been continuously monitored via a submarine cable since 1982 [*Shoosmith et al.*, 2005; *Meinen et al.*, 2010]. Since only the geostrophic shear can be estimated from hydrography, the barotropic flow must be determined using a constraint. One common approach is to use mass conservation to solve for the barotropic flow [*Bryan*, 1962; *Bryden and Hall*, 1980; *Hall and Bryden*, 1982; *Talley*, 1999, 2003; *Talley et al.*, 2003]; another is to use inverse methods [*Ganachaud and Wunsch*, 2000; *Lumpkin and Speer*, 2003; *McDonagh and King*, 2005; *Lumpkin and Speer*, 2007; *McDonagh et al.*, 2010].

Ganachaud and Wunsch [2000] utilize hydrographic sections, transports of boundary currents, and Ekman transports estimated from satellite wind observations to estimate transports across several sections in each ocean basin (Figure 2b). In the Atlantic, the solution yields 16±2 Sv across 24°N and 14±2 Sv across the slanted 43°–48°N section. *Lumpkin and Speer* [2003, 2007] extend the inverse solution of *Ganachaud and Wunsch* [2000] by including air-sea flux estimates to constrain deep water formation rates. They find transports of 17.2±1.8 Sv across 24°N and 13.8±2.1 Sv across 43°N (Figure 2a), similar to estimates obtained by *Ganachaud and Wunsch* [2000]. Direct hydrographic methods and inverse box models indicate a peak Atlantic OHT of 1–1.5 PW at about 20°N; various historical estimates of the mean Atlantic OHT are shown in Figure 3b.

Several studies have utilized repeat hydrographic sections to estimate the variability of the AMOC and Atlantic OHT. *Roemmich and Wunsch* [1985] use a hierarchy of geostrophic models to estimate the AMOC and OHT at 24.5°N and 36.25°N from hydrographic sections taken in 1957 and 1981. They conclude that both the AMOC and OHT are very similar for the two years, but the deep southward flows exhibit a significant shift toward greater depths in the 1981 sections. On the other hand, *Bryden et al.* [2005] note a 30% decline in the AMOC based on repeat trans-Atlantic sections at 26.5°N (1957, 1981, 1992, 1998, and 2004). However, the decline is strongly dependent on a single AMOC estimate in 1957, and the observations are thought to be aliased by higher-frequency (including seasonal) variability [*Kanzow et al.*, 2010]. A subsequent attempt to estimate the variability of the AMOC at 26.5°N from boundary dynamic height observations (as well as Florida Current and Ekman transports) finds significant annual/intra-annual variability (~10 Sv) but no statistically significant trends over the period 1980–2005 [*Longworth et al.*, 2011]. Inverse calculations utilizing repeat sections at 48°N show no evidence for significant AMOC changes during the 1990s [*Lumpkin et al.*, 2008]. Direct observations of western boundary currents at 43°N and 53°N (1999–2010) show significant intra-annual variability, but much smaller decadal variability and no significant trends [*Schott et al.*, 2004, 2006; *Fischer et al.*, 2010; *Xu et al.*, 2013].

Argo data and satellite altimetry have also been used to infer AMOC and Atlantic OHT variability. If a single vertical mode (e.g., the first baroclinic mode) dominates, the geostrophic component of the AMOC theoretically can be estimated from sea surface height (SSH) alone [e.g., *Wunsch*, 2008]. However, this is not possible in practice because (1) higher-order vertical modes dominate at the boundary and (2) the resolution of satellite SSH observations may be insufficient to capture the rapid decrease of SSH near the western boundary [*Hirschi et al.*, 2009; *Kanzow et al.*, 2009; *Szuts et al.*, 2102]. Combining satellite SSH data with Argo observations allows estimation of the AMOC at latitudes where the continental slope is steep [*Willis*, 2010]; in regions with shallow continental slopes, the AMOC cannot be estimated accurately due to the lack of Argo data in regions shallower than 2000 m. *Willis* [2010] and *Hobbs and Willis* [2012] utilize satellite altimetry and Argo profiles and drift velocities (2002–2009) to estimate a mean strength of AMOC at 41°N of 15.5 ± 2.4 Sv and a mean Atlantic OHT of 0.50 ± 0.1 PW (see Figure 3b); they conclude that there is no significant trend in the AMOC or OHT strength at this latitude between 2002 and 2009. Furthermore, *Hobbs and Willis* [2012] demonstrate that the majority of intra-annual-to-interannual OHT variability is due to overturning cells forced by Ekman transport variability. *Hernández-Guerra et al.* [2010] utilize ocean observations (Florida Strait transports and Argo profiles/drift velocities) and an inverse calculation to estimate the strength of the AMOC at 24°N and 36°N over the period 2003–2007. Comparison to previous AMOC estimates from hydrographic surveys suggests that within the error bars of the estimation, the upper limb of the AMOC is unlikely to have changed significantly since 1957.

4.1.2. AMOC Observing Arrays

The RAPID-MOCHA array is designed to provide a continuous estimate of the strength of the AMOC and Atlantic OHT at 26.5°N. The array is based on the dynamic method, which relates buoyancy on the boundaries of a zonal transect to meridional transports (relative to a reference level) [*Lee and Marotzke*, 1998; *Hirschi et al.*, 2003; *Baehr et al.*, 2004; *Marotzke and Scott*, 1999]. Mooring arrays that measure temperature and salinity are located on eastern and western boundaries of the basin and on either side of the Mid-Atlantic Ridge (see Figure 4). Additionally, moorings near the western boundary are equipped with current meters and upward looking acoustic Doppler current profilers (ADCPs) to directly measure strong western boundary currents.

The RAPID-MOCHA array moorings, combined with Florida Current cable transports [*Shoosmith et al.*, 2005; *Meinen et al.*, 2010] and scatterometer winds, have enabled the AMOC strength to be measured at 26.5°N since March 2004 [*Cunningham et al.*, 2007; *Kanzow et al.*, 2010; *Johns et al.*, 2011]. The AMOC estimate is accomplished by adapting equation (9) for the specific geometry of 26.5°N and the observational methods employed by the RAPID program:

$$\tilde{\Psi}(z) = \underbrace{\int_z^{\eta} T_{gs}\phi(z)\,\mathrm{d}z}_{\Psi_{gs}(z)} + \underbrace{\int_{x_{iw}}^{x_{mw}}\int_z^{\eta} v\,\mathrm{d}z}_{\Psi_{wbw}(z)} + \underbrace{\int_z^{\eta}\frac{1}{f}\int_{z_{ref}}^{z}(b(x_e)-b(x_{mw}))\,\mathrm{d}z\,\mathrm{d}z}_{\Psi_{tw}(z)} + \underbrace{\int_{x_{iw}}^{x_e}\int_z^{\eta} v_{ek}\,\mathrm{d}z\,\mathrm{d}x}_{\Psi_{ek}(z)} + \underbrace{A(z)\,\overline{v}_b}_{\Psi_{ext}(z)}. \tag{10}$$

Specifically, two new terms are introduced: Ψ_{gs} and Ψ_{wbw}. The term Ψ_{gs} reflects the fact that at 26.5°N the majority of the Gulf Stream transport is restricted to the Florida Straits (between the Florida coast, x_w,

and Abaco, x_{iw}), which has been monitored by a submarine cable and repeat ship sections since 1982 [*Meinen et al.*, 2010]. The transport in each layer is calculated by projecting the measured transport T_{gs} on the first baroclinic mode $\phi(z)$ and the transport is integrated with depth to obtain Ψ_{gs} [*Kanzow et al.*, 2010]. The contribution Ψ_{wbw} reflects the fact that the transport in the western boundary wedge (WBW) between x_{iw} and mooring WB2 (x_{mw}) is measured using current meters and ADCPs [*Johns et al.*, 2008].

The thermal wind component relative to a deep reference level $z_{ref} = -4740$ m, Ψ_{tw}, is estimated from moorings that record temperature and salinity at discrete depths near the eastern and western boundaries of the basin and on both sides of the Mid-Atlantic Ridge. For simplicity we have not explicitly represented the contributions on each side of the Mid-Atlantic Ridge (below 3700 db); more details on these contributions, which mainly affect the deep structure of the mean AMOC, are described in *McCarthy et al.* [2015]. Several different wind products have been used to calculate the Ekman component, Ψ_{ek}, including Quick Scatterometer measurements (available through November 2009) [*Schlax et al.*, 2001], CCMP level 3.0 [*Atlas et al.*, 2011], and ERA-Interim [*Dee et al.*, 2011]. Current RAPID releases use ERA-Interim winds, as they are available for the entire time period without delay, but calculations are not found to be very sensitive to the wind product used [*McCarthy et al.*, 2015]. The Ekman transport is assumed to be evenly distributed between the surface and 100 m depth. A compensating transport, which is assumed to be spatially uniform in the horizontal and zonal direction, is calculated by assuming mass conservation at each 10 day time step, an approximation shown to be valid for timescales 10 days and longer [*Kanzow et al.*, 2007]. Integrating this compensating transport vertically and zonally yields Ψ_{ext}.

The strength of the AMOC and each of its components is defined as the maximum of the stream function over the water column (see equation (2); at 26.5°N $z_{max} \approx 1100$ m):

$$\underbrace{\bar{\Psi}(z_{max})}_{\text{AMOC}} = \underbrace{\Psi_{gs}(z_{max})}_{\text{Gulf Stream}} + \underbrace{\Psi_{wbw}(z_{max}) + \Psi_{tw}(z_{max}) + \Psi_{ext}(z_{max})}_{\text{Upper Mid-Ocean}} + \underbrace{\Psi_{ek}(z_{max})}_{\text{Ekman}}. \tag{11}$$

Here the various contributions have been lumped together and labeled according to the conventions of the RAPID program. It is worth noting that this decomposition is not unique; choices have been made, including that of a reference level of $z_{ref} = -4740$ m and the incorporation of the mass conservation term in the Upper Mid-Ocean transport. In fact, some analyses assume that the Ekman transport is returned barotropically and thus include a portion of Ψ_{ext} in the Ekman rather than Upper Mid-Ocean term [*Baehr et al.*, 2004; *Blaker et al.*, 2015]. Including a barotropic return flow in the Ekman term appears justified on short timescales [*Jayne and Marotzke*, 2001], but on longer timescales, the Ekman transport is returned baroclinically (e.g., subtropical overturning cells) [see *Elipot et al.*, 2014].

The observed strength of the AMOC at 26.5°N and its various components are shown in Figure 8. The mean AMOC is 17.2 Sv, and its strength varies substantially, with a 10 day filtered root-mean-square variability of 4.6 Sv [*McCarthy et al.*, 2015]. The nature of AMOC variability depends strongly on timescale. It exhibits large intra-annual and seasonal variability [*Rayner et al.*, 2011], suggesting that estimates based on synoptic hydrographic surveys separated by many years may suffer from severe aliasing of the fast components, compromising our ability to detect long-term trends in such observations [see also *Baehr et al.*, 2007; *Baehr*, 2011]. In contrast, interannual AMOC variability is much smaller; from April 2004 to March 2009, annual mean AMOC anomalies have a standard deviation of only 1 Sv [*McCarthy et al.*, 2012]. However, between April 2009 and May 2010, the annual mean AMOC declined by 30% due to both a reduction in the Ekman transport and a strengthening of the southward geostrophic flow in the upper 1100 m, resulting from a deepening of the thermocline on the western boundary [*McCarthy et al.*, 2012]. The changes in the geostrophic flow appear to be driven by local and remote atmospheric forcing [*Hirschi et al.*, 2013; *Roberts et al.*, 2013b; *Zhao and Johns*, 2014]. However, AMOC trends are quite small, especially compared to the large seasonal and intra-annual variability. For example, *Smeed et al.* [2014] estimate that the AMOC strength decreased by 0.54 ± 0.45 Sv over the period 2004–2012, a trend which is not significantly different from that expected due to internal AMOC variability [*Roberts et al.*, 2014].

The separation of the AMOC into its (observationally estimated) components is also insightful for understanding mechanisms of AMOC variability. On timescales longer than about 10 days, there is a large compensation between various components [*Kanzow et al.*, 2007]. Just as the mean strength of the AMOC is set by the

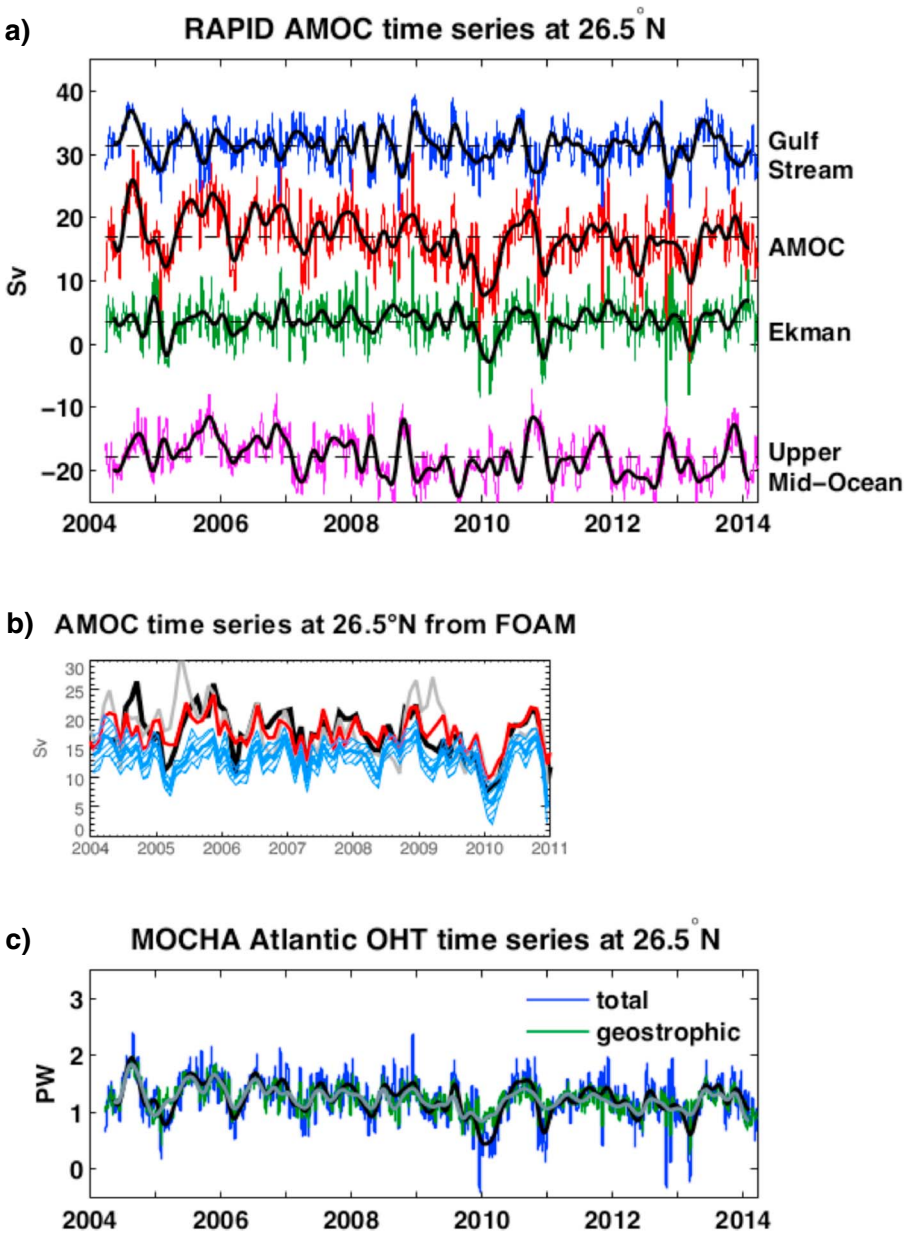

Figure 8. (a) Estimate of the AMOC and its components (as defined in equation (11)) at 26.5°N from the RAPID-MOCHA array for the period April 2004 to March 2014. Ten day (colors) and 3 month low-pass (black) time series of AMOC (red), Gulf Stream transport (blue), Ekman transport (green), and Upper Mid-Ocean transport (magenta). Horizontal dashed black lines are time series means. Positive transports correspond to northward flow. Time series were downloaded from the RAPID website and plotted as in *McCarthy et al.* [2012]. (b) Monthly mean AMOC time series at 26.5°N from the FOAM ocean forecasting model (red and grey lines show two different assimilation techniques) is compared to the RAPID AMOC time series (black). When the model is driven by atmospheric forcing alone (no data assimilation, blue lines with hatching covering ±2 standard deviations of the ensemble members), it is able to reproduce much of the time variability of the AMOC, including the 2009–2010 event. Transports are defined as the value of the overturning stream function at a depth of 1050 m [from *Roberts et al.*, 2013b]. (c) Atlantic OHT time series from the RAPID-MOCHA array for the period April 2004 to March 2014. Blue (heavy black) lines show the 10 day (3 month low-pass-filtered) time series of the total OHT. Green (heavy grey) lines show the 10 day (3 month low-pass-filtered) time series of the geostrophic OHT, obtained by setting Q_{ek} constant in equation (12). Time series was provided by Bill Johns, extending the calculation presented in *Johns et al.* [2011].

partial compensation between northward transport in the Gulf Stream and Ekman layer and southward transport in the geostrophic interior, the sum of the Ekman and Gulf Stream transports is highly anticorrelated with the Upper Mid-Ocean transport. The Ekman component is dominated by high-frequency variability. The Upper Mid-Ocean and Gulf Stream transports are responsible for the low-frequency variability, and at low frequencies these terms are strongly anticorrelated.

The portion of AMOC variability due to changes in the geostrophic circulation (Ψ_g) can be quantified by removing the time-variable Ekman transport (replacing v_{ek} with its mean value in equation (10)) [see *Johns et al.*, 2011]. Removing Ekman transport variability significantly reduces high-frequency variability, while low-frequency variability of Ψ_g is very similar to that of Ψ. The contribution of the western boundary to Ψ_g, henceforth referred to as Ψ_{gw}, can be isolated by replacing b_e with its time-mean; similarly, the contribution of the eastern boundary to Ψ_g, henceforth called Ψ_{ge}, can be isolated by replacing b_w, Ψ_{gs}, and Ψ_{wbw} with their time-means. *Bryden et al.* [2009] and *Elipot et al.* [2014] find that the variance of Ψ_{gw} is significantly larger than that of Ψ_{ge}, although the eastern boundary contribution plays a dominant role in the seasonal cycle of AMOC variability [*Chidichimo et al.*, 2010; *Kanzow et al.*, 2010]. The importance of buoyancy anomalies on the western boundary is fundamental for understanding mechanisms of low-frequency AMOC variability, as will be developed in section 5.

The RAPID-MOCHA array has also been utilized to estimate the Atlantic OHT at 26.5°N [*Johns et al.*, 2011; *McCarthy et al.*, 2015] (see Figure 8c). The temperature transport of each of the components is estimated from the mass transport and temperature, and then each of these terms are combined to estimate the Atlantic OHT as

$$Q = \underbrace{\rho_o\, C_p\, T_{gs}\, \theta_{FW}}_{Q_{GS}} + \underbrace{\rho_o\, C_p \int_{x_{iw}}^{x_{mw}} \int_{z}^{\eta} v\, \theta \, dz\, dx}_{Q_{WBW}} + \underbrace{\frac{C_p}{f} \int_{x_{iw}}^{x_e} \tau_x\, \theta_{Ek}\, dx}_{Q_{Ek}} + \underbrace{\rho_o\, C_p \int_{x_{mw}}^{x_e} \int_{z}^{\eta} [v_g]\, [\theta(z)]\, dz\, dx}_{Q_{MO}} + \underbrace{\rho_o\, C_p \int_{z}^{\eta} \int_{x_{mw}}^{x_e} v_g'\, \theta(z)'\, dz\, dx}_{Q_{eddy}}, \quad (12)$$

where θ_{FW} is a seasonal climatology of the flow-weighted temperature and θ_{Ek} is a weighted average of θ over the top 50 m derived from Argo. Square brackets are zonal means, and primes are deviations from zonal means. The temperature transports in the Gulf Stream (Q_{GS}), the western boundary wedge (Q_{WBW}), Ekman layer (Q_{Ek}), and Upper Mid-Ocean (Q_{MO}), as well as an estimate of the eddy transport (Q_{eddy}) from hydrographic sections, are combined to estimate the total Atlantic OHT (Q). Temperatures in the basin interior used to calculate Q_{MO} and Q_{eddy} are derived from an objective analysis with weekly resolution of available Argo profiles and temperature and salinity profiles from the RAPID moorings, merged with a seasonal temperature climatology below 2000 m based on the RAPID Hydrobase product [*Johns et al.*, 2011]. (In *Johns et al.* [2011], θ_{Ek} is instead set to SST from *Reynolds and Smith* [1994], and estimates of Q_{MO} and Q_{eddy} use seasonal climatologies of θ.)

The mean Atlantic OHT at 26.5°N for 2004–2014 is 1.25 ± 0.11 PW (Figure 3b). Variability of the heat transport is large, with a standard deviation (for 10 day low-pass-filtered data) of 0.36 PW (Figure 8c) [*McCarthy et al.*, 2015]. About half of this variability can be directly attributed to Ekman transport changes; the remainder is due to geostrophic circulation changes (quantified by replacing τ_x with its mean value in equation (12)) [see *Johns et al.*, 2011] (Figure 8c). The meridional heat transport is highly correlated with changes in the strength of the meridional overturning circulation (as can be seen by inspection of Figure 8), and AMOC variability explains over 90% of the estimated Atlantic OHT variability at this latitude [*Johns et al.*, 2011].

Recent work has attempted to extend the RAPID time series back in time by developing proxies for the Upper Mid-Ocean transport derived from RAPID mooring observations. *Duchez et al.* [2014] hypothesize that the Upper Mid-Ocean geostrophic transport is wind driven and can be approximated by the geostrophic Sverdrup transport at interannual and longer timescales. They use numerical simulations to verify that the AMOC calculated using this approximation captures a substantial portion of the AMOC variability on interannual and decadal timescales. *Frajka-Williams* [2015] uses the RAPID array observations to develop a regression model relating interannual anomalies of the Upper Mid-Ocean transport to sea surface height (SSH) in the western basin. She shows that the regression can explain 80% of the Upper Mid-Ocean transport variability at 26.5°N,

and when combined with the Florida Current and Ekman transport observations, it can recover 90% of the interannual AMOC variability at 26.5°N. She then applies the regression model to estimate interannual AMOC anomalies over the satellite era (1993–2012) and finds that the AMOC does not exhibit any statistically significant trends over this period.

In addition to the RAPID array, several contemporaneous mooring arrays in the western basin have been used to monitor the DWBC, including 53°N near the exit of the Labrador Sea [*Fischer et al.*, 2010], Line W off the coast of New England [*Toole et al.*, 2011; *Fischer et al.*, 2013], and the Meridional Overturning Variability Experiment (MOVE) array at 16°N [*Kanzow et al.*, 2006; *Send et al.*, 2011]. Results from the MOVE array indicate that over the period January 2000 to June 2009, either (1) the southward transport in the NADW layer decreased by 20% or (2) the level of no motion (boundary between northward and southward flowing layers) deepened by 100 m. The authors argue that these changes may be associated with natural multidecadal fluctuations of the AMOC.

An array, which uses techniques similar to those employed at 26.5°N by the RAPID array, recently has been deployed in the South Atlantic at 34.5°S [*Meinen et al.*, 2013; *Ansorge et al.*, 2014]. Preliminary results from the South Atlantic MOC Basin-wide Array (SAMBA), indicate that the AMOC in the South Atlantic exhibits significant high-frequency variability. From March 2009 to December 2010 the 10 day low-pass-filtered AMOC varies between 3 and 39 Sv. As seen at 26.5°N, Ekman transport variability primarily contributes at high frequencies, while geostrophic transports dominate at lower frequencies. Unlike in the North Atlantic, buoyancy anomalies on the eastern and western margins contribute approximately equally to AMOC variability on all timescales observed by the array [*Meinen et al.*, 2013].

Recent work has focused on an alternative method of estimating the AMOC using ocean bottom pressure measurements from bottom pressure recorders and Gravity Recovery and Climate Experiment (GRACE) satellites. While sensor drifts in ocean bottom pressure recorders remain a problem for long-term AMOC estimates, *Elipot et al.* [2014] show that ocean bottom pressure gradients can capture a significant portion of geostrophic AMOC variability (at both 26°N and 41°N) on the western boundary on semiannual and longer timescales. *Landerer et al.* [2015] use GRACE bottom pressure measurements to estimate the AMOC at 26.5°N; they show that the correlation of their estimate with the RAPID AMOC estimate is relatively high on interannual timescales, although the correlation is mainly due to the ability of the GRACE measurements to capture the large 2009–2010 AMOC anomaly.

4.2. Model-Based AMOC and Atlantic OHT Estimates

Here we discuss estimates of the mean AMOC and its historical variability using ocean hindcasts, ocean state estimates, and coupled models. These model-based estimates yield a complete description of the AMOC in space and time but are compromised by model imperfections, including the representation of small-scale ocean eddies, convection, overflows, mixing, and the complex geometry of the Atlantic Ocean basin. Ocean hindcasts are ocean models forced with observational estimates of atmospheric forcing, typically from atmospheric reanalyses. In state estimation, assimilation of ocean observations is used to constrain ocean models that are forced by atmospheric fields from reanalyses (ocean state estimation) or coupled to an assimilative atmospheric model (coupled state estimation). Both ocean hindcasts and state estimates may suffer from errors in atmospheric forcing and ocean initialization. Coupled models provide long time series of the AMOC and attempt to capture coupled feedbacks in the climate system, but they are only constrained by observed (or projected) external forcing and may have large mean state biases.

Models tend to have difficulty in representing the mean AMOC; the strength and the depth of the AMOC appear to be sensitive to model details, such as resolution, overflow parameterizations, and mesoscale eddy fluxes. For example, the maximum of the mean AMOC in CMIP5 models occurs at latitudes between 20° and 60°N and ranges in strength between 13 and 31 Sv [*Zhang and Wang*, 2013; *Kostov et al.*, 2014]. A similar diversity in the mean strength of the AMOC is seen in ocean hindcasts, even when forced by the same atmospheric forcing. For example, in ocean models forced by the second phase of the Coordinated Ocean-ice Reference Experiments (CORE II) [*Large and Yeager*, 2009] the maximum AMOC ranges from 8 to 28 Sv, and the peak Atlantic OHT ranges from 0.4 to 1.1 PW [*Danabasoglu et al.*, 2014]. Although including observational constraints can potentially enhance agreement between models and improve agreement with observations, the mean AMOC and Atlantic OHT varies between state estimates and many state estimates are inconsistent with direct AMOC and OHT observations [*Munoz et al.*, 2011; *Karspeck et al.*, 2015]. For example, state estimates produced by the Estimating the Circulation and Climate of the Ocean (ECCO) project [*Wunsch et al.*, 2007, 2009; *Wunsch and Heimbach*, 2013a] and the Geophysical Fluid Dynamics Laboratory (GFDL) ensemble

coupled data assimilation (ECDA) [*Chang et al.*, 2012] underestimate the AMOC at 26°N compared to RAPID observations and underestimate the peak Atlantic OHT compared to direct ocean estimates (see Figure 3b). This is likely due to spurious mixing in overflow regions that leads to a weaker DWBC and overturning cell [*Forget et al.*, 2008a, 2008b]. These results suggest that current ocean observations do not provide sufficient constraints to correct model errors, particularly in the deep ocean [see also *Zhang and Rosati*, 2010].

Models exhibit AMOC variability on a wide range of timescales, with large variability on intra-annual and seasonal timescales (order 100% of its mean value) and much smaller variability on interannual to decadal timescales (order a few Sverdrups). Atlantic OHT variability is closely related to AMOC variability in the tropics/subtropics [*Jayne and Marotzke*, 2001; *Wunsch and Heimbach*, 2006], while in the subpolar gyre OHT variations do not follow AMOC variations closely, as gyre circulation variations and temperature anomalies advected by the mean current also play prominent roles [*Dong and Sutton*, 2002; *Piecuch and Ponte*, 2012; *Kwon and Frankignoul*, 2014].

Both ocean hindcasts and ocean state estimates are generally able to reproduce much of the large intra-annual AMOC variability observed by the RAPID array at 26.5°N (see Figure 8b) [*Hirschi et al.*, 2013; *Roberts et al.*, 2013b; *Blaker et al.*, 2015]. Much of this ability seems to come from specifying the atmospheric forcing alone. For example, *Roberts et al.* [2013b] find that 70–80% of monthly AMOC variability observed by the RAPID array can be reproduced if ocean models are driven by observed winds (see Figure 8b). The largest part of the response is through Ekman transports driven directly by the wind and Upper Mid-Ocean anomalies associated with wind-induced heaving of isopycnals. These results do not require data assimilative models but rather reflect the importance of the short timescale response of the upper ocean and its stratification to wind changes. One important result of these studies is that the dramatic AMOC anomaly seen in the RAPID observations during 2009/2010 (sudden weakening followed by a rebound) can be captured in ensemble simulations without data assimilation. This suggests that the "event" was connected to local wind effects and thus is unlikely to have a dramatic impact over remote regions. Nevertheless, some investigators have implicated the drop in the AMOC during 2009/2010 as a precursor to the subsequent severe winter over western Europe [*Maidens et al.*, 2013; *Cunningham et al.*, 2013; *Bryden et al.*, 2014], as will be discussed in section 6.2.

Modeling historical AMOC changes on longer (interannual to decadal) timescales remains challenging since observations to validate AMOC estimates are lacking and remote (in space and time) forcings become increasingly important. In general, ocean hindcast experiments forced with various atmospheric data products show increasing trends in the North Atlantic MOC in the 1980s to the mid-1990s and decreasing trends thereafter [e.g., *Häkkinen*, 1999; *Beismann and Barnier*, 2004; *Bentsen et al.*, 2004; *Böning et al.*, 2006; *Deshayes and Frankignoul*, 2008; *Robson et al.*, 2012; *Danabasoglu et al.*, 2016]. These trends are thought to be related to changes in the NAO [*Eden and Willebrand*, 2001; *Bentsen et al.*, 2004; *Böning et al.*, 2006; *Deshayes and Frankignoul*, 2008; *Lohmann et al.*, 2009; *Robson et al.*, 2012]. However, the magnitude, timing, and latitude-depth patterns of AMOC changes differ substantially between models [*Danabasoglu et al.*, 2016]. While one might expect the inclusion of ocean observations to lead to greater agreement between AMOC estimates, AMOC and Atlantic OHT trends found in state estimates depend on both the period of analysis and the specific ocean model and assimilation technique. For example, *Wunsch and Heimbach* [2006, 2009] find no significant trends in the AMOC or Atlantic OHT in ECCO state estimates (which begin in 1992), and the AMOC appears statistically stable with fluctuations indistinguishable from those of a stationary Gaussian stochastic process [*Wunsch and Heimbach*, 2013b]. More significant AMOC trends are found in longer state estimates, but even the sign of the trend differs between estimates [*Tett et al.*, 2014; *Karspeck et al.*, 2015]. For example, at 26.5°N German ECCO (GECCO) [*Kohl and Stammer*, 2008; *Wang et al.*, 2010] and Simple Ocean Data Assimilation (SODA) [*Carton and Santorelli*, 2008; *Tett et al.*, 2014] exhibit increasing trends since 1960; the European Centre for Medium-Range Weather Forecasts operational ocean estimate (1959–2008) [*Balmaseda et al.*, 2007] shows decreasing trends since 1960; and National Center for Environmental Prediction (NCEP) ocean reanalysis produces an increase in the AMOC from 1980 to 1995 followed by a reduction from 1995 to 2008 [*Huang et al.*, 2012]. Furthermore, *Karspeck et al.* [2015] suggest that AMOC trends from ocean state estimates are less consistent with each other than those from corresponding nonassimilative ocean hindcasts, indicating that AMOC estimates are sensitive to assimilation techniques [see also *Balmaseda et al.*, 2013]. These results suggest that (1) AMOC trends over the last 50 years are likely weak and (2) current ocean observations do not provide sufficient constraints on models [see *Forget and Wunsch*, 2007] to enable ocean state estimates to realistically reproduce these small trends. Model improvements, additional observations, and improved assimilation techniques are thus necessary in order to improve estimates of the AMOC and its variability.

Coupled models have been primarily utilized to quantify the mean AMOC and its response to external forcing (e.g., anthropogenic forcing; see section 2.5). However, coupled modeling studies have also focused on establishing "fingerprints" of the AMOC, which may be used to estimate the AMOC strength from better observed quantities in the absence of direct AMOC observations. Potential fingerprints of the AMOC include sea level from altimetry [*Häkkinen*, 2001; *Lorbacher et al.*, 2010; *Ivchenko et al.*, 2011] or tide gauges [*Bingham and Hughes*, 2009], SST [*Latif et al.*, 2004, 2006; *Dima and Lohmann*, 2010; *Rahmstorf et al.*, 2015], and ocean temperature anomalies [*Zhang*, 2008, 2010a; *Mahajan et al.*, 2011]. For example, *Zhang* [2008] show that a dipole of upper ocean temperature anomalies between the subpolar gyre and Gulf Stream path is a fingerprint of the AMOC in the GFDL coupled model, CM2.1. *Mahajan et al.* [2011] attempt to use this fingerprint to predict the AMOC from observations. The difficulty with such estimates is that they generally rely on models to diagnose patterns of SST, etc., that are related to the AMOC, and these patterns differ between models and may not represent AMOC signals in the real system.

4.3. Model Explorations of AMOC Mechanisms

Models have been utilized to explore AMOC variability on a wide range of timescales, and mechanisms of variability are found to depend strongly on timescale. The Ekman component plays a substantial role in AMOC and Atlantic OHT variability on short timescales [*Häkkinen*, 1999; *Sato and Rossby*, 2000; *Klinger and Marotzke*, 2000; *Jayne and Marotzke*, 2001; *Dong and Sutton*, 2001, 2003; *Hobbs and Willis*, 2012; *Xu et al.*, 2014], whereas the geostrophic component dominates on longer (interannual to decadal) timescales [*Hirschi et al.*, 2007; *Cabanes et al.*, 2008]. The AMOC is not coherent between the subtropical and subpolar gyres on interannual timescales [*Bingham et al.*, 2007; *Balan Sarojini et al.*, 2011]; within the subtropical gyre interannual AMOC variability is dominant, while in the subpolar latitudes decadal AMOC variability is stronger [*Balmaseda et al.*, 2007; *Wunsch*, 2013; *Wunsch and Heimbach*, 2013b], a fact that *Wunsch and Heimbach* [2013b] attribute to the increase of the baroclinic Rossby wave crossing timescale with latitude.

On decadal timescales models generally exhibit meridionally coherent modes of AMOC and Atlantic OHT variability (see Figure 9a) [*Delworth et al.*, 1993; *Delworth and Mann*, 2000; *Knight et al.*, 2005; *Danabasoglu*, 2008; *Msadek and Frankignoul*, 2009; *Danabasoglu et al.*, 2012]. However, the precise timescale at which the AMOC and Atlantic OHT are meridionally coherent is not known; gyre-specific AMOC changes may occur even on decadal timescales [*Lozier et al.*, 2010; *Fan and Schneider*, 2011; *Williams et al.*, 2014]. Meridionally coherent AMOC anomalies are thought to originate from subpolar regions [*Zhang*, 2010a; *Balan Sarojini et al.*, 2011] and reflect the response to time-variable buoyancy forcing [*Böning et al.*, 2006; *Biastoch et al.*, 2008a; *Robson et al.*, 2012; *Yeager and Danabasoglu*, 2014].

The processes important for setting the dominant timescales of low-frequency modes of AMOC variability are not well understood, and, in fact, dominant timescales vary markedly between models (e.g., CMIP5 models) [*Zhang and Wang*, 2013] and even between subsequent versions of models produced by a single modeling center. For example, the Community Climate System Model version 3 (CCSM3) exhibits strong multidecadal AMOC variability, but version 4 of the same model (CCSM4) exhibits a broad spectrum of AMOC variability with a considerably smaller amplitude [*Danabasoglu*, 2008; *Danabasoglu et al.*, 2012]. A number of idealized [*Marshall et al.*, 2001b; *te Raa and Dijkstra*, 2002; *Lee and Wang*, 2010] and GCM [*te Raa et al.*, 2004; *Hirschi et al.*, 2007; *Frankcombe and Dijkstra*, 2009; *Zanna et al.*, 2011, 2012; *Buckley et al.*, 2012] studies suggest that the dominant timescale of AMOC variability is related to the time it takes for baroclinic Rossby waves to propagate across the basin. Other studies suggest that dominant timescales are set by advective processes, such as the spin-up/spin-down of the gyre circulation [*Delworth et al.*, 1997; *Dong and Sutton*, 2005] or the accumulation of high-/low-density water in deep water formation regions [*Griffies and Tziperman*, 1995; *Dong and Sutton*, 2005; *Msadek and Frankignoul*, 2009].

There is currently no consensus on the mechanisms responsible for low-frequency AMOC variability. Part of the lack of consensus is related to a diverse range of (often statistical) techniques used to analyze models, which sometimes make it difficult to determine the similarities/differences between proposed mechanisms of AMOC variability. Perhaps a more fundamental issue is that AMOC variability in models may depend on highly uncertain parameterizations, leading to AMOC variability that is model dependent. Despite this, previous work on mechanisms of AMOC variability can be grouped into two broad categories: (1) changes in convection and water mass formation and (2) baroclinic Rossby waves.

A dominant paradigm is that decadal AMOC variability results from changes in convection/water mass formation. This paradigm is based on a variety of modeling studies that demonstrate the following:

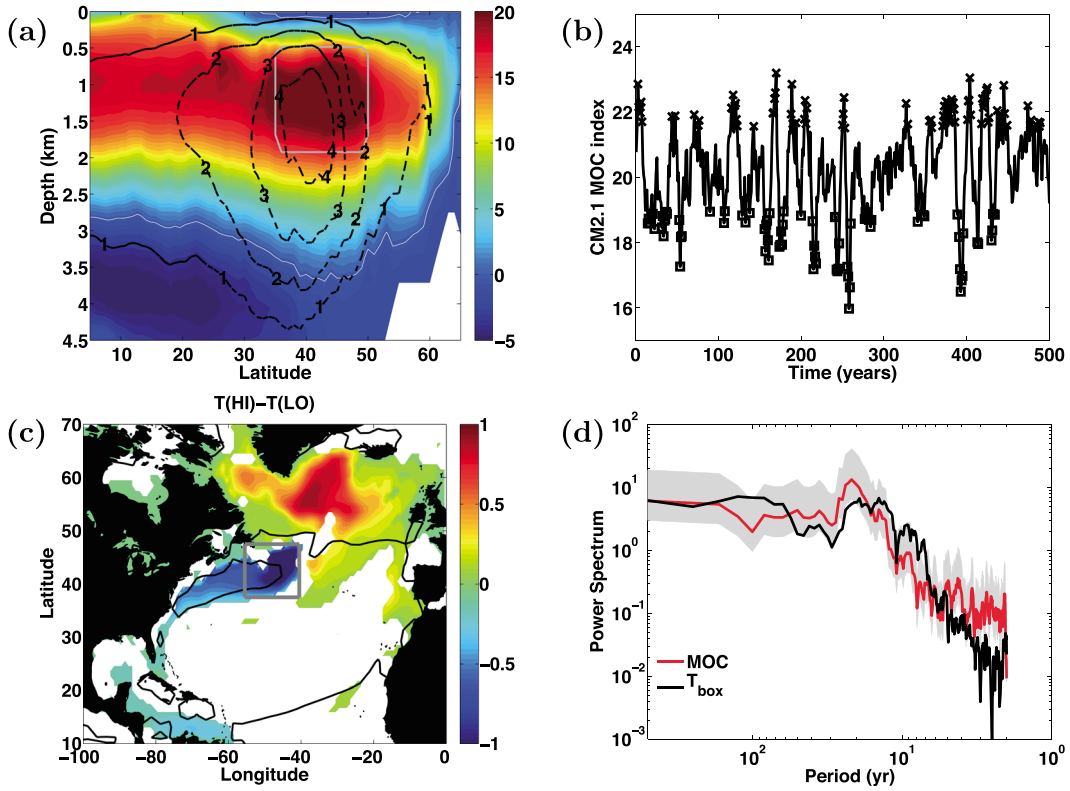

Figure 9. (a) Eulerian mean AMOC (Sv, colors) from the coupled climate model CM2.1 and AMOC anomaly (Sv, black contours) formed by (HI)-(LO) composites described in Figure 9b. (b) Time series of the AMOC index, defined as the average AMOC from 35°N to 50°N and from 500 to 1800 m depth, as indicated by the grey box in Figure 9a. Years marked by crosses (squares) denote years that are more than one standard deviation above (below) the time-mean. These are used to construct (HI)-(LO) composite maps, shown in Figures 9a and 9c. (c) Composite (HI)-(LO) map of temperature averaged over the top 1 km. White shading indicates regions that are not significant at the 95% confidence level. (d) Normalized power spectra of the AMOC index (red) and temperature (black) (K) averaged over the top 1 km in the gray box region (shown in Figure 9c). The gray shading is a 95% confidence interval. Figure provided by R. Tulloch (personal communication, 2013), modified from *Tulloch and Marshall* [2012].

1. Lagged correlations suggest that the AMOC responds to changes in subpolar regions. Correlations between the first principle component time series of North Atlantic subsurface temperature and the AMOC at various latitudes suggest that AMOC anomalies are communicated meridionally (Figure 10). *Zhang* [2010a] uses a visual impression of propagation to argue that buoyancy anomalies originate in the Labrador Sea and are then communicated southward into the subpolar and subtropical gyres. Additionally, lagged correlations between the AMOC and mixed layer depth anomalies/convective variability suggest that anomalies in regions of deep convection lead AMOC anomalies [*Delworth et al.*, 1993; *Dong and Sutton*, 2005; *Danabasoglu*, 2008; *Deshayes and Frankignoul*, 2008; *Frankignoul et al.*, 2009; *Msadek and Frankignoul*, 2009; *Kwon and Frankignoul*, 2012; *Danabasoglu et al.*, 2012; *Jackson and Vellinga*, 2012; *Medhaug et al.*, 2012; *Roberts et al.*, 2013a].
2. Ocean-only experiments suggest that decadal AMOC variability in the North Atlantic primarily results from buoyancy forcing over subpolar regions [*Böning et al.*, 2006; *Biastoch et al.*, 2008b; *Robson et al.*, 2012; *Yeager and Danabasoglu*, 2014]. In fact, some model experiments suggest that decadal AMOC variability can be explained by buoyancy forcing only over very localized regions [*Böning et al.*, 2006; *Biastoch et al.*, 2008b], such as the Labrador Sea [*Yeager and Danabasoglu*, 2014].
3. Large AMOC changes can be induced by a disruption in deep convection [e.g., *Zhang and Delworth*, 2005], as well as changes in overflow waters [e.g., *Zhang et al.*, 2011]. Water hosing experiments, in which large quantities of freshwater are added to the subpolar North Atlantic, show a disruption in deep convection and

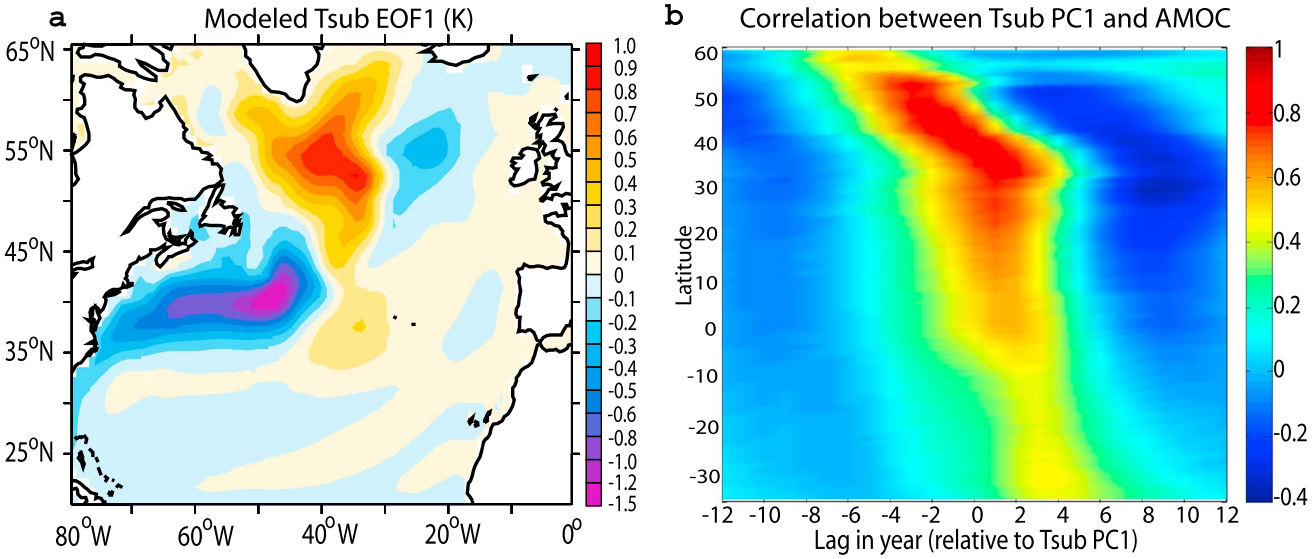

Figure 10. (a) First empirical orthogonal function (EOF1) of temperature at 400 m (T_{sub}) (K, 24.8% of variance) from a 1000 year control run of GFDL CM2.1 [from *Zhang*, 2008]. (b) Correlation between the first principle component (PC1) time series of T_{sub} and AMOC strength variations at all latitudes. The AMOC strength at each latitude is defined as the maximum of the annual mean zonally integrated Atlantic overturning stream function in density space [from *Zhang*, 2010a].

a strong reduction or collapse in the strength of the AMOC [e.g., *Zhang and Delworth*, 2005; *Stouffer et al.*, 2006; *Zhang*, 2007]. However, it is not clear to what extent these large perturbation experiments shed light on the relationship between deep convection and AMOC anomalies on decadal timescales.

Despite the significant number of studies linking AMOC variability to changes in convective regions, studies do not agree on the origin of convective variability. Proposed processes include variability of atmospheric forcing over convective regions [*Mignot and Frankignoul*, 2005; *Condron and Renfrew*, 2013; *Yeager and Danabasoglu*, 2014] and time-variable heat/freshwater transports into convective regions from the Arctic [*Delworth et al.*, 1997; *Jungclaus et al.*, 2005; *Frankcombe and Dijkstra*, 2011] or the subtropics [*Delworth et al.*, 1993; *Delworth and Greatbatch*, 2000; *Dong and Sutton*, 2005; *Häkkinen and Rhines*, 2009; *Msadek and Frankignoul*, 2009; *Häkkinen et al.*, 2011a; *Burkholder and Lozier*, 2011b; *Wouters et al.*, 2012]. Processes important in variations in convective regions may depend on highly uncertain parameterizations, leading to AMOC variability that is model dependent. For example, *Danabasoglu et al.* [2012] hypothesize that AMOC variability in CCSM4 results from buoyancy anomalies in the Labrador Sea and demonstrates that parameterized mesoscale eddy fluxes contribute substantially to the buoyancy budget in this region.

However, as outlined in *Lozier* [2010, 2012], the direct causal link between water mass formation and the AMOC is now being questioned because there seems to be only a rather tenuous connection between convection/water mass formation, the DWBC, and overturning. For example, while strong variability of LSW formation rates has been observed [*Rhein et al.*, 2002; *Kieke et al.*, 2006, 2007; *Yashayaev*, 2007; *Yashayaev and Loder*, 2009; *Vage et al.*, 2009; *Rhein et al.*, 2011], observations have not been able to link this to variability of the AMOC [*Pickart and Spall*, 2007; *Schott and Brandt*, 2007]. Changes in rates of LSW formation may lead to changes in volumes of water masses rather than significant changes in export [*Mauritzen and Häkkinen*, 1999; *Deshayes et al.*, 2007]. Furthermore, export of LSW and overturning are not simply related to dense water formation; they also depends on the strength of the gyre circulation and the efficiency with which fluid is exchanged between the interior and the boundary current [*Spall*, 2004; *Straneo*, 2006; *Palter et al.*, 2008]. In addition, Lagrangian studies indicate a lack of connectivity of LSW pathways to the north and south of the Grand Banks [*Bower et al.*, 2009, 2011; *Gary et al.*, 2011], suggesting that the influence of variability in the Labrador Sea on subtropical AMOC anomalies may be modest.

While the aforementioned studies question whether AMOC anomalies can penetrate southward from deep convection regions, a number of studies suggest an alternative mechanism involving anomalies arriving from the east via westward propagating baroclinic Rossby waves [*te Raa and Dijkstra*, 2002; *te Raa et al.*, 2004;

Hirschi et al., 2007; *Cabanes et al.*, 2008; *Frankcombe and Dijkstra*, 2009; *Frankcombe et al.*, 2010; *Zanna et al.*, 2011, 2012; *Buckley et al.*, 2012; *Sévellec and Fedorov*, 2012]. In each of these studies, AMOC variability is related to buoyancy anomalies that propagate westward in the subpolar gyre or on the boundary between the subtropical and subpolar gyres and reach the western boundary. Baroclinic Rossby waves may result from stochastic atmospheric wind and/or buoyancy forcing integrated along Rossby wave characteristics [*Frankignoul et al.*, 1997; *Marshall et al.*, 2001a; *Buckley et al.*, 2012] or excited by baroclinic instability [*Colin de Verdiére and Huck*, 1999; *Buckley et al.*, 2012].

While numerous modeling studies link AMOC anomalies to Rossby waves, such a link has not been established observationally. Observations of Rossby waves are primarily restricted to subtropical latitudes and intra-annual to interannual timescales due to the shortness of the observational record (about two decades for SSH) and the slower wave crossing time at high latitudes. Similarly, AMOC observations are lacking on decadal timescales, and continuous observations are limited to 26.5°N. The impact of Rossby waves and eddies on the AMOC has been studied extensively at 26.5°N using satellite altimetry and dynamic height profiles at RAPID array moorings [*Wunsch*, 2008; *Kanzow et al.*, 2009; *Clément et al.*, 2014]. These studies suggest that Rossby waves (crossing the Atlantic at 26.5°N) play a significant role in intra-annual AMOC variability at 26.5°N but little role on interannual timescales. However, the diminished impact of local (at a given latitude) Rossby waves on interannual timescales does not preclude remote Rossby waves (such as those propagating on the subtropical-subpolar gyre boundary) from influencing the AMOC on decadal timescales.

Despite the diversity of proposed mechanisms of low-frequency AMOC variability, several common features emerge. Examining the contributions of buoyancy anomalies on the eastern and western boundaries separately (calculating Ψ_{tw} in equation (9) but only allowing either $b(x_e)$ or $b(x_w)$ to vary) demonstrates that buoyancy anomalies along the western boundary make a larger contribution to geostrophic AMOC variability [*Cabanes et al.*, 2008; *Buckley et al.*, 2012; *Tulloch and Marshall*, 2012; *Polo et al.*, 2014]. Thus, understanding the origin of buoyancy anomalies on the western boundary is an essential aspect of understanding of AMOC variability. Furthermore, idealized [*Zanna et al.*, 2011; *Buckley et al.*, 2012] and GCM [*Danabasoglu*, 2008; *Zhang*, 2008; *Biastoch et al.*, 2008a; *Tziperman et al.*, 2008; *Hawkins and Sutton*, 2009; *Tulloch and Marshall*, 2012] studies isolate the subpolar gyre/the boundary between the subtropical and subpolar gyres as the pacemaker region for decadal AMOC variability. For example, *Zanna et al.* [2012] find that optimal initial conditions for generating AMOC anomalies are characterized by buoyancy anomalies in the subpolar gyre, which amplify through nonnormal dynamics.

4.4. Robust Features of AMOC in Observations and Models

Analysis of AMOC observations, coupled and ocean-only GCMs, and state estimates have yielded the following important insights into AMOC variability.

1. *Magnitude of AMOC variability*. Array-based AMOC estimates, GCMs, and state estimates all indicate that the AMOC exhibits large variability on intra-annual and seasonal timescales (order 100% of its mean value) and much smaller variability on interannual to decadal timescales (order a few Sverdrups). Neither observational estimates nor models suggest that large systematic changes in the AMOC have occurred over the last 10–50 years. Intra-annual AMOC variability is primarily the local response to wind variability, through Ekman transports driven directly by the winds [*Hirschi et al.*, 2007; *Kanzow et al.*, 2007; *Cabanes et al.*, 2008; *Rayner et al.*, 2011] and geostrophic anomalies associated with wind-induced heaving of isopycnals [*Hirschi et al.*, 2013; *Roberts et al.*, 2013b]. On interannual and longer timescales, the geostrophic component of the AMOC dominates.
2. *Meridional Coherence of the AMOC*. Modeling studies [*Bingham et al.*, 2007], ocean state estimates [*Wunsch and Heimbach*, 2013b], and observations [*Mielke et al.*, 2013] indicate that the AMOC is not coherent between the subtropical and subpolar gyres on interannual timescales. Within the subtropical gyre interannual AMOC variability is dominant, while in the subpolar latitudes decadal AMOC variability is stronger [*Balmaseda et al.*, 2007; *Wunsch and Heimbach*, 2013b]. On decadal timescales models and state estimates generally exhibit meridionally coherent modes of AMOC variability.
3. *Importance of buoyancy anomalies on the western boundary*. Observations [*Bryden et al.*, 2009; *Longworth et al.*, 2011], theory, ocean state estimates [*Cabanes et al.*, 2008], and models [*Buckley et al.*, 2012; *Tulloch and Marshall*, 2012] demonstrate that upper ocean (top kilometer) buoyancy anomalies on the western boundary play a key role in variability of AMOC. On decadal timescales, meridionally coherent western

boundary buoyancy anomalies appear to originate in the subpolar gyre [*Böning et al.*, 2006; *Biastoch et al.*, 2008b; *Robson et al.*, 2012; *Yeager and Danabasoglu*, 2014] or along the subtropical-subpolar gyre boundary [*Danabasoglu*, 2008; *Buckley et al.*, 2012].

5. Framework for Understanding Decadal AMOC Variability

We focus here on the origin of large-scale, meridionally coherent decadal modes of AMOC variability. We are therefore primarily concerned with the geostrophic component, since the Ekman component responds to wind forcing and dominates on shorter timescales. Currently, there is no accepted mechanism for decadal AMOC variability. Insights about mechanisms have largely come from models, but, as we have reviewed, the magnitude and timescale of AMOC variability vary markedly across models and model formulations. Despite these uncertainties, we use the robust features of AMOC variability identified in section 4.4 to order our discussion of likely mechanisms.

Low-frequency AMOC variability (at a given latitude) is related to buoyancy anomalies at the western boundary of the basin (point 3 above). Models suggest that meridionally coherent AMOC anomalies originate in the subpolar gyre and/or along the subtropical-subpolar gyre boundary (points 2 and 3 above). These results suggest that understanding decadal AMOC variability requires an understanding of the origin of western boundary buoyancy anomalies that are able to propagate meridionally.

5.1. The Transition Zone as the Pacemaker of AMOC Variability

Here we set forth the hypothesis that a consensus on mechanisms of decadal AMOC variability is possible with a focus on the dynamics at the western margin of the subtropical-subpolar gyre boundary, the region we refer to as the TZ. Decadal AMOC anomalies are generally maximal near 40°N (see Figures 9 and 10), which suggests that AMOC anomalies may originate from this region. *Tulloch and Marshall* [2012] show that decadal AMOC variability in two coupled climate models (CM2.1 and CCSM3) covaries with upper ocean (top kilometer) thermal anomalies in the TZ (Figure 9). The buoyancy anomalies in the TZ are part of a large-scale pattern that propagates around the subpolar gyre and likely acts as a "pacemaker" of AMOC variability. Here we use the word pacemaker to refer to a region or process that sets the timescale of variability and suggest that the TZ sets the variability of the AMOC on decadal timescales. Focus on the TZ as an important region controlling variability of the North Atlantic circulation is not new; *Rossby* [1996] argues that variability in the TZ, specifically variations in the strength of the Mann Eddy at the heart of the TZ, plays an important role in modifying the strength of the NAC.

Variability in this key region is implicitly reflected in the AMOC indices commonly utilized by the modeling community, such as (1) time series of the strength of the AMOC at the latitude of the maximum of the mean AMOC [*Knight et al.*, 2005; *Zhang*, 2008], (2) time series of the maximum AMOC in the North Atlantic [*Delworth et al.*, 1993; *Delworth and Greatbatch*, 2000; *Mignot and Frankignoul*, 2005; *Guemas and Salas-Mélia*, 2008; *Danabasoglu*, 2008; *Danabasoglu et al.*, 2012], and (3) the first principle component time series of the (generally annual mean or low-pass-filtered) AMOC [*Dong and Sutton*, 2005; *Danabasoglu*, 2008; *Danabasoglu et al.*, 2012]. These indices typically covary with buoyancy anomalies in the TZ because the maximum mean and variance of the AMOC is typically found at about 40°N and decadal AMOC variability is related to buoyancy anomalies on the western boundary.

Lagrangian studies indicate that the TZ is an important region for both near-surface and deep AMOC pathways. *Burkholder and Lozier* [2011a] identify the TZ as a bifurcation point of the near-surface flow, as it contains both pathways for recirculated waters in the subtropical gyre and throughput pathways related to the AMOC. Back trajectories from near the surface in the eastern subpolar gyre show two pathways for waters supplying the region: a dominant subtropical to subpolar subsurface pathway and a less traveled surface pathway carrying recirculated waters from the western subpolar gyre [*Burkholder and Lozier*, 2014]. Importantly, both pathways pass through the TZ where strong modifications of the parcels' temperatures occur, indicating strong buoyancy transformations in this region. Both Lagrangian and tracer studies indicate important changes in deep AMOC pathways in the TZ. The majority of both real and model-simulated floats deployed in the DWBC are detrained from the boundary current between the Flemish Cap and the Tail of the Grand Banks [*Bower et al.*, 2009, 2011]; *Getzlaff et al.* [2006] argue that the intense eddy activity around the Grand Banks is responsible for the detrainment of waters from the DWBC. Floats remaining in the DWBC at the Tail of the Grand Banks, i.e., within the TZ, are likely to be exported to the subtropical gyre via the DWBC. Tracer studies (e.g., CFCs; see section 2.1) indicate that the TZ is a region where tracer ages in the DWBC increase

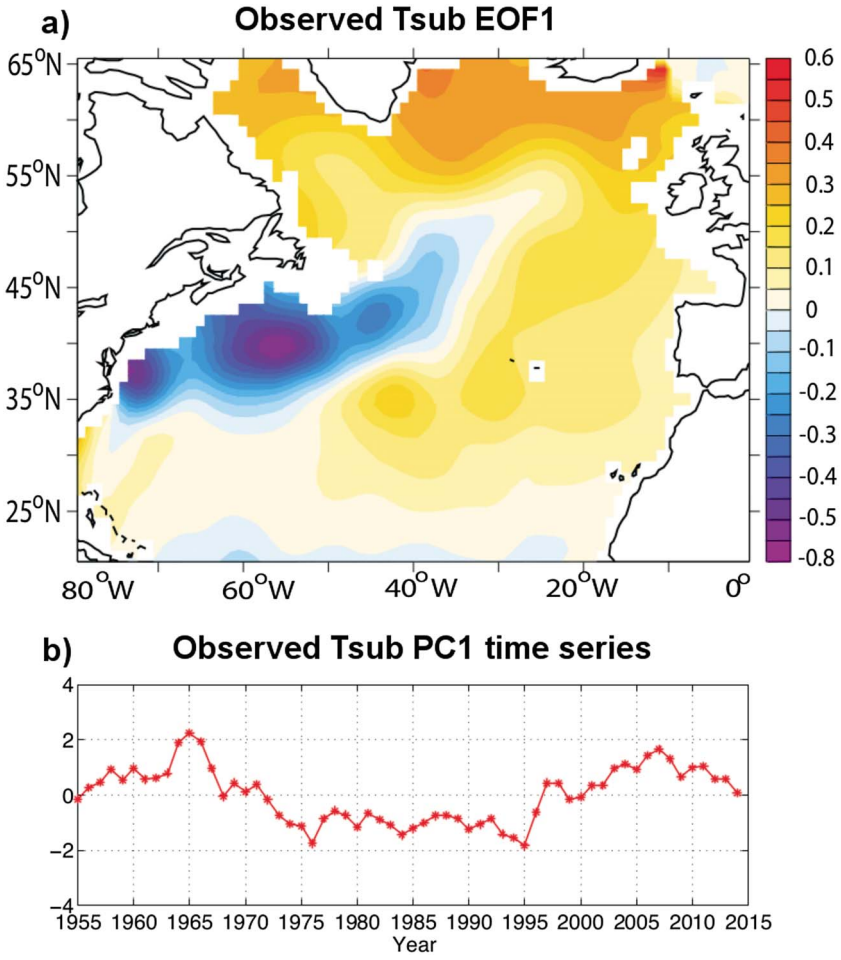

Figure 11. Variability of observed annual mean anomalies of ocean temperature at 400 m (T_{sub}) from an objectively analyzed ocean temperature data set [*Levitus et al.*, 2005]. (a) The first empirical orthogonal function (EOF1) of observed North Atlantic T_{sub} (K, 30%) for 1955–2014. (b) First principle component (PC1) time series of observed T_{sub} during 1955–2014 (normalized). Figure provided by R. Zhang (personal communication, 2015), updated from *Zhang* [2008].

abruptly, indicating strong mixing of newly formed (young) waters with older waters (Figure 5) [*Gary et al.*, 2012; *Rhein et al.*, 2015]. These studies indicate that (1) buoyancy anomalies in the TZ may be communicated to both the subtropical and subpolar gyre and (2) the TZ is not a passive conduit for buoyancy anomalies, as strong modifications of water mass properties occur in this region.

Since decadal observations of the AMOC are not available, the connection between large-scale AMOC anomalies and variability in the TZ cannot be established via observations alone. However, observations indicate that there is significant low-frequency variability of SST, UOHC, SSH, and ocean currents in the TZ [*Häkkinen and Rhines*, 2004; *Zhang*, 2008; *Lumpkin et al.*, 2008; *Häkkinen et al.*, 2013]. For example, Figure 11 shows the variability of observed annual mean anomalies of temperature at 400 m (T_{sub}) from an empirical orthogonal function analysis (1955–2014) (updated from *Zhang* [2008]). Note the large variability in T_{sub} along the path of the Gulf Stream/NAC and in the TZ. Yearly snapshots of absolute zonal velocities across the AR19 (48°N) section also show that variability in currents is large near 45°W in the vicinity of the Mann Eddy at the heart of the TZ [see *Lumpkin et al.*, 2008, Figure 7].

As we now review, buoyancy anomalies in the TZ are not solely locally forced; rather, they are the result of a wide array of ocean processes. Thus, the TZ can be thought of as an integrator of processes from disparate regions of the Atlantic, a view that may reconcile various proposed mechanisms of AMOC variability, such as the remote influences of deep convection and Rossby waves (see section 4.3). Many such processes likely play a role in setting buoyancy anomalies in the TZ, and their relative roles certainly depend on timescale.

5.2. Mechanisms for Creating Buoyancy Anomalies in the Transition Zone

We now review processes contributing to the creation of buoyancy anomalies in the TZ , including local atmospheric forcing, advection of anomalies by mean currents, westward propagating (wind or buoyancy forced) baroclinic Rossby waves, anomalies resulting from large-scale ocean circulation changes (such as shifts of the Gulf Stream path), and anomalies advected/propagated from high latitudes.

5.2.1. Local Atmospheric Forcing

Can upper ocean buoyancy anomalies in the TZ be created by local atmospheric forcing, which is notably strong in the region? Indeed, the "null hypothesis" for the origin of midlatitude SST anomalies is that they reflect the passive response of the ocean to stochastic atmospheric forcing [*Frankignoul and Hasselmann*, 1977]. Statistical analyses [*Frankignoul and Hasselmann*, 1977; *Frankignoul*, 1985; *Cayan*, 1992a, 1992b], mixed layer models [*Seager et al.*, 2000], and heat budget analyses [*Buckley et al.*, 2014a, 2015] indicate that in many regions (particularly gyre interiors) SSTs primarily reflect the response to stochastic atmospheric forcing (Figure 7a). Enhanced persistence of SST anomalies in the subpolar gyre is consistent with deeper mixed layer depths (MLDs) in these regions and the reemergence of SST anomalies isolated below the summer thermocline [*Alexander and Deser*, 1995]. However, the TZ is a place where ocean advection is likely to play a key role. Interannual to decadal UOHC anomalies in the Gulf Stream region are forced by changes in ocean geostrophic advection and are damped by air-sea heat fluxes [*Marshall et al.*, 2001a; *Dong and Kelly*, 2004; *Dong et al.*, 2007; *Zhai and Sheldon*, 2012; *Buckley et al.*, 2014a, 2015] (see Figure 7a). *Buckley et al.* [2014a] isolate the TZ as a place where ocean dynamics, including geostrophic advection, eddies, and diffusion, are important in the UOHC budget (see Figure 7b). So although the null hypothesis may explain UOHC variability in many regions, ocean processes appear to play a significant role in setting UOHC in this key region.

5.2.2. Advection of Buoyancy Anomalies by Mean Currents

Buoyancy anomalies may be advected into the TZ by the mean ocean circulation. *Tulloch and Marshall* [2012] argue that buoyancy anomalies in CCSM3 and CM2.1 originate along the subtropical/subpolar gyre boundary and are advected cyclonically by the mean subpolar gyre circulation (see Figure 9c). When these anomalies reach the western boundary, they lead to AMOC variability in accord with the thermal wind relation. *Kwon and Frankignoul* [2012] suggest that AMOC anomalies in CCSM3 are due to buoyancy anomalies that originate near the western boundary and are advected by the mean subpolar gyre circulation into the Labrador Sea. *Sutton and Allen* [1997] use analyses of monthly mean SST compiled from ship observations for the period 1945–1989 to investigate predictability of North Atlantic SST associated with oceanic advection. They find substantial lagged correlations between SSTs over the Gulf Stream separation region and SSTs along the path of the Gulf Stream/NAC, with anomalies taking 5–6 years to travel from the Gulf Stream separation to the TZ.

Saravanan and McWilliams [1998] recognize that the interaction between spatially coherent (but temporally incoherent) atmospheric patterns and ocean advection can lead to the generation of preferred timescales in the atmosphere-ocean system through a mechanism which they term spatial resonance. A standing atmospheric pattern with length scale L generates SST anomalies that are advected by the mean ocean current V. The preferred timescale L/V picked out by spatial resonance is the timescale for which atmospheric forcing constructively reinforces SST anomalies as they are advected. This mechanism may explain, for example, the surprisingly large lagged correlations between SST anomalies along the Gulf Stream path found by *Sutton and Allen* [1997].

5.2.3. Buoyancy Signals Communicated by Baroclinic Rossby Waves

As outlined in section 4.3, modeling studies have linked AMOC variability to baroclinic Rossby waves [*te Raa and Dijkstra*, 2002; *te Raa et al.*, 2004; *Hirschi et al.*, 2007; *Cabanes et al.*, 2008; *Frankcombe and Dijkstra*, 2009; *Frankcombe et al.*, 2010; *Zanna et al.*, 2011, 2012; *Buckley et al.*, 2012; *Sévellec and Fedorov*, 2012]. In each of these studies, AMOC variability is induced by buoyancy anomalies that propagate westward in the subpolar gyre or on the boundary between the subtropical and subpolar gyres and reach the western boundary in the vicinity of the TZ (or an idealized analogue thereof).

Although observations of the AMOC are too sparse to relate baroclinic Rossby waves to the strength of the AMOC (with the exception of at 26.5°N), observational studies demonstrate that Rossby wave models forced by wind stress anomalies successfully capture much of the observed SSH and thermocline depth variability measured by tide gauges [*Sturges and Hong*, 1995], hydrographic data [*Sturges et al.*, 1998; *Schneider and Miller*, 2001], and satellite altimetry [*Fu and Qui*, 2002; *Qiu*, 2002; *Qiu and Chen*, 2006]. However, most of these studies are restricted to the subtropics and intra-annual to interannual timescales. Despite this,

observations indicate that Rossby wave amplitudes increase toward the west, consistent with the accumulation of stochastic forcing along Rossby wave characteristics. Wave amplitudes are significantly larger west of the Mid-Atlantic Ridge than east of the ridge [*Chelton and Schlax*, 1996; *Challenor et al.*, 2001; *Osychny and Cornillon*, 2004], with the largest amplitudes occurring where the Gulf Stream crosses bathymetric features (the continental slope, New England Seamounts, and the Newfoundland Ridge) and in the TZ. *Chelton and Schlax* [1996] hypothesize that the Mid-Atlantic Ridge plays a role in amplifying or generating Rossby waves. In contrast, *Osychny and Cornillon* [2004] suggest that a key source of baroclinic Rossby waves in the western North Atlantic is located southeast of the Grand Banks where the Gulf Stream/NAC and DWBC interact with each other and the Newfoundland Ridge.

In summary, models have linked decadal AMOC variability to baroclinic Rossby waves, primarily along the subtropical-subpolar gyre boundary. While observations suggest that Rossby waves play an important role in SSH and thermocline height variability, observations of Rossby waves are primarily restricted to subtropical latitudes and intra-annual to interannual timescales due to the shortness of the observational record (about two decades for SSH) and the slower wave crossing time at high latitudes. Similarly, observations of the AMOC are lacking on decadal timescales, and continuous observations are limited to 26.5°N. Therefore, determining the role of Rossby waves in low-frequency AMOC variability from observations remains difficult.

5.2.4. Gyre Wobbles and Shifts in the Gulf Stream Path

Shifts in the Gulf Stream path lead to large temperature anomalies along the front. Both wind and buoyancy forcing play a role, as well as interaction of the Gulf Stream with the DWBC. Observations [*Frankignoul et al.*, 2001; *Joyce and Zhang*, 2010] and models [*Sasaki and Schneider*, 2011] document the relationship between northward (southward) shifts in the Gulf Stream path and strong warming (cooling) of SST along the Gulf Stream front (see Figure 12). The patterns of SST variability associated with changes in the Gulf Stream path resembles the dominant modes of interannual to decadal SST variability [see *Joyce and Zhang*, 2010, Figure 3] and include significant anomalies in the TZ.

A variety of processes play a role in setting the path of the Gulf Stream. Basic theory suggests that the spin-up/spin-down of the gyre circulation is the result of stochastic atmospheric forcing (generally taken to be wind forcing) integrated along Rossby wave characteristics [*Frankignoul et al.*, 1997]. Wind stress curl anomalies associated with a positive (negative) phase of the NAO lead to a spin-up of an anomalous anticyclonic (cyclonic) intergyre gyre [*Marshall et al.*, 2001a] and buoyancy anomalies in the key region identified above [*Zhai and Sheldon*, 2012]. The decadal timescale of SST anomalies is expected from the crossing time of first baroclinic mode Rossby waves.

While both observations [*Joyce et al.*, 2000; *Frankignoul et al.*, 2001] and models [*de Coëtlogon et al.*, 2006; *Sasaki and Schneider*, 2011] connect northward (southward) shifts in the Gulf Stream path to positive (negative) phases of the NAO in accord with the theory suggested by *Marshall et al.* [2001a], the timescale of the response is not consistent between various studies. One reason for this may be that many studies seek lagged correlations between the Gulf Stream position and the NAO index at a specific time [e.g., *Frankignoul et al.*, 2001], rather than the NAO integrated over the Rossby wave crossing time. Additionally, a surfeit of processes that are not included in the simple model of *Marshall et al.* [2001a], including dissipation, instability, buoyancy forcing, and interaction with bathymetry, also may be important in determining variability in the Gulf Stream path. Observations and models suggest that Rossby waves are unable to cross the gyre at middle and high latitudes due to (1) their slow crossing time (decadal), which may be longer than dissipative timescales, and (2) the potential instability of the waves [*LaCasce and Pedlosky*, 2004; *Isachsen et al.*, 2007]. As a result, variability in the Gulf Stream path may reflect stochastic atmospheric forcing integrated over a more localized region near the western boundary and the dominant timescale may be given by the damping timescale. For example, *Sasaki and Schneider* [2011] find that the Gulf Stream position in an eddy-resolving model lags the NAO by approximately 2 years and attribute the time lag to westward propagation of the undulation of the jet axis from the central to the western part of the gyre.

Buoyancy forcing may also play a role in variability in the Gulf Stream path. Cooling along the Gulf Stream path leads to a strengthening of the jet and a southeastward shift in the separation path [*Nurser and Williams*, 1990]. *Frankignoul et al.* [2001] argue that the fast response (1 year time lag) of the Gulf Stream path to NAO forcing is due to buoyancy forcing over the recirculation gyres. Similarly, *Häkkinen and Rhines* [2004] suggest that the leading mode of SSH variability in the North Atlantic, consisting of anomalies along the Gulf Stream path and anomalies of the opposite polarity over the northern/western subpolar gyre, is related to buoyancy forcing over the subpolar gyre.

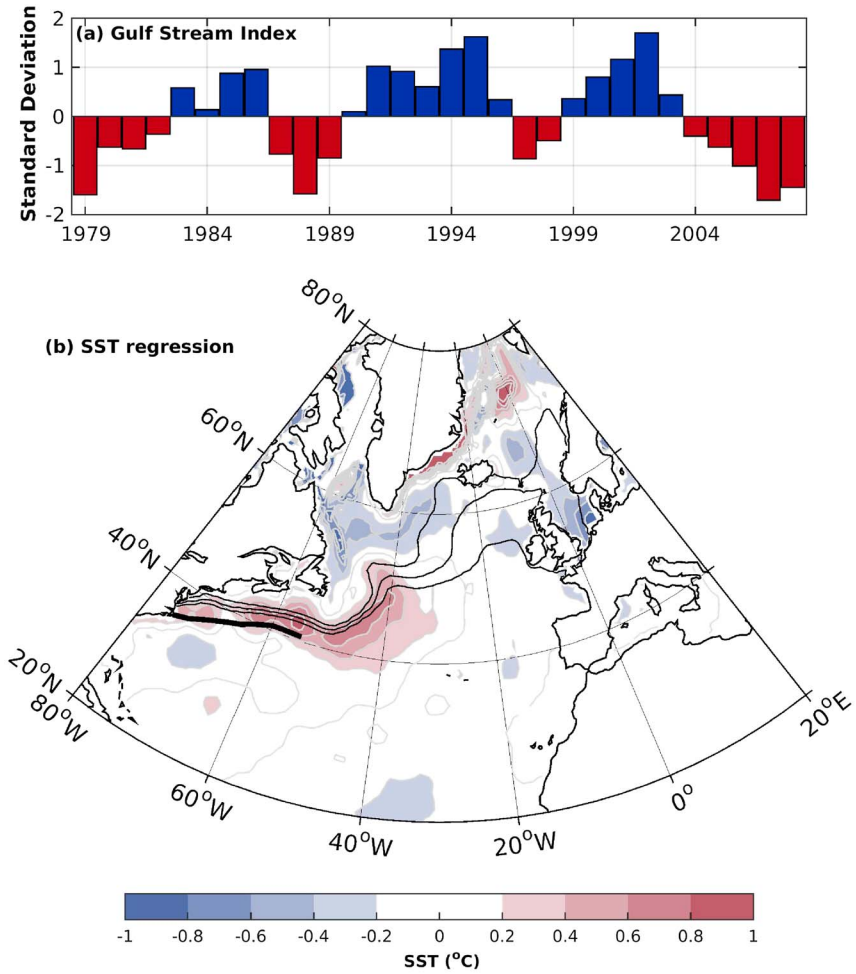

Figure 12. (a) Winter (January-February-March, JFM) Gulf Stream path index time series. The index is the leading principal component (PC) for the temperature anomalies at 200 m along the mean Gulf Stream path, as defined by *Joyce et al.* [2000]. Positive (negative) anomalies indicate a northward (southward) shift in the Gulf Stream path. (b) Regression of the JFM SST anomalies on the JFM Gulf Stream index when the Gulf Stream path leads by 1 year. Magnitudes of SST anomalies shown are based on two standard deviations of the PC time series, and the area contoured is almost exclusively within the 90% confidence level based on the Student's *t* test. The mean Gulf Stream path is indicated by the thick black line. Isotherms of the mean JFM SST for 6°, 8°, and 10°C are plotted with thin black contours. Figure is based on the Figure 10 of *Kwon and Joyce* [2013] and was provided by Young-Oh Kwon (personal communication, 2015).

Finally, many modeling studies demonstrate that the presence of the DWBC affects the separation of the Gulf Stream from the coast and its subsequent path into the interior [*Thompson and Schmitz*, 1989; *Spall*, 1996; *Zhang and Vallis*, 2007]. Bottom vortex stretching induced by a downslope DWBC south of the Grand Banks leads to the formation of a cyclonic northern recirculation gyre, the separation of the Gulf Stream from the coast downstream of Cape Hatteras, and thus a more southerly Gulf Stream path [*Zhang and Vallis*, 2007]. The relationship between the DWBC and Gulf Stream path has led to the hypothesis that meridional excursions in the Gulf Stream might be induced by variations in the strength of the DWBC. Observational [*Peña Molino and Joyce*, 2008; *Joyce and Zhang*, 2010; *Toole et al.*, 2011; *Peña Molino et al.*, 2012] and modeling studies [*Zhang*, 2008; *Joyce and Zhang*, 2010] find that southward displacements of the Gulf Stream are associated with a stronger DWBC, with changes in the DWBC leading changes in the Gulf Stream by several months [*Joyce and Zhang*, 2010].

While shifts in the Gulf Stream path are an effective mechanism for creating buoyancy anomalies due to large buoyancy gradients along the front, some studies have suggested that changes in the strength of the subtropical and subpolar gyres are important in creating Atlantic SST anomalies, including the NAO tripole [*Schneider and Fan*, 2012] and the AMV [*Häkkinen et al.*, 2011b, 2013]. A weakening of the subtropical and subpolar gyres

driven by changes in the wind stress curl allows greater penetration of warm subtropical waters into the subpolar gyre [*Häkkinen and Rhines*, 2004; *Hátún et al.*, 2005; *Häkkinen and Rhines*, 2009; *Häkkinen et al.*, 2011a]. While the meridional extent of the gyre circulations is primarily related to the NAO, modulations in the mean gyre strength appear to be associated with changes in blocking between Greenland and western Europe [*Häkkinen et al.*, 2011b].

5.2.5. Changes in Deep Convection and Water Mass Formation

Changes in convection and water mass formation can lead to buoyancy anomalies in remote sites, including the TZ. Several observational studies attempt to trace buoyancy, potential vorticity, and layer thickness anomalies from the Labrador Sea to regions within the DWBC as a function of latitude. Water properties at Line W southeast of Cape Cod document a large change between November 2001 and April 2008, and the structure of these anomalies is consistent with observations in the Labrador Sea 4–9 years earlier [*Peña Molino et al.*, 2011]. *Curry et al.* [1998] and *van Sebille et al.* [2011] argue that temperature, salinity, and thickness anomalies of LSW observed at middepth near Bermuda can be traced back to anomalies in the Labrador Sea 5–9 years earlier (although the correlations are not found to be statistically significant in *van Sebille et al.* [2011]). In contrast, *Bower et al.* [2009] and *Lozier et al.* [2013] focus on the lack of connectivity of the DWBC to the north and south of the Grand Banks, suggesting that the impact of changes in the subpolar DWBC on the subtropical circulation may be modest. Most Lagrangian (float) trajectories originating in the DWBC at 50°N enter the interior in several regions around the Grand Banks. Back trajectories of floats arriving at Line W (69°W) show that few trajectories pass northward of the Grand Banks; most of the DWBC in the subtropical gyre is transporting waters that are recirculating in the northern recirculation gyre. Although the aforementioned two groups of studies suggest quite different meridional coherence of anomalies between the subtropical and subpolar regions, they both suggest that the TZ is likely a region that is highly influenced by variability in both the subtropical and subpolar gyres.

5.2.6. Role of Salinity

Observations suggest that there have been significant shifts in the salinity of the subpolar gyre in recent decades [*Holliday*, 2003]. One hypothesis is that a weakening of the subtropical and subpolar gyres driven by changes in the wind stress curl (see section 5.2.4) allows greater penetration of warm, salty subtropical waters into the subpolar gyre [*Häkkinen and Rhines*, 2004; *Hátún et al.*, 2005; *Lozier and Stewart*, 2008; *Häkkinen and Rhines*, 2009; *Burkholder and Lozier*, 2011a; *Häkkinen et al.*, 2011a, 2011b, 2013]. The potential impact to these salinity changes on the AMOC remains to be determined.

In considering the contribution of salinity to buoyancy anomalies, the following should be noted:

1. Salinity plays a larger role in creating buoyancy anomalies in the (cold) subpolar gyre than in the (warm) tropics/subtropics.
2. Ice formation and the resulting brine rejection increase salinity, and the melting of ice decreases salinity.
3. Whereas low-frequency SST anomalies tend to be damped via air-sea heat fluxes, freshwater fluxes are not dependent on sea surface salinity (SSS). As a result, low-frequency SSS anomalies will likely experience less damping than SST anomalies.

A fundamental question is whether a two-component equation of state (temperature and salinity) is essential to AMOC variability or whether AMOC variability can be understood considering a single variable (buoyancy). Some idealized models exhibit AMOC oscillations despite only considering a single-variable equation of state [*Welander*, 1967; *Greatbach and Zhang*, 1995; *Chen and Ghil*, 1996; *Huck et al.*, 1999]. In other idealized studies, AMOC variability is dependent on a two-component equation of state [*Welander*, 1986; *Delworth et al.*, 1993; *Griffies and Tziperman*, 1995; *Dong and Sutton*, 2005]. For example, *Griffies and Tziperman* [1995] find that the different damping timescales of temperature and salinity (see point 3 above) are essential for AMOC variability in an idealized box model. A strengthened AMOC leads to increased salt and heat transport into the sinking region. The salt anomalies decrease the buoyancy in the sinking region, providing a positive feedback on the AMOC (salinity-advection feedback), while the temperature anomalies increase buoyancy and provide a negative feedback (temperature-advection feedback). However, the temperature anomalies are initially damped, and thus the negative feedback is delayed, leading to an oscillation in the strength of the AMOC. AMOC oscillations in ocean-only models often depend on the types of boundary conditions used for temperature and salinity (restoring, fixed-flux, or mixed) [*Arzel et al.*, 2006].

The relative importance of temperature and salinity in modes of AMOC variability depends on timescale. It is well documented that salinity plays a role in the mean AMOC: the higher salinity of the Atlantic compared to

that of the Pacific is essential for the deep overturning circulation in the Atlantic [*Ferreira et al.*, 2010]. As a result of less vigorous damping, salinity anomalies likely play a more significant role in AMOC variability on longer timescales [*Deshayes et al.*, 2014]. For example, *Delworth and Zeng* [2012] suggest that salinity anomalies propagating from the Southern Ocean play a role in centennial AMOC variability in GFDL CM2.1. *Vellinga and Wu* [2004] propose that centennial AMOC variability in the Hadley Centre Coupled Model version 3 (HadCM3) results from interactions between the AMOC, the position of the ITCZ, and tropical salinity anomalies.

A number of studies have examined the relative roles of temperature and salinity in determining buoyancy anomalies in regions thought to be important for decadal AMOC variability. In the GFDL coupled model [*Delworth et al.*, 1993; *Tulloch and Marshall*, 2012], HadCM3 [*Dong and Sutton*, 2005], the Institut Pierre-Simon Laplace climate model [*Msadek and Frankignoul*, 2009], and CCSM4 [*Danabasoglu et al.*, 2012] buoyancy anomalies in convective regions are due to salinity anomalies resulting from salt transport convergences by ocean currents. In contrast, in the Max Planck Institute for Meteorology coupled model [*Zhu and Jungclaus*, 2008] buoyancy anomalies in the Labrador Sea are mainly due to temperature anomalies, with smaller compensating salinity anomalies. In CCSM3 temperature and salinity contribute roughly equally to density in the Labrador Sea and are nearly in phase [*Danabasoglu*, 2008], although it is stressed that the amplitude and phasing of the contributions of temperature and salinity to density anomalies depend highly on the region considered. *Tulloch and Marshall* [2012] demonstrate that buoyancy anomalies in the TZ in both CM2.1 and CCSM3 are largely the result of temperature anomalies with smaller, compensating salinity anomalies.

5.3. Meridional Communication of Buoyancy Anomalies

In order to create meridionally coherent AMOC anomalies, there must be a mechanism by which buoyancy anomalies are communicated meridionally. Here we have suggested that the TZ is an important region for in this meridional communication, while much previous work has focused on meridional communication from regions of deep convection. Two mechanisms for the meridional communication of buoyancy (and hence AMOC) anomalies have been proposed: (1) slow advection of buoyancy anomalies by the mean DWBC or interior pathways and (2) rapid meridional propagation of anomalies via boundary waves [e.g., *Kawase*, 1987; *Johnson and Marshall*, 2002a].

Observational studies attempting to track buoyancy anomalies along the western boundary as a function of latitude generally find slow propagation of anomalies, suggesting that buoyancy anomalies are communicated via advective pathways. Since observations are sparse, advective timescales are typically calculated by finding the lag that maximizes the correlation between anomalies in one region (e.g., the Labrador Sea) and downstream locations in the DWBC, such as Line W [*Peña Molino et al.*, 2011] and sections at 48°N, 36°N, and 24°N [*Curry et al.*, 1998; *Koltermann et al.*, 1999; *van Sebille et al.*, 2011]. A velocity can be inferred from this time lag, under the assumption that this velocity is constant over the distance along the DWBC; such studies generally find spreading rates on the order of a few centimeters per second. Tracer observations and Lagrangian trajectories provide a more rigorous way of estimating advective timescales from observations. Both tracer ages calculated from CFCs (see Figure 5 and section 2.1) and Lagrangian particle transit times find timescales on the order of 30 years for waters to travel from the Labrador Sea to the subtropics. Average spreading rates are on the order of a few centimeters per second, but there are significant regional variations. Observed spreading rates are much slower than velocities measured within the DWBC, which are on the order of 10–20 cm s^{-1} [e.g., *Johns et al.*, 1993; *Schott et al.*, 1993; *Fischer et al.*, 2015]. Slower-than-expected spreading rates likely are signatures of eddy-driven recirculation gyres generated by the instabilities of the Gulf Stream/NAC system [*Lozier et al.*, 1997; *Lozier*, 1999; *Gary et al.*, 2011].

Theoretical studies and idealized models tend to implicate boundary waves in the southward communication of AMOC variability [*Kawase*, 1987; *Johnson and Marshall*, 2002a, 2002b; *Deshayes and Frankignoul*, 2005; *Schloesser et al.*, 2012]. Buoyancy anomalies on the western boundary excite boundary waves that propagate rapidly southward from the subpolar gyre to the equator, eastward along the equator, and poleward along the eastern boundary in both hemispheres. Since pressure anomalies decrease with latitude along the western boundary (while maintaining the same transport anomaly), pressure anomalies reaching the equatorial region are tiny. When these anomalies are communicated poleward along the eastern boundary, the pressure anomalies do not reamplify since energy is radiated via Rossby waves. Therefore, pressure anomalies on the eastern boundary are small, and the equator acts as a buffer to AMOC variability [*Johnson and Marshall*, 2002a, 2002b]. While the propagation along the ocean boundaries and the equator is typically thought to be due to Kelvin waves, *Marshall and Johnson* [2013] show that Kelvin waves are only important

for period less than a few months. At longer timescales, propagation occurs through short and long Rossby waves at the western and eastern boundaries, respectively.

In contrast, the relative importance of advection and boundary waves in communicating AMOC signals in GCMs appears to be model dependent. Some GCM studies observe significant time lags between buoyancy/AMOC anomalies in the subpolar gyre and the subtropics and suggest that advective processes communicate buoyancy anomalies meridionally [*Marotzke and Klinger*, 2000; *Zhang*, 2010a; *Buckley et al.*, 2012]. Other studies find that buoyancy anomalies are communicated rapidly in accord with expectations from boundary wave theory [*Biastoch et al.*, 2008a]. *Kohl* [2005] and *Heimbach et al.* [2011] examine the adjoint sensitivities of the AMOC to perturbations and find that buoyancy anomalies that travel rapidly along the boundaries are involved in the communication of AMOC signals with latitude. *Getzlaff et al.* [2005] and *Zhang* [2010a] suggest that the relative roles of advection and boundary waves depend on latitude: AMOC anomalies travel at advective speeds in the subpolar gyre and at faster boundary wave speeds in the subtropical gyre (see Figure 10). *Marshall and Johnson* [2013] show that the speed of boundary waves may be model dependent (due to being inversely proportional to the boundary layer width), which may help explain the wide range of meridional communication speeds seen in models. However, it also casts doubt on the typical use of signal speeds to distinguish between meridional communication by advection and boundary waves.

While previous work has primarily focused on meridional communication from regions of deep convection, both Eulerian and Lagrangian studies indicate changes in meridional communication at the TZ. As outlined in section 5.1, Lagrangian studies show that most floats deployed in the DWBC are detrained from the boundary current between the Flemish Cap and the Tail of the Grand Banks [*Bower et al.*, 2009, 2011]. Tracer studies indicate that the TZ is a region where tracer ages in the DWBC increase abruptly (Figure 5), indicating strong mixing of newly formed (young) waters with older waters [*Gary et al.*, 2012; *Rhein et al.*, 2015]. Eulerian studies also show strong changes in the strength of the DWBC in this region: *Dengler et al.* [2006] report a mean LSW layer DWBC transport of about −17 Sv at 56°N, while *Schott et al.* [2006] report only −7 Sv at 43°N. These studies suggest that any anomalies formed in regions of deep convection are likely strongly modified before reaching the subtropical gyre. In contrast, anomalies in the DWBC within the TZ are likely to be exported to the subtropical gyre.

5.4. Interaction of the AMOC With Other Ocean Basins

Thus far, we have focused on modes of decadal AMOC variability that originate in the North Atlantic. However, it is important to place these modes in the context of other sources of AMOC variability originating from outside the North Atlantic.

Dong et al. [2011] show that changes in the AMOC at 34°S are primarily in response to inter-ocean exchanges with the Pacific and Indian Oceans. Using an ocean model with an embedded two-way nesting scheme that resolves mesoscale dynamics in the Agulhas region, *Biastoch et al.* [2008a] demonstrate that the Agulhas leakage acts as source of decadal AMOC variability. Low-frequency undulations in thermocline depth originating in the Agulhas region travel across the South Atlantic as Rossby waves and along the western boundary into the North Atlantic as coastal Kelvin waves. The resulting decadal AMOC transport signal gradually diminishes from south to north, but the amplitude in the tropical Atlantic is comparable in magnitude to AMOC anomalies that originate in the North Atlantic. *Biastoch et al.* [2009] show that poleward shifts in the westerlies associated with climate change [*Kushner et al.*, 2001; *Thompson and Solomon*, 2002; *Marshall*, 2003; *Fu et al.*, 2006] lead to an increase the Agulhas leakage; however, on decadal timescales significant impacts on the AMOC are confined to the South Atlantic [*Biastoch and Böning*, 2013]. *Delworth and Zeng* [2012] suggest that centennial variability in the AMOC in CM2.1 is related to the century-scale propagation of salinity anomalies from the Southern Ocean to the subpolar North Atlantic.

Numerous studies focus on the role of changes in winds over the Southern Ocean in modifying the strength of the AMOC. While formation of dense water can be thought of as the "push" that drives the AMOC, mixing of this dense water back to the surface, the "pull," is required to sustain the circulation [*Sandström*, 1908; *Visbeck*, 2007]. A significant portion of dense water formed in the North Atlantic upwells adiabatically along isopycnals that outcrop in the Southern Ocean, driven by the westerly winds in this region [*Toggweiler and Samuels*, 1995; *Gnanadesikan*, 1999; *Marshall and Speer*, 2012]. Increasing the strength of winds over the Southern Ocean and/or shifting them poleward results in an increase in Ekman-driven upwelling and hence of the AMOC [*Delworth and Zeng*, 2008; *Klinger and Cruz*, 2009; *Wei et al.*, 2012]. However, changes in poleward eddy fluxes largely compensate for the enhanced equatorward Ekman transport in the Southern Ocean

[*Marshall and Radko*, 2003; *Abernathey et al.*, 2011], and hence, the response of the AMOC to Southern Ocean winds is relatively modest [*Hallberg and Gnanadesikan*, 2006; *Farneti et al.*, 2010; *Farneti and Delworth*, 2010; *Farneti and Gent*, 2011; *Gent and Danabasoglu*, 2011; *Bryan et al.*, 2013; *Gent*, 2015].

It takes many decades to a century or more for the North Atlantic MOC to respond to altered winds over the Southern Ocean, so it appears unlikely that intrinsic wind variability (e.g., the Southern Annular Mode, which has a nearly white spectrum) can induce decadal changes in the AMOC. Thus, Southern Ocean winds are likely to play a role in AMOC changes on longer timescales, including the response of the AMOC to anthropogenic climate change [*Spence et al.*, 2009; *Spooner et al.*, 2013], but not for decadal changes in the AMOC which are our focus here.

5.5. Summary

Decadal AMOC variability responds to buoyancy anomalies on the western boundary near the TZ, a region where significant low-frequency buoyancy anomalies are observed (see Figures 6c, 11, and 12b). As outlined in section 5.2, a myriad of processes may be involved in creating buoyancy anomalies in this key region, including local atmospheric forcing, advection by mean ocean currents, westward propagating baroclinic Rossby waves, shifts in the Gulf Stream path, and anomalies advected and/or propagated from outside the North Atlantic. Stochastic atmospheric forcing likely plays a significant role in all of these mechanisms of variability. Ocean processes can provide memory and, to the extent that they feed back on the atmosphere, color the spectrum of atmospheric variability. Of course, changes in the AMOC and resulting changes in Atlantic OHT convergence may also play an active role in creating buoyancy anomalies in this key region, but the importance of this mechanism for creating buoyancy anomalies must be assessed in relationship to the myriad of other processes that lead to buoyancy anomalies in this complex region.

6. The AMOC and Climate Variability and Predictability

6.1. The Impact of the AMOC and the AMV on the Atmosphere

The AMOC can influence climate due to its role in variability of OHT, atmospheric heat transport (AHT), SST, and air-sea heat fluxes. As outlined in sections 2.3 and 3.2, the AMOC plays a key role in modulating Atlantic OHT variability. On sufficiently long timescales changes in OHT manifest themselves in changes in SST and air-sea energy fluxes and thus can influence the atmosphere. *Bjerknes* [1964] hypothesizes that on decadal timescales OHT anomalies are compensated by AHT anomalies. The key assumptions behind the Bjerknes compensation hypothesis are that (1) rates of change of ocean heat storage are sufficiently small that they can be neglected, an assumption that becomes increasing relevant at long (multidecadal) timescales, and (2) top-of-the-atmosphere radiative fluxes do not vary substantially. *Shaffrey and Sutton* [2006] and *van der Swaluw et al.* [2007] evaluate the hypotheses and mechanisms underlying Bjerknes compensation and find that in the northern extratropics decadal anomalies of AHT are indeed highly anticorrelated with anomalies of Atlantic OHT. Moreover, OHT changes are related to variability of the AMOC. They suggest that during periods of enhanced poleward OHT, meridional SST gradients decrease, as does atmospheric baroclinicity and eddy activity, leading to a decrease in AHT. It should be noted, however, that Bjerknes compensation does not hold in the tropics because changes in meridional OHT are associated with large changes in top-of-the-atmosphere fluxes. Additionally, to the extent the near-surface branches of both the atmospheric and oceanic overturnings can be thought of as the Ekman drift associated with the same surface stress, AHT and OHT in the tropics are expected to covary [*Held*, 2001].

The AMOC is often invoked as the dominant player in low-frequency SST variability observed in the Atlantic Basin (e.g., the AMV), although the relative contributions of atmospheric forcing, ocean dynamics, and external (anthropogenic and volcanic) forcing remain to be quantified (see section 2.4). The AMV impacts regional and global climate, including temperatures across North America and Europe [*Collins and Sinha*, 2003; *Sutton and Hodson*, 2005; *Pohlmann et al.*, 2006; *Ting et al.*, 2011], rainfall in the United States [*Patricola et al.*, 2013] and African Sahel [*Folland et al.*, 1986; *Zhang and Delworth*, 2006; *Ting et al.*, 2011], and frequency and intensity of Atlantic hurricanes [*Knight et al.*, 2006; *Zhang and Delworth*, 2006]. If the AMV is indeed the result of AMOC variability, then the AMOC plays a central role in regional and global climate variability on decadal timescales.

As an indication of the possible global impact of the AMV, Figure 13 shows (a) the asymmetry in zonal mean tropospheric temperature and (b) global mean precipitation regressed on to the AMV time series (shown in Figure 6a). When the AMV is anomalously high, the NH troposphere is anomalously warm and the ITCZ is displaced poleward of its annual mean position. Moreover, the impacts are not local to the Atlantic but

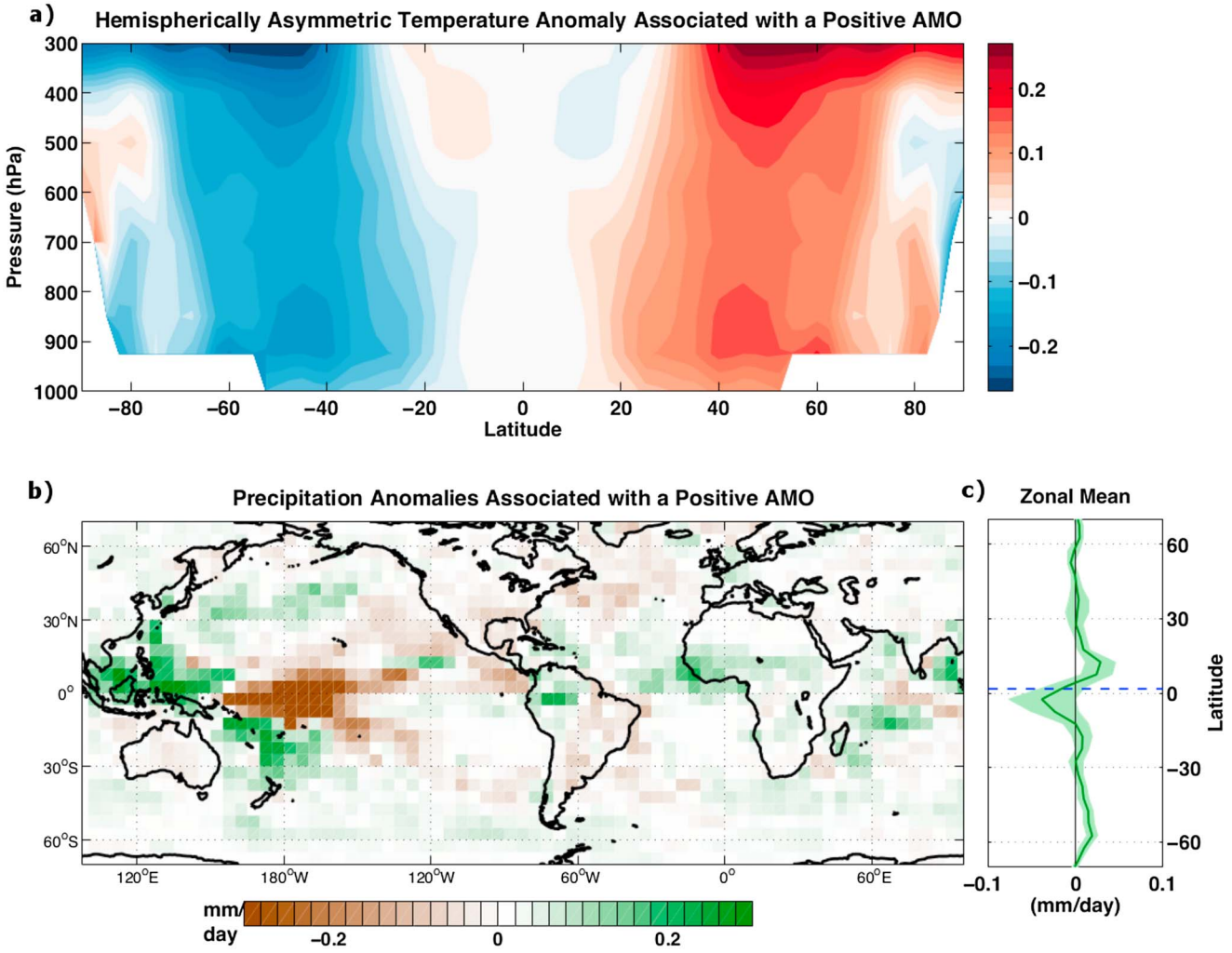

Figure 13. AMV index (see Figure 6a) regressed onto (a) hemispherically asymmetric zonal mean atmospheric temperature anomalies, (b) precipitation anomalies, and (c) zonally averaged precipitation anomalies. All regressions use low-pass-filtered time series with a cutoff period of 10 years. Temperature regression in panel (a) uses the NCEP/NCAR reanalysis from 1948 to 2012 [*Kalnay et al.*, 1996]; NCEP reanalysis data provided by the NOAA/OAR/ESRL PSD, Boulder, Colorado, USA, from their website at http://www.esrl.noaa.gov/psd/. Precipitation regressions in panels (b) and (c) use the *Smith et al.* [2012] reconstruction from 1900 to 2008. Shading in panel (c) indicates 1σ confidence interval, and the dashed blue line represents the time-mean ITCZ position. From Brian Green, MIT (personal communication, 2014).

global in scale. The temperature and precipitation patterns associated with the AMV match those expected to be associated with an increase in strength of the AMOC and meridional OHT [*Chiang and Bitz*, 2005; *Zhang and Delworth*, 2005; *Kang et al.*, 2008, 2009; *Zhang*, 2010c]. The global impact of variations in Atlantic SST, particularly in the tropics, is one of the most compelling pieces of evidence that the AMV is indeed related to hemispheric changes in OHT and corresponding changes in AHT.

6.2. Predictability of the AMOC and Associated Climate Signals

The community's focus on the AMOC and the deployment of AMOC observing arrays is motivated by attempts to exploit knowledge of the state of the North Atlantic Ocean to augment seasonal-to-interannual-to-decadal prediction systems for North America and Europe [see, e.g., *Sutton and Hodson*, 2005; *Collins et al.*, 2006; *Latif and Keenlyside*, 2011]. Furthermore, if AMOC variations lead SST changes, monitoring the AMOC may provide an "early warning system" for future changes in SST and the climate system, even in the absence of the ability to make skillful AMOC predictions [*Hawkins and Sutton*, 2008]. Yet as outlined in this review, the RAPID array and subsequent observational and modeling studies have demonstrated that on intra-annual timescales there is very large AMOC variability (see point 1 in section 4.4). This AMOC variability is directly related to the

local wind field (Ekman transports and wind-induced heaving of isopycnals) and thus exhibits little meridional coherence (see point 2 in section 4.4) and has little predictability. Moreover, it is not clear that on such short timescales the AMOC and its associated OHT are expressed in SST variability and can thus affect the atmosphere above (see section 2.4). On longer timescales (interannual to decadal) AMOC variability is much smaller (order 1 Sv) and is associated with the relatively slowly varying ocean density field (see point 3 of section 4.4), which has considerable memory. Moreover, these are the timescales that the AMOC and associated Atlantic OHT variability may impact SST and thus the atmosphere above (see section 2.4). However, the extent to which predictability of AMOC can be leveraged for prediction of meteorological variables over land is much less clear. Fundamentally, this is because atmosphere-ocean coupling in middle latitudes is much weaker than in the tropics.

We discuss these issues in the context of two interrelated questions:

1. Does the AMOC possess any predictability, and if so, what are its predictability horizons? How does predictability of the AMOC compare to that of SST or UOHC?
2. Can any predictability in the AMOC and/or Atlantic SST be leveraged for predictability of atmospheric variables, such as air temperature and precipitation?

6.2.1. Does the AMOC Possess Any Predictability?

The RAPID AMOC estimate at 26.5°N provides an observational data set against which seasonal to interannual AMOC hindcasts and predictions can be evaluated. However, as discussed at the beginning of this section, large intra-annual variability in the AMOC is the direct response to local wind variability and thus is thought to have little predictability [*Sinha et al.*, 2013]. Attempts to predict AMOC anomalies on intra-annual to interannual timescales have yielded mixed results, with various studies differing on whether skillful predictions can be made. *Matei et al.* [2012a] report skill for up to 4–5 years, as measured by correlations between observed and modeled monthly mean AMOC transport anomalies at various lead times. This predictability appears to originate from the Upper Mid-Ocean component of the AMOC, associated with east-west density differences; the eastern influence dominates, likely because the seasonal cycle of the AMOC is dominated by the eastern boundary at this latitude [*Chidichimo et al.*, 2010; *Kanzow et al.*, 2010]. *Vecchi et al.* [2012] argue that the predictability seen by *Matei et al.* [2012a] is due to the dominance of the seasonal cycle over the short observational record and question whether *Matei et al.* [2012a] outperform reference forecasts based on the seasonal cycle (but see the reply by *Matei et al.* [2012b]).

As the RAPID AMOC time series is only about a decade long, we lack AMOC observations to evaluate decadal AMOC hindcasts and predictions. Thus, two main approaches have been utilized: (1) the "perfect model" approach and (2) initialized predictions. Statistical models have also been utilized to estimate predictability of SST and the AMOC, including linear inverse models based on observations [*Zanna*, 2012; *Wunsch*, 2013] and regression models trained on coupled climate model integrations [*Branstator et al.*, 2012; *Branstator and Teng*, 2012; *DelSole et al.*, 2013; *Branstator and Teng*, 2014].

In the perfect model approach, a large ensemble of simulations is created by adding small random perturbations to the model's atmospheric initial conditions and assessing how well ensemble members track the original, unperturbed model evolution. Such studies find potential predictability of the AMOC several years to decades in advance (see Figure 14a) [*Griffies and Bryan*, 1997a, 1997b; *Collins and Sinha*, 2003; *Pohlmann et al.*, 2004; *Collins et al.*, 2006; *Hawkins and Sutton*, 2008; *Msadek et al.*, 2010], but the degree of predictability is found to depend on the initial state of the AMOC [*Msadek et al.*, 2010; *Hermanson and Sutton*, 2010]. Perfect model experiments are limited in the sense that predictability depends on the model utilized. Furthermore, these experiments assume perfect knowledge of ocean initial conditions; hence, they show only potential predictability, rather than the predictability that can be realized with the present ocean observational network. More realistic simulations have been carried out in which observations are only supplied in certain areas [*Dunstone and Smith*, 2010]. Observations over the top 2 km of the ocean, in particular in the subpolar gyre of the North Atlantic, appear to be a key source of information required to initialize the system; in contrast, the initial state of the atmosphere plays a small role (see Figures 14b and 14c).

Predictions made with models initialized with observations have the potential to assess predictability of the AMOC in a more realistic setting. However, model drift is a substantial limitation, as models initialized with observations tend to drift back to their own climatologies. Anomaly initialization can reduce drift by initializing the model near its own climatology [*Smith et al.*, 2007; *Keenlyside et al.*, 2008; *Pohlmann et al.*, 2009; *Robson et al.*, 2012; *Kröger et al.*, 2012]. Alternatively, model drift can be estimated from ensembles and removed

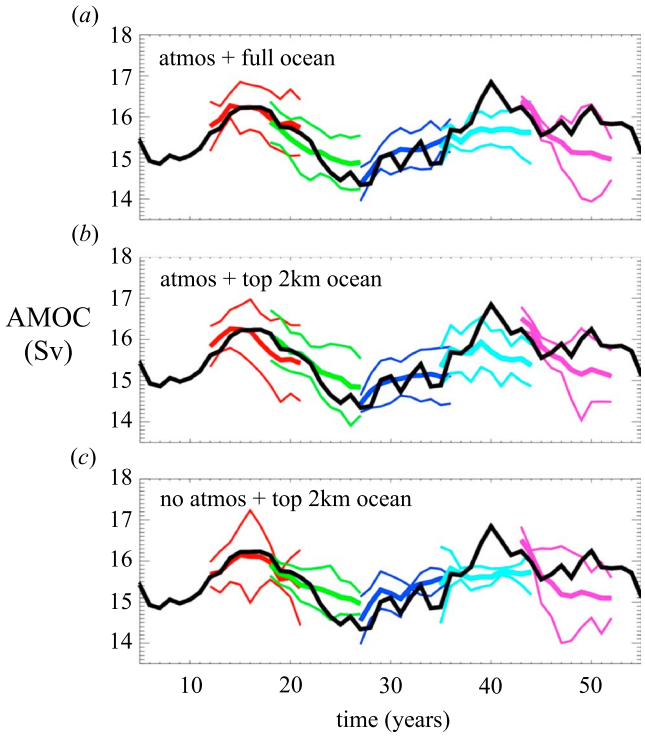

Figure 14. Idealized coupled model experiments to explore the predictability of the AMOC at 30°N (1000 m depth) when an ensemble is created with knowledge of (a) all variables in the atmosphere and ocean instantaneously, (b) monthly mean ocean temperature and salinity data globally in the top 2000 m and atmospheric information (6-hourly surface pressure, three-dimensional winds, and potential temperature), and (c) only monthly mean ocean temperature and salinity data globally in the top 2000 m (no atmospheric data). The black line shows the evolution of the original control run (the "truth"), different colored thick lines represent the ensemble mean of the different hindcast start dates, and the thin lines show the 90% confidence interval assessed from the spread of the ensemble members. Note that skill in predicting the AMOC evolution, as assessed by the root-mean-square error statistic, is similar between all three experiments, meaning that specifying temperature and salinity in the top 2000 m is sufficient to predict the evolution of the AMOC at this latitude. Figure provided by N. Dunstone [from *Dunstone*, 2014], modified from *Dunstone and Smith* [2010].

during data processing [*CLIVAR* 2011; *Yeager et al.*, 2012]. Since direct AMOC observations against which hindcasts can be compared are not available on decadal timescales, predictions are compared to ocean reanalyses from the same model [*Kröger et al.*, 2012; *Tiedje et al.*, 2012] or "independent" ocean state estimates [*Pohlmann et al.*, 2009, 2013]. The former generally shows a higher degree of "potential predictability," while the latter is an independent means of evaluation, but predictability is affected by errors in both the models used to produce predictions and the reference ocean state estimate. Some initialized prediction systems find predictability of the AMOC on interannual to decadal timescales [*Keenlyside et al.*, 2008], whereas others exhibit little skill beyond persistence or a trend [*Pohlmann et al.*, 2009; *Kröger et al.*, 2012]. These differences likely depend on the model, initialization technique, and forecast verification method. Furthermore, predictability of the AMOC and Atlantic OHT varies strongly with latitude; *Tiedje et al.* [2012] find potential predictability of 3–5 years in the gyre interiors and little predictability on the gyre boundaries.

In summary, perhaps counterintuitively, prediction of intra-annual to interannual variability of the AMOC may be a much tougher proposition than the decadal problem. This is because it relies much more strongly on the ability to predict changes in the wind field on these timescales [*Sinha et al.*, 2013]. This is very difficult given the essentially random nature of synoptic eddies in middle latitudes. Moreover, it is not clear that on such short timescales the AMOC and its associated heat transport are expressed in SST variability and can affect the atmosphere above. In contrast, on decadal timescales AMOC variations are associated with the slowly varying density field and thus are likely to have predictability. Furthermore, on these timescales SST and perhaps the atmosphere above are much more likely to be driven by the ocean, rather than the other way around.

Yet prediction systems have evolved from consideration of short timescales (numerical weather prediction) to increasingly longer timescales, at which ocean dynamics become more important. For these reasons we suggest that SST and UOHC may be more useful metrics for predictability studies [e.g., *Smith et al.*, 2007; *Pohlmann et al.*, 2009; *Yeager et al.*, 2012; *Branstator et al.*, 2012; *Branstator and Teng*, 2012; *Kröger et al.*, 2012; *Robson et al.*, 2012; *DelSole et al.*, 2013; *Hu et al.*, 2013; *Karspeck et al.*, 2014; *Hermanson et al.*, 2014; *Bombardi et al.*, 2014] than the AMOC. In short, UOHC reflects an integration of air-sea heat fluxes and ocean transports and thus does not have the issue of large, but arguably irrelevant, transport anomalies driven by the instantaneous wind field that are present in AMOC variability. By analyzing long control integrations of nine coupled GCMs, *Branstator and Teng* [2014] find that predictability of the annual mean AMOC (about a decade) is less than that of North Atlantic UOHC, a fact which they attribute to the substantial high-frequency variability present in the AMOC. *Pohlmann et al.* [2009] show that a coupled model initialized with the GECCO state estimate is able to make skillful predictions of North Atlantic SST and UOHC on interannual to decadal timescales, but AMOC predictions are only more skillful than damped persistence on timescales of about 5 years. SST and UOHC may be preferred predictability metrics since these quantities are better constrained by observations than the AMOC, providing more accurate data sets against which predictions can be evaluated. Furthermore, the AMOC is often poorly represented in models used to make decadal predictions.

Before proceeding, we return to the question of whether observations of the ocean circulation, specifically the AMOC, can be used as an "early warning" for future SST changes and atmospheric and climate impacts. The focus of monitoring the AMOC is in part due to the hypothesis that AMOC variations may lead variations in SST and UOHC, imparting some predictability in these quantities by virtue of time lags, even in the absence of the ability to accurately predict the AMOC. Unfortunately, separating the climate-relevant AMOC signal from the large, local wind-driven variations is extremely difficult, particularly given the short observational record. However, if, as we have argued in this review, the TZ is important in low-frequency AMOC variability, monitoring and predicting UOHC anomalies in this region may be important for predicting low-frequency, climate-relevant variability of the AMOC and potentially for decadal variability of SST in the entire North Atlantic region. The importance of monitoring the subpolar gyre for AMOC predictions has been noted previously [*Häkkinen and Rhines*, 2004; *Bingham et al.*, 2007; *Tziperman et al.*, 2008; *Hawkins and Sutton*, 2009; *Zhang*, 2010b; *Zanna et al.*, 2011; *Buckley et al.*, 2012]. For example, *Mahajan et al.* [2011] use fingerprints of AMOC variability on subsurface temperature and SSH (derived from CM2.1), which have significant anomalies in the TZ region, to predict interannual AMOC variations.

6.2.2. Can Ocean Predictability Be Leveraged for Atmospheric Predictability?

On seasonal to interannual timescales the NAO and atmospheric blocking [*Häkkinen et al.*, 2011b] are the biggest players influencing the climate of the North Atlantic and surrounding landmasses. The NAO is generally thought to be driven by internal atmospheric processes, and current forecast systems exhibit little or no skill in predicting the NAO. Despite this, an experimental coupled forecast system currently being developed at the UK Met Office exhibits modest skill in predicting the wintertime NAO from initializations in November [*Scaife et al.*, 2011, 2014]. Analyses of extreme events, such as the record-breaking cold, negative NAO winters of 2009–2010, indicate that there may be some periods in which the NAO responds more strongly to SST anomalies, rather than being primarily forced by internal atmospheric processes. Experiments with an atmospheric model forced by observed SST anomalies indicate that North Atlantic SST did not substantially contribute to the development of the negative NAO and cold winter of 2009–2010, but SST anomalies did contribute to the negative NAO phase in November and December 2010 [*Maidens et al.*, 2013; *Buchan et al.*, 2014]. The reemergence of SST anomalies in the North Atlantic likely contributed to the development of a SST pattern that favored the persistence of the negative NAO pattern [*Taws et al.*, 2011; *Buchan et al.*, 2014; *Blaker et al.*, 2015]. The reemergence of locally forced SST anomalies likely dominates since on these timescales the ocean circulation is thought to have only a modest impact on SST and the atmospheric circulation. Despite this, several studies [*Maidens et al.*, 2013; *Cunningham et al.*, 2013; *Bryden et al.*, 2014] boldly argue that the temporary reduction in strength of the AMOC observed by the RAPID array during 2009/2010 led to a cooling of the subtropical Atlantic and, furthermore, that this may have contributed to the anomalously cold winter in northern Europe the following year. These results have not yet been reproduced by other forecast centers. Should they stand the test of time, current perceptions of midlatitude predictability on seasonal-to-interannual timescales, and the role of the ocean therein, will have to be modified substantially.

On decadal timescales there is considerable evidence that variability of the ocean circulation, including the AMOC, plays an important role in setting SST anomalies, with possible impacts on a host of other climate

variables, including surface air temperature, precipitation, and winds. For example, *Pohlmann et al.* [2009] find that predictability of surface air temperature tends to be higher over the oceans, in particular in regions with high SST predictability, such as the North Atlantic. The importance of SST anomalies on predictions of atmospheric quantities can also be seen by quantifying the impact of ocean initialization on decadal prediction experiments. Initialization of coupled models with observed SST anomalies can lead to significantly improved decadal predictions over the North Atlantic, North America, western Europe, and northern Africa [*Keenlyside et al.*, 2008; *Müller et al.*, 2012, 2014].

7. Conclusions and Outlook

The AMOC is a shorthand, zonally averaged description of the three-dimensional, time-dependent circulation of the Atlantic Ocean. The Atlantic is arguably the ocean's most complex basin, with the circulation reflecting a fascinating interplay between wind and buoyancy driven flows, as well as eddies and mixing. As we have seen, AMOC dynamics, both in its mean and variability, reflect this fundamental complexity and are not fully understood. Nevertheless, observational programs, such as RAPID, and models of ever increasing resolution, complexity, and fidelity have yielded the following robust features of the AMOC and its variability:

1. Large systematic changes in AMOC have not been observed over the last 50 years. However, the AMOC exhibits considerable variability on intra-annual and seasonal timescales, which can be as large as the mean. On interannual to decadal timescales, the variability is much smaller and does not exhibit a significant trend.
2. The Ekman component of the AMOC plays a significant role on short timescales, while the geostrophic component, reflecting east-west density contrasts across the basin, dominates on interannual to decadal timescales. Buoyancy anomalies in the upper kilometer of the ocean in the transition zone (TZ), at the terminus of the separated Gulf Stream just off the Grand Banks, appear to play a key role in decadal variability of the AMOC.
3. On short timescales, meridional coherence of the AMOC is limited to that of the wind field, while on longer timescales (decadal and longer) the AMOC exhibits increasing meridional coherence.
4. The mechanisms driving the AMOC clearly depend on timescale. Winds dominate on short timescales, but on decadal timescales the AMOC appears to be controlled by buoyancy anomalies that reach the TZ. The TZ is a place where water masses from many disparate regions of the Atlantic converge, with myriad processes contributing. It is therefore, perhaps, not surprising that decadal AMOC variability differs greatly across models and within the same model when its parameters are changed.

Despite being confined to the rather small Atlantic Basin, the AMOC plays a central role in climate. For example, the mean position of the Intertropical Convergence Zone in the Northern Hemisphere is thought to be the result of the northward cross-equatorial ocean heat transport achieved by the AMOC. The AMOC is a key means by which anthropogenic heat and carbon can be transported from the surface to the deep ocean, and thus the AMOC modulates the trajectory of climate change. On decadal timescales, variability of the AMOC has been linked to low-frequency variability of Atlantic sea surface temperatures, termed the Atlantic Multidecadal Oscillation/Variability, with a host of implications for climate variability over surrounding landmasses.

Such climate impacts are prime motivators for exploring whether and on what timescales the AMOC might be predictable. Our view is that predicting intra-annual to interannual variability of AMOC is a very challenging proposition because it depends on predictability of the midlatitude wind stress, which is dominated by chaotic synoptic systems. Somewhat counterintuitively, perhaps, decadal predictability of AMOC and its associated climate signals has a firmer mechanistic underpinning and is a tantalizing possibility, although it has yet to be realized. As an indication of the potential importance of predicting the AMOC, some studies have suggested that the recent "hiatus" in warming of global mean surface temperature (little warming since 1998) is due to variations in the Atlantic Ocean circulation [*Tung and Zhou*, 2013; *Chen and Tung*, 2014; *Steinman et al.*, 2015]. However, other studies suggest the importance of the Pacific [*Trenberth and Fasullo*, 2013; *Trenberth et al.*, 2014; *England et al.*, 2014] and changes in external forcing [*Solomon et al.*, 2010, 2011; *Kaufmann et al.*, 2011]; yet others suggest that the SST hiatus may, in fact, be an artifact due to data biases [*Karl et al.*, 2015]. Furthermore, *Meehl et al.* [2014] claim that the hiatus would have been predictable had decadal predictions been run in 1998. Thus, understanding and potentially predicting internal climate variability, including variability of the AMOC, has potential to aid in making accurate climate projections, even on a global scale.

Finally, just as RAPID drove the community to a deeper understanding of North Atlantic ocean variability, observational programs directed at other components of the AMOC are now being planned and implemented [*Cunningham and Marsh*, 2010; *Srokosz et al.*, 2012; *Blunden and Arndt*, 2013]. A pilot array has recently been deployed in the South Atlantic at 34.5°S [*Meinen et al.*, 2013]. Measuring the AMOC and its variability at this latitude has the potential to enhance understanding of the stability of the AMOC and the connection between the AMOC and other ocean basins. An array in the subpolar North Atlantic was deployed in the summer of 2014 as part of the Overturning in the Subpolar North Atlantic Program. The purpose of this array, which extends from Labrador to the Scottish coast, is to provide a continuous record of the full-water column, trans-basin fluxes of heat, mass, and freshwater; determine overflow water pathways; and, in conjunction with other observational arrays, assess the meridional coherence of the AMOC.

Glossary

AHT:	atmospheric heat transport.
AMOC:	Atlantic Meridional Overturning Circulation.
AMV:	Atlantic Multidecadal Variability.
CCSM3, CCSM4:	Community Climate System Model, versions 3 and 4.
CFC:	chlorofluorocarbons.
CMIP5:	Coupled Model Intercomparison Project, version 5.
CM2.1:	GFDL Coupled Model, version 2.1.
DWBC:	Deep Western Boundary Current.
EMIC:	Earth system models of intermediate complexity.
ECCO:	Estimating the Circulation and Climate of the Ocean (ocean state estimate).
FWT:	freshwater transport.
GCM:	general circulation model.
GECCO:	German Estimating the Circulation and Climate of the Ocean (ocean state estimate).
GRACE:	Gravity Recovery and Climate Experiment (satellite).
HadCM3:	Hadley Centre Coupled Model, version 3.
HadISST:	Hadley Centre Sea Ice and Sea Surface Temperature data set.
ITCZ:	Intertropical Convergence Zone.
IPCC:	Intergovernmental Panel on Climate Change.
LSW:	Labrador Sea Water.
MLD:	mixed layer depth.
MOC:	Meridional Overturning Circulation.
MOCHA:	Meridional Overturning and Heatflux Array.
NAC:	North Atlantic Current.
NADW:	North Atlantic Deep Water.
NAO:	North Atlantic Oscillation.
NH:	Northern Hemisphere.
OHT:	ocean heat transport.
RAPID:	Rapid Climate Change.
SSH:	sea surface height.
SST:	sea surface temperature.
SH:	Southern Hemisphere.
TZ:	transition zone.
UOHC:	upper ocean heat content.

Acknowledgments

The data presented in this paper are available by request to M.B. (marthabuckley@gmail.com). Funding for M.B. at AER was provided by NOAA grants NA10OAR4310199 and NA13OAR4310134 (Climate Variability and Predictability). Funding for continuation of this work by M.B. at GMU was provided by NOAA (NA150AR4310100, NA09OAR4310058, and NA14OAR4310160), NSF (1338427), and NASA (NNX14AM19G). J.M. thanks the NASA MAPP program for their support. We would like to acknowledge Rong Zhang, Young-Oh Kwon, Ross Tulloch, Brian Green, and Nicholas Barrier for making figures for this paper, as well as Rym Msadek, Bill Johns, and You-Soon Chang for providing data. We would also like to thank Susan Lozier, Ed Schneider, Wilbert Weijer, Laurie Trenary, the Editor of *Reviews of Geophysics*, and two anonymous reviewers for providing helpful comments on the manuscript. Finally, we would like to acknowledge the support of the U.S. AMOC program and the U.S. AMOC Science Teams. Figure 1 has been made by using NCAR Command Language (version 6.0.0, 2011, Boulder, Colorado, UCAR/NCAR/CISL/VETS, http://dx.doi.org/10.5065/D6WD3XH5).

References

Abernathey, R., J. Marshall, and D. Ferreira (2011), The dependence of Southern Ocean meridional overturning on wind stress, *J. Phys. Oceanogr.*, *41*(12), 2261–2278, doi:10.1175/JPO-D-11-023.1.

Abraham, J. P., et al. (2013), A review of global ocean temperature observations: Implications for ocean heat content estimates and climate change, *Rev. Geophys.*, *51*(3), 450–483, doi:10.1002/rog.20022.

Alexander, M. A., and C. Deser (1995), A mechanism for the recurrence of wintertime midlatitude SST anomalies, *J. Phys. Oceanogr.*, *25*(1), 122–137, doi:10.1175/1520-0485(1995)025<0122:AMFTRO>2.0.CO;2.

Alley, R., et al. (2002), *Abrupt Climate Change: Inevitable Surprises*, Natl. Acad. Press, Washington, D. C.

Alley, R. B. (2007), Wally was right: Predictive ability of the North Atlantic "conveyor belt" hypothesis for abrupt climate change, *Ann. Rev. Earth Planet. Sci.*, *35*(1), 241–272, doi:10.1146/annurev.earth.35.081006.131524.

Andrews, T., J. M. Gregory, M. J. Webb, and K. E. Taylor (2012), Forcing, feedbacks and climate sensitivity in CMIP5 coupled atmosphere-ocean climate models, *Geophys. Res. Lett.*, *39*, L09712, doi:10.1029/2012GL051607.

Ansorge, I. J., et al. (2014), Basin-wide oceanographic array bridges the South Atlantic, *Eos Trans. AGU*, *95*(6), 53–54, doi:10.1002/2014EO060001.

Arzel, O., T. Huck, and A. Colin de Verdiére (2006), The different nature of the interdecadal variability of the thermohaline Circulation under mixed and flux boundary conditions, *J. Phys. Oceanogr.*, *36*(9), 1703–1718, doi:10.1175/JPO2938.1.

Atkinson, C., H. Bryden, S. Cunningham, and B. King (2012), Atlantic transport variability at 25°N in six hydrographic sections, *Ocean Sci.*, *8*(4), 497–523.

Atlas, R., R. N. Hoffman, J. Ardizzone, S. M. Leidner, J. C. Jusem, D. K. Smith, and D. Gombos (2011), A cross-calibrated, multiplatform ocean surface wind velocity product for meteorological and oceanographic applications, *Bull. Am. Meteorol. Soc.*, *92*(2), 157–174, doi:10.1175/2010BAMS2946.1.

Baehr, J. (2011), Detecting changes in the meridional overturning circulation at 26°N in the Atlantic from observations, *Deep Sea Res., Part II*, *58*(17–18), 1833–1836, doi:10.1016/j.dsr2.2010.10.062.

Baehr, J., J. Hirschi, J.-O. Beismann, and J. Marotzke (2004), Monitoring the meridional overturning circulation in the North Atlantic: A model-based array design study, *J. Mar. Res.*, *62*, 283–312, doi:10.1357/0022240041446191.

Baehr, J., H. Haak, S. Alderson, S. A. Cunningham, J. H. Jungclaus, and J. Marotzke (2007), Timely detection of changes in the Meridional Overturning Circulation at 26°N in the Atlantic, *J. Clim.*, *20*(23), 5827–5841, doi:10.1175/2007JCLI1686.1.

Balan Sarojini, B., J. M. Gregory, R. Tailleux, G. R. Bigg, A. T. Blaker, D. R. Cameron, N. R. Edwards, A. P. Megann, L. C. Shaffrey, and B. Sinha (2011), High frequency variability of the Atlantic meridional overturning circulation, *Ocean Sci.*, *7*(4), 471–486, doi:10.5194/os-7-471-2011.

Balmaseda, M. A., G. C. Smith, K. Haines, D. Anderson, T. N. Palmer, and A. Vidard (2007), Historical reconstruction of the Atlantic Meridional Overturning Circulation from the ECMWF operational ocean reanalysis, *Geophys. Res. Lett.*, *34*, L23615, doi:10.1029/2007GL031645.

Balmaseda, M. A., K. Mogensen, and A. T. Weaver (2013), Evaluation of the ECMWF ocean reanalysis system ORAS4, *Q. J. R. Meteorol. Soc.*, *139*(674), 1132–1161, doi:10.1002/qj.2063.

Baringer, M. O., and S. L. Garzoli (2007), Meridional heat transport determined with expendable bathythermograph—Part I: Error estimates from model and hydrographic data, *Deep Sea Res., Part I*, *54*(8), 1390–1401, doi:10.1016/j.dsr.2007.03.011.

Barsugli, J. J., and D. S. Battisti (1998), The basic effects of atmosphere–ocean thermal coupling on midlatitude variability, *J. Atmos. Sci.*, *55*(4), 477–493, doi:10.1175/1520-0469(1998)055<0477:TBEOAO>2.0.CO;2.

Beismann, J.-O., and B. Barnier (2004), Variability of the meridional overturning circulation of the North Atlantic: Sensitivity to overflows of dense water masses, *Ocean Dyn.*, *54*(1), 92–106, doi:10.1007/s10236-003-0088-x.

Bentsen, M., H. Drange, T. Furevik, and T. Zhou (2004), Simulated variability of the Atlantic meridional overturning circulation, *Clim. Dyn.*, *22*(6–7), 701–720, doi:10.1007/s00382-004-0397-x.

Biastoch, A., and C. W. Böning (2013), Anthropogenic impact on Agulhas leakage, *Geophys. Res. Lett.*, *40*, 1138–1143, doi:10.1002/grl.50243.

Biastoch, A., C. W. Böning, and J. R. E. Lutjeharms (2008a), Agulhas leakage dynamics affects decadal variability in Atlantic overturning circulation, *Nature*, *456*, 489–492, doi:10.1038/nature07426.

Biastoch, A., C. W. Böning, J. Getzlaff, J.-M. Molines, and G. Madec (2008b), Causes of interannual-decadal variability in the meridional overturning circulation of the midlatitude North Atlantic Ocean, *J. Clim.*, *21*, 6599–6615, doi:10.1175/2008JCLI2404.1.

Biastoch, A., C. W. Boning, F. U. Schwarzkopf, and J. R. E. Lutjeharms (2009), Increase in Agulhas leakage due to poleward shift of Southern Hemisphere westerlies, *Nature*, *462*(7272), 495–498.

Bingham, R., C. Hughes, V. Roussenov, and R. Williams (2007), Meridional coherence of the North Atlantic meridional overturning circulation, *Geophys. Res. Lett.*, *34*, L23606, doi:10.1029/2007GL031731.

Bingham, R. J., and C. W. Hughes (2009), Signature of the Atlantic meridional overturning circulation in sea level along the east coast of North America, *Geophys. Res. Lett.*, *36*, L02603, doi:10.1029/2008GL036215.

Bjerknes, J. (1964), Atlantic air-sea interaction, *Adv. Geophys.*, *10*, 1–82, doi:10.1016/S0065-2687(08)60005-9.

Blaker, A., J. J. M. Hirschi, G. McCarthy, B. Sinha, S. Taws, R. Marsh, A. Coward, and B. de Cuevas (2015), Historical analogues of the recent extreme minima observed in the Atlantic meridional overturning circulation at 26°N, *Clim. Dyn.*, *44*(1–2), 457–473, doi:10.1007/s00382-014-2274-6.

Blunden, J., and D. S. Arndt (2013), State of the climate in 2012, *Bull. Am. Meteorol. Soc.*, *94*(8), S1–S258, doi:10.1175/2013BAMSStateoftheClimate.1.

Boccaletti, G., R. Ferrari, A. Adcroft, D. Ferreira, and J. Marshall (2005), The vertical structure of ocean heat transport, *Geophys. Res. Lett.*, *32*, L10603, doi:10.1029/2005GL022474.

Boé, J., A. Hall, and X. Qu (2009), Deep ocean heat uptake as a major source of spread in transient climate change simulations, *Geophys. Res. Lett.*, *36*, L22701, doi:10.1029/2009GL040845.

Bombardi, R. J., et al. (2014), Evaluation of the CFSv2 CMIP5 decadal predictions, *Clim. Dyn.*, *44*, 543–557, doi:10.1007/s00382-014-2360-9.

Böning, C. W., M. Scheinert, J. Dengg, A. Biastoch, and A. Funk (2006), Decadal variability of subpolar gyre transport and its reverberation in the North Atlantic overturning, *Geophys. Res. Lett.*, *33*, L21S01, doi:10.1029/2006GL026906.

Booth, B., N. Dunstone, P. Halloran, T. Andrews, and N. Bellouin (2012), Aerosols implicated as the primary driver of twentieth-century North Atlantic climate variability, *Nature*, *484*, 228–232, doi:10.1038/nature10946.

Bower, A. S., and M. S. Lozier (1994), A closer look at particle exchange in the Gulf Stream, *J. Phys. Oceanogr.*, *24*(6), 1399–1418, doi:10.1175/1520-0485(1994)024<1399:ACLAPE>2.0.CO;2.

Bower, A. S., H. T. Rossby, and J. L. Lillibridge (1985), The Gulf Stream—Barrier or blender?, *J. Phys. Oceanogr.*, *15*(1), 24–32, doi:10.1175/1520-0485(1985)015<0024:TGSOB>2.0.CO;2.

Bower, A. S., M. S. Lozier, S. F. Gary, and C. W. Böning (2009), Interior pathways of the North Atlantic meridional overturning circulation, *Nature*, *459*, 243–247, doi:10.1038/nature07979.

Bower, A. S., S. Lozier, and S. Gary (2011), Export of Labrador Sea Water from the subpolar North Atlantic: A Lagrangian perspective, *Deep Sea Res., Part II*, *58*, 1798–1818, doi:10.1016/j.dsr2.2010.10.060.

Brambilla, E., and L. D. Talley (2006), Surface drifter exchange between the North Atlantic subtropical and subpolar gyres, *J. Geophys. Res.*, *111*, C07026, doi:10.1029/2005JC003146.

Branstator, G., and H. Teng (2012), Potential impact of initialization on decadal predictions as assessed for CMIP5 models, *Geophys. Res. Lett.*, *39*, L12703, doi:10.1029/2012GL051974.

Branstator, G., and H. Teng (2014), Is AMOC more predictable than North Atlantic heat content?, *J. Clim.*, *27*(10), 3537–3550, doi:10.1175/JCLI-D-13-00274.1.

Branstator, G., H. Teng, G. A. Meehl, M. Kimoto, J. R. Knight, M. Latif, and A. Rosati (2012), Systematic estimates of initial-value decadal predictability for six AOGCMs, *J. Clim.*, *25*(6), 1827–1846, doi:10.1175/JCLI-D-11-00227.1.

Broecker, W. S. (1991), The great ocean conveyor, *Oceanography*, *4*, 79–89.

Broecker, W. S. (1997), Thermohaline circulation, the Achilles heel of our climate system: Will man-made CO_2 upset the current balance?, *Science*, *278*(5343), 1582–1588.

Broecker, W. S. (1998), Paleocean circulation during the last deglaciation: A bipolar seesaw?, *Paleoceanography*, *13*(2), 119–121, doi:10.1029/97PA03707.

Broecker, W. S. (2003), Does the trigger for abrupt climate change reside in the ocean or in the atmosphere?, *Science*, *300*(5625), 1519–1522.

Broecker, W. S. (2007), Musings about the connection between thermohaline circulation and climate, in *Ocean Circulation: Mechanisms and Impacts—Past and Future Changes of Meridional Overturning*, edited by A. Schmittner, J. C. H. Chiang, and S. R. Hemming, pp. 265–278, AGU, Washington, D. C., doi:10.1029/173GM17.

Bryan, F. O., P. R. Gent, and R. Tomas (2013), Can Southern Ocean eddy effects be parameterized in climate models?, *J. Clim.*, *27*(1), 411–425, doi:10.1175/JCLI-D-12-00759.1.

Bryan, K. (1962), Measurements of meridional heat transport by ocean currents, *J. Geophys. Res.*, *67*(9), 3403–3414, doi:10.1029/JZ067i009p03403.

Bryden, H. L. (1993), Ocean heat transport across 24°N latitude, in *Interactions Between Global Climate Subsystems: The Legacy of Hann*, edited by G. A. McBean and M. Hantel, pp. 65–75, AGU, Washington, D. C., doi:10.1029/GM075p0065.

Bryden, H. L., and M. M. Hall (1980), Heat transport by currents across 25°N latitude in the Atlantic Ocean, *Science*, *207*(4433), 884–886, doi:10.1126/science.207.4433.884.

Bryden, H. L., H. Longworth, and S. Cunningham (2005), Slowing of the Atlantic meridional overturning circulation at 25°N, *Nature*, *438*, 655–657, doi:10.1038/nature04385.

Bryden, H. L., A. Mujahid, S. A. Cunningham, and T. Kanzow (2009), Adjustment of the basin-scale circulation at 26°N to variations in Gulf Stream, deep western boundary current and Ekman transports as observed by the RAPID array, *Ocean Sci.*, *5*(4), 421–433, doi:10.5194/os-5-421-2009.

Bryden, H. L., B. A. King, and G. D. McCarthy (2011), South Atlantic overturning circulations at 24°S, *J. Mar. Res.*, *69*(1), 39–56, doi:10.1357/002224011798147633.

Bryden, H. L., B. A. King, G. D. McCarthy, and E. L. McDonagh (2014), Impact of a 30% reduction in Atlantic meridional overturning during 2009–2010, *Ocean Sci.*, *10*, 683–691, doi:10.5194/os-10-683-2014.

Buchan, J., J. J. M. Hirschi, A. T. Blaker, and B. Sinha (2014), North Atlantic SST anomalies and the cold North European weather events of winter 2009/10 and December 2010, *Mon. Weather Rev.*, *142*(2), 922–932, doi:10.1175/MWR-D-13-00104.1.

Buckley, M. W., D. Ferreira, J.-M. Campin, J. Marshall, and R. Tulloch (2012), On the relationship between decadal buoyancy anomalies and variability of the Atlantic Meridional Overturning Circulation, *J. Clim.*, *25*, 8009–8030, doi:10.1175/JCLI-D-11-00505.1.

Buckley, M. W., R. M. Ponte, G. Forget, and P. Heimbach (2014a), Low-frequency SST and upper-ocean heat content variability in the North Atlantic, *J. Clim.*, *27*(13), 4996–5018, doi:10.1175/JCLI-D-13-00316.1.

Buckley, M. W., R. M. Ponte, G. Forget, and P. Heimbach (2014b), Corrigendum, *J. Clim.*, *27*(19), 7502–7525, doi:10.1175/JCLI-D-14-00523.1.

Buckley, M. W., R. M. Ponte, G. Forget, and P. Heimbach (2015), Determining the origins of advective heat transport convergence variability in the North Atlantic, *J. Clim.*, *28*(10), 3943–3956, doi:10.1175/JCLI-D-14-00579.1.

Burkholder, K. C., and M. S. Lozier (2011a), Subtropical to subpolar pathways in the North Atlantic: Deductions from Lagrangian trajectories, *J. Geophys. Res.*, *116*, C07017, doi:10.1029/2010JC006697.

Burkholder, K. C., and M. S. Lozier (2011b), Mid-depth Lagrangian pathways in the North Atlantic and their impact on the salinity of the eastern subpolar gyre, *Deep Sea Res., Part I*, *58*(12), 1196–1204, doi:10.1016/j.dsr.2011.08.007.

Burkholder, K. C., and M. S. Lozier (2014), Tracing the pathways of the upper limb of the North Atlantic Meridional Overturning Circulation, *Geophys. Res. Lett.*, *41*, 4254–4260, doi:10.1002/2014GL060226.

Cabanes, C., T. Lee, and L.-L. Fu (2008), Mechanisms of interannual variations of the Meridional Overturning Circulation of the North Atlantic Ocean, *J. Phys. Oceanogr.*, *38*(2), 467–480, doi:10.1175/2007JPO3726.1.

Carton, J. A., and A. Santorelli (2008), Global decadal upper-ocean heat content as viewed in nine analyses, *J. Clim.*, *21*(22), 6015–6035, doi:10.1175/2008JCLI2489.1.

Cayan, D. R. (1992a), Latent and sensible heat flux anomalies over the northern oceans: Driving the sea surface temperature, *J. Phys. Oceanogr.*, *22*(8), 859–881, doi:10.1175/1520-0485(1992)022<0859:LASHFA>2.0.CO;2.

Cayan, D. R. (1992b), Latent and sensible heat flux anomalies over the northern oceans: The connection to monthly atmospheric circulation, *J. Clim.*, *5*(4), 354–369, doi:10.1175/1520-0442(1992)005<0354:LASHFA>2.0.CO;2.

Challenor, P. G., P. Cipollini, and D. Cromwell (2001), Use of the 3D Radon transform to examine the properties of oceanic Rossby waves, *J. Atmos. Oceanic Technol.*, *18*(9), 1558–1566, doi:10.1175/1520-0426(2001)018<1558:UOTRTT>2.0.CO;2.

Chang, Y.-S., S. Zhang, A. Rosati, T. L. Delworth, and W. F. Stern (2012), An assessment of oceanic variability for 1960–2010 from the GFDL ensemble coupled estimate, *Clim. Dyn.*, *40*(3–4), 775–803, doi:10.1007/s00382-012-1412-2.

Chelton, D. B., and M. G. Schlax (1996), Global observations of oceanic Rossby waves, *Science*, *272*(5259), 234–238, doi:10.1126/science.272.5259.234.

Chen, F., and M. Ghil (1996), Interdecadal variability in a hybrid coupled ocean-atmosphere model, *J. Phys. Oceanogr.*, *26*(8), 1561–1578, doi:10.1175/1520-0485(1996)026<1561:IVIAHC>2.0.CO;2.

Chen, H., E. Schneider, and Z. Wu (2015), Mechanisms of internally generated decadal-to-multidecadal variability of SST in the Atlantic Ocean in a coupled GCM, *Clim. Dyn.*,1–30, doi:10.1007/s00382-015-2660-8.

Chen, X., and K.-K. Tung (2014), Varying planetary heat sink led to global-warming slowdown and acceleration, *Science*, *345*(6199), 897–903.

Cheng, W., C. M. Bitz, and J. C. H. Chiang (2007), Adjustment of the global climate to an abrupt slowdown of the Atlantic meridional overturning circulation, in *Ocean Circulation: Mechanisms and Impacts—Past and Future Changes of Meridional Overturning*, pp. 295–313, AGU, Washington, D. C., doi:10.1029/173GM19

Cheng, W., J. C. H. Chiang, and D. Zhang (2013), Atlantic Meridional Overturning Circulation (AMOC) in CMIP5 models: RCP and historical simulations, *J. Clim.*, *26*(18), 7187–7197, doi:10.1175/JCLI-D-12-00496.1.

Chiang, J. H., and C. Bitz (2005), Influence of high latitude ice cover on the marine Intertropical Convergence Zone, *Clim. Dyn.*, *25*(5), 477–496, doi:10.1007/s00382-005-0040-5.

Chidichimo, M. P., T. Kanzow, S. A. Cunningham, W. E. Johns, and J. Marotzke (2010), The contribution of eastern-boundary density variations to the Atlantic meridional overturning circulation at 26.5°N, *Ocean Sci.*, *6*(2), 475–490.

Church, J. A. (2007), A change in circulation?, *Science*, *317*(5840), 908–909, doi:10.1126/science.1147796.

Chylek, P., C. K. Folland, H. A. Dijkstra, G. Lesins, and M. K. Dubey (2011), Ice-core data evidence for a prominent near 20 year time-scale of the Atlantic Multidecadal Oscillation, *Geophys. Res. Lett.*, *38*, L13704, doi:10.1029/2011GL047501.

Chylek, P., C. Folland, L. Frankcombe, H. Dijkstra, G. Lesins, and M. Dubey (2012), Greenland ice core evidence for spatial and temporal variability of the Atlantic Multidecadal Oscillation, *Geophys. Res. Lett.*, *39*, L09705, doi:10.1029/2012GL051241.

Clark, P. U., N. G. Pisias, T. F. Stocker, and A. J. Weaver (2002), The role of the thermohaline circulation in abrupt climate change, *Nature*, *415*(6874), 863–869.

Clément, L., E. Frajka-Williams, Z. B. Szuts, and S. A. Cunningham (2014), Vertical structure of eddies and Rossby waves, and their effect on the Atlantic meridional overturning circulation at 26.5°N, *J. Geophys. Res. Oceans*, *119*, 6479–6498, doi:10.1002/2014JC010146.

CLIVAR (Ed.) (2011), *Data and Bias Correction for Decadal Climate Predictions, CLIVAR Publ. Ser.*, 150 pp., International CLIVAR Project Office. [Available at http://eprints.soton.ac.uk/171975/1/ICPO150_Bias.pdf.]

Colin de Verdiére, A., and T. Huck (1999), Baroclinic instability: An oceanic wavemaker for interdecadal variability, *J. Phys. Oceanogr.*, *29*(5), 893–910.

Collins, M., and B. Sinha (2003), Predictability of decadal variations of the thermohaline circulation and climate, *Geophys. Res. Lett.*, *30*(6), 1306, doi:10.1029/2002GL016504.

Collins, M., et al. (2006), Interannual to decadal climate predictability in the North Atlantic: A multimodel-ensemble study, *J. Clim.*, *19*(7), 1195–1203, doi:10.1175/JCLI3654.1.

Condron, A., and I. A. Renfrew (2013), The impact of polar mesoscale storms on northeast Atlantic Ocean circulation, *Nat. Geosci.*, *6*(1), 34–37, doi:10.1038/NGEO1661.

Cowan, T., and W. Cai (2013), The response of the large-scale ocean circulation to 20th century Asian and non-Asian aerosols, *Geophys. Res. Lett.*, *40*, 2761–2767, doi:10.1002/grl.50587.

Cunningham, S. A., and R. Marsh (2010), Observing and modeling changes in the Atlantic MOC, *WIREs Clim. Change*, *1*(2), 180–191, doi:10.1002/wcc.22.

Cunningham, S. A., et al. (2007), Temporal variability of the Atlantic Meridional Overturning Circulation at 26.5°N, *Science*, *317*, 935–937, doi:10.1126/science.1141304.

Cunningham, S. A., C. D. Roberts, E. Frajka-Williams, W. E. Johns, W. Hobbs, M. D. Palmer, D. Rayner, D. A. Smeed, and G. McCarthy (2013), Atlantic Meridional Overturning Circulation slowdown cooled the subtropical ocean, *Geophys. Res. Lett.*, *40*, 6202–6207, doi:10.1002/2013GL058464.

Curry, R. G., M. S. McCartney, and T. M. Joyce (1998), Oceanic transport of subpolar climate signals to mid-depth subtropical waters, *Nature*, *391*, 575–577.

Czaja, A. (2009), Atmospheric control on the thermohaline circulation, *J. Phys. Oceanogr.*, *39*(1), 234–247, doi:10.1175/2008JPO3897.1.

Czaja, A., and J. Marshall (2001), Observations of atmosphere-ocean coupling in the North Atlantic, *Q. J. R. Meteorol. Soc.*, *127*(576), 1893–1916, doi:10.1002/qj.49712757603.

Czaja, A., and J. Marshall (2006), The partitioning of poleward heat transport between the atmosphere and ocean, *J. Atmos. Sci.*, *63*(5), 1498–1511, doi:10.1175/JAS3695.1.

Danabasoglu, G. (2008), On multidecadal variability of the Atlantic Meridional Overturning Circulation in the Community Climate System Model version 3, *J. Clim.*, *21*(21), 5524–5544, doi:10.1175/2008JCLI2019.1.

Danabasoglu, G., S. Yeager, Y.-O. Kwon, J. Tribbia, A. Phillips, and J. Hurrell (2012), Variability of the Atlantic Meridional Overturning Circulation in CCSM4, *J. Clim.*, *25*, 5153–5172, doi:10.1175/JCLI-D-11-00463.1.

Danabasoglu, G., et al. (2014), North Atlantic simulations in Coordinated Ocean-ice Reference Experiments phase II (CORE-II). Part I: Mean states, *Ocean Model.*, *73*, 76–107, doi:10.1016/j.ocemod.2013.10.005.

Danabasoglu, G., et al. (2016), North Atlantic simulations in Coordinated Ocean-ice Reference Experiments phase II (CORE-II). Part II: Inter-annual to decadal variability, *Ocean Model.*, *97*, 65–90, doi:10.1016/j.ocemod.2015.11.007.

de Coëtlogon, G., C. Frankignoul, M. Bentsen, C. Delon, H. Haak, S. Masina, and A. Pardaens (2006), Gulf Stream variability in five oceanic general circulation models, *J. Phys. Oceanogr.*, *36*(11), 2119–2135, doi:10.1175/JPO2963.1.

de Vries, P., and S. L. Weber (2005), The Atlantic freshwater budget as a diagnostic for the existence of a stable shut down of the meridional overturning circulation, *Geophys. Res. Lett.*, *32*, L09606, doi:10.1029/2004GL021450.

Dee, D. P., et al. (2011), The ERA-Interim reanalysis: Configuration and performance of the data assimilation system, *Q. J. R. Meteorol. Soc.*, *137*(656), 553–597, doi:10.1002/qj.828.

DelSole, T., L. Jia, and M. K. Tippett (2013), Decadal prediction of observed and simulated sea surface temperatures, *Geophys. Res. Lett.*, *40*, 2773–2778, doi:10.1002/grl.50185.

Delworth, T., S. Manabe, and R. J. Stouffer (1993), Interdecadal variations of the thermohaline circulation in a coupled ocean-atmosphere model, *J. Clim.*, *6*(11), 1993–2011, doi:10.1175/1520-0442(1993)006<1993:IVOTTC>2.0.CO;2.

Delworth, T. L., and K. W. Dixon (2006), Have anthropogenic aerosols delayed a greenhouse gas-induced weakening of the North Atlantic thermohaline circulation?, *Geophys. Res. Lett.*, *33*, L02606, doi:10.1029/2005GL024980.

Delworth, T. L., and R. J. Greatbatch (2000), Multidecadal thermohaline circulation variability driven by atmospheric surface flux forcing, *J. Clim.*, *13*(9), 1481–1495, doi:10.1175/1520-0442(2000)013<1481:MTCVDB>2.0.CO;2.

Delworth, T. L., and M. Mann (2000), Observed and simulated multidecadal variability in the Northern Hemisphere, *Clim. Dyn.*, *16*, 661–676.

Delworth, T. L., and F. Zeng (2008), Simulated impact of altered Southern Hemisphere winds on the Atlantic Meridional Overturning Circulation, *Geophys. Res. Lett.*, *35*, L20708, doi:10.1029/2008GL035166.

Delworth, T. L., and F. Zeng (2012), Multicentennial variability of the Atlantic meridional overturning circulation and its climatic influence in a 4000 year simulation of the GFDL CM2.1 climate model, *Geophys. Res. Lett.*, *39*, L13702, doi:10.1029/2012GL052107.

Delworth, T. L., S. Manabe, and R. Stouffer (1997), Multidecadal climate variability in the Greenland Sea and surrounding regions: A coupled model simulation, *Geophys. Res. Lett.*, *24*(3), 257–260.

Delworth, T. L., R. Zhang, and M. Mann (2007), Decadal to centennial variability of the Atlantic from observations and models, in *Ocean Circulation: Mechanisms and Impacts*, edited by A. Schmittner, J. C. H. Chiang, and S. R. Hemming, pp. 131–148, AGU, Washington, D. C., doi:10.1029/173GM10.

Dengler, M., F. A. Schott, C. Eden, P. Brandt, J. Fischer, and R. J. Zantopp (2004), Break-up of the Atlantic deep western boundary current into eddies at 8°S, *Nature*, *432*(7020), 1018–1020.

Dengler, M., J. Fischer, F. A. Schott, and R. Zantopp (2006), Deep Labrador Current and its variability in 1996–2005, *Geophys. Res. Lett.*, *33*, L21S06, doi:10.1029/2006GL026702.

Deser, C., and M. L. Blackmon (1993), Surface climate variations over the North Atlantic Ocean during winter: 1900–1989, *J. Clim.*, *6*, 1743–1753.

Deser, C., M. A. Alexander, S.-P. Xie, and A. S. Phillips (2010), Sea surface temperature variability: Patterns and mechanisms, *Annu. Rev. Mar. Sci.*, *2*, 115–143, doi:10.1146/annurev-marine-120408-151453.
Deshayes, J., and C. Frankignoul (2005), Spectral characteristics of the response of the Meridional Overturning Circulation to deep-water formation, *J. Phys. Oceanogr.*, *35*(10), 1813–1825, doi:10.1175/JPO2793.1.
Deshayes, J., and C. Frankignoul (2008), Simulated variability of the circulation in the North Atlantic from 1953 to 2003, *J. Clim.*, *21*(19), 4919–4933, doi:10.1175/2008JCLI1882.1.
Deshayes, J., C. Frankignoul, and H. Drange (2007), Formation and export of deep water in the Labrador and Irminger Seas in a GCM, *Deep Sea Res., Part I*, *54*(4), 510–532, doi:10.1016/j.dsr.2006.12.014.
Deshayes, J., et al. (2013), Oceanic hindcast simulations at high resolution suggest that the Atlantic MOC is bistable, *Geophys. Res. Lett.*, *40*, 3069–3073, doi:10.1002/grl.50534.
Deshayes, J., R. Curry, and R. Msadek (2014), CMIP5 model intercomparison of freshwater budget and circulation in the North Atlantic, *J. Clim.*, *27*(9), 3298–3317, doi:10.1175/JCLI-D-12-00700.1.
Dijkstra, H. A. (2007), Characterization of the multiple equilibria regime in a global ocean model, *Tellus A*, *59*(5), 695–705, doi:10.1111/j.1600-0870.2007.00267.x.
Dima, M., and G. Lohmann (2010), Evidence for two distinct modes of large-scale ocean circulation changes over the last century, *J. Clim.*, *23*(1), 5–16, doi:10.1175/2009JCLI2867.1.
Ding, Y., J. A. Carton, G. A. Chepurin, G. Stenchikov, A. Robock, L. T. Sentman, and J. P. Krasting (2014), Ocean response to volcanic eruptions in Coupled Model Intercomparison Project 5 simulations, *J. Geophys. Res.*, *119*, 5622–5637, doi:10.1002/2013JC009780.
Dong, B., and R. Sutton (2001), The dominant mechanisms of variability in Atlantic Ocean heat transport in a coupled ocean-atmospheric GCM, *Geophys. Res. Lett.*, *28*(12), 2445–2448.
Dong, B., and R. Sutton (2002), Variability in North Atlantic heat content and heat transport in a coupled ocean–atmosphere GCM, *Clim. Dyn.*, *19*(5–6), 485–497, doi:10.1007/s00382-002-0239-7.
Dong, B., and R. Sutton (2003), Variability of Atlantic Ocean heat transport and its effects on the atmosphere, *Ann. Geophys.*, *46*(1), 87–97, doi:10.4401/ag-3391.
Dong, B., and R. Sutton (2005), Mechanism of interdecadal thermohaline circulation variability in a coupled ocean-atmosphere GCM, *J. Clim.*, *18*, 1117–1135, doi:10.1175/JCLI3328.1.
Dong, S., and K. A. Kelly (2004), Heat budget in the Gulf Stream region: The importance of heat storage and advection, *J. Phys. Oceanogr.*, *34*(5), 1214–1231, doi:10.1175/1520-0485(2004)034<1214:HBITGS>2.0.CO;2.
Dong, S., S. L. Hautala, and K. A. Kelly (2007), Interannual variations in upper-ocean heat content and heat transport convergence in the western North Atlantic, *J. Phys. Oceanogr.*, *37*(11), 2682–2697, doi:10.1175/2007JPO3645.1.
Dong, S., S. Garzoli, M. Baringer, C. Meinen, and G. Goni (2009), Interannual variations in the Atlantic meridional overturning circulation and its relationship with the net northward heat transport in the South Atlantic, *Geophys. Res. Lett.*, *36*, L20606, doi:10.1029/2009GL039356.
Dong, S., S. Garzoli, and M. Baringer (2011), The role of interocean exchanges on decadal variations of the meridional heat transport in the South Atlantic, *J. Phys. Oceanogr.*, *41*(8), 1498–1511, doi:10.1175/2011JPO4549.1.
Dong, S., M. O. Baringer, G. J. Goni, C. S. Meinen, and S. L. Garzoli (2014), Seasonal variations in the South Atlantic Meridional Overturning Circulation from observations and numerical models, *Geophys. Res. Lett.*, *41*, 4611–4618, doi:10.1002/2014GL060428.
Drijfhout, S., W. Hazeleger, F. Selten, and R. Haarsma (2008), Future changes in internal variability of the Atlantic Meridional Overturning Circulation, *Clim. Dyn.*, *30*(4), 407–419, doi:10.1007/s00382-007-0297-y.
Drijfhout, S., G. J. van Oldenborgh, and A. Cimatoribus (2012), Is a decline of AMOC causing the warming hole above the North Atlantic in observed and modeled warming patterns?, *J. Clim.*, *25*(24), 8373–8379, doi:10.1175/JCLI-D-12-00490.1.
Drijfhout, S. S., and W. Hazeleger (2007), Detecting Atlantic MOC changes in an ensemble of climate change simulations, *J. Clim.*, *20*(8), 1571–1582, doi:10.1175/JCLI4104.1.
Drijfhout, S. S., S. Weber, and E. van der Swaluw (2011), The stability of the MOC as diagnosed from model projections for pre-industrial, present and future climates, *Clim. Dyn.*, *37*(7–8), 1575–1586, doi:10.1007/s00382-010-0930-z.
Duchez, A., et al. (2014), A new index for the Atlantic Meridional Overturning Circulation at 26°N, *J. Clim.*, *27*(17), 6439–6455, doi:10.1175/JCLI-D-13-00052.1.
Dunstone, N. J. (2014), A perspective on sustained marine observations for climate modelling and prediction, *Philos. Trans. R. Soc. A*, *372*, 20130340, doi:10.1098/rsta.2013.0340.
Dunstone, N. J., and D. M. Smith (2010), Impact of atmosphere and sub-surface ocean data on decadal climate prediction, *Geophys. Res. Lett.*, *37*, L02709, doi:10.1029/2009GL041609.
Eden, C., and J. Willebrand (2001), Mechanism of interannual to decadal variability of the North Atlantic circulation, *J. Clim.*, *14*(10), 2266–2280, doi:10.1175/1520-0442(2001)014<2266:MOITDV>2.0.CO;2.
Elipot, S., E. Frajka-Williams, C. W. Hughes, and J. K. Willis (2014), The observed North Atlantic Meridional Overturning Circulation: Its meridional coherence and ocean bottom pressure, *J. Phys. Oceanogr.*, *44*(2), 517–537, doi:10.1175/JPO-D-13-026.1.
Emile-Geay, J., M. A. Cane, N. Naik, R. Seager, A. C. Clement, and A. van Geen (2003), Warren revisited: Atmospheric freshwater fluxes and "Why is no deep water formed in the North Pacific", *J. Geophys. Res.*, *108*(C6), 3178, doi:10.1029/2001JC001058.
Enfield, D. B., A. M. Mestas-Nuñez, and P. J. Trimble (2001), The Atlantic Multidecadal Oscillation and its relation to rainfall and river flows in the continental U.S., *Geophys. Res. Lett.*, *28*(10), 2077–2080, doi:10.1029/2000GL012745.
England, M. H., S. McGregor, P. Spence, G. A. Meehl, A. Timmermann, W. Cai, A. S. Gupta, M. J. McPhaden, A. Purich, and A. Santoso (2014), Recent intensification of wind-driven circulation in the Pacific and the ongoing warming hiatus, *Nat. Clim. Change*, *4*(3), 222–227.
Fan, M., and E. K. Schneider (2011), Observed decadal North Atlantic tripole SST variability. Part I: Weather noise forcing and coupled response, *J. Atmos. Sci.*, *69*(1), 35–50, doi:10.1175/JAS-D-11-018.1.
Farneti, R., and T. L. Delworth (2010), The role of mesoscale eddies in the remote oceanic response to altered Southern Hemisphere winds, *J. Phys. Oceanogr.*, *40*(10), 2348–2354, doi:10.1175/2010JPO4480.1.
Farneti, R., and P. R. Gent (2011), The effects of the eddy-induced advection coefficient in a coarse-resolution coupled climate model, *Ocean Model.*, *39*(1–2), 135–145, doi:10.1016/j.ocemod.2011.02.005.
Farneti, R., T. L. Delworth, A. J. Rosati, S. M. Griffies, and F. Zeng (2010), The role of mesoscale eddies in the rectification of the Southern Ocean response to climate change, *J. Phys. Oceanogr.*, *40*(7), 1539–1557, doi:10.1175/2010JPO4353.1.
Ferrari, R., and D. Ferreira (2011), What processes drive the ocean heat transport?, *Ocean Model.*, *38*(3–4), 171–186, doi:10.1016/j.ocemod.2011.02.013.
Ferreira, D., and J. Marshall (2015), Freshwater transport in the coupled ocean-atmosphere system: A passive ocean, *Ocean Dyn.*, *65*(7), 1029–1036, doi:10.1007/s10236-015-0846-6.

Ferreira, D., J. Marshall, and J.-M. Campin (2010), Localization of deep water formation: Role of atmospheric moisture transport and geometrical constraints on ocean circulation, *J. Clim.*, *23*(6), 1456–1476, doi:10.1175/2009JCLI3197.1.
Feulner, G., S. Rahmstorf, A. Levermann, and S. Volkwardt (2013), On the origin of the surface air temperature difference between the hemispheres in Earth's present-day climate, *J. Clim.*, *26*(18), 7136–7150, doi:10.1175/JCLI-D-12-00636.1.
Fine, R. A., M. Rhein, and C. Andrié (2002), Using a CFC effective age to estimate propagation and storage of climate anomalies in the deep western North Atlantic Ocean, *Geophys. Res. Lett.*, *29*(24), 2227, doi:10.1029/2002GL015618.
Fischer, J., and F. A. Schott (2002), Labrador Sea Water tracked by profiling floats—From the boundary current into the open North Atlantic, *J. Phys. Oceanogr.*, *32*(2), 573–584, doi:10.1175/1520-0485(2002)032<0573:LSWTBP>2.0.CO;2.
Fischer, J., F. A. Schott, and M. Dengler (2004), Boundary circulation at the exit of the Labrador Sea, *J. Phys. Oceanogr.*, *34*(7), 1548–1570, doi:10.1175/1520-0485(2004)034<1548:BCATEO>2.0.CO;2.
Fischer, J., M. Visbeck, R. Zantopp, and N. Nunes (2010), Interannual to decadal variability of outflow from the Labrador Sea, *Geophys. Res. Lett.*, *37*, L24610, doi:10.1029/2010GL045321.
Fischer, J., et al. (2015), Intra-seasonal variability of the DWBC in the western subpolar North Atlantic, *Prog. Oceanogr.*, *132*, 233–249, doi:10.1016/j.pocean.2014.04.002.
Fischer, M., A. Biastoch, E. Behrens, and J. Baehr (2013), Simulations of a Line W-based observing system for the Atlantic meridional overturning circulation, *Ocean Dyn.*, *63*(8), 865–880, doi:10.1007/s10236-013-0632-2.
Folland, C. K., T. N. Palmer, and D. E. Parker (1986), Sahel rainfall and worldwide sea temperatures, 1901–85, *Nature*, *320*(6063), 602–607.
Forget, G., and R. M. Ponte (2015), The partition of regional sea level variability, *Prog. Oceanogr.*, *137*(Part A), 173–195, doi:10.1016/j.pocean.2015.06.002.
Forget, G., and C. Wunsch (2007), Estimated global hydrographic variability, *J. Phys. Oceanogr.*, *37*(8), 1997–2008, doi:10.1175/JPO3072.1.
Forget, G., B. Ferron, and H. Mercier (2008a), Combining Argo profiles with a general circulation model in the North Atlantic. Part 1: Estimation of hydrographic and circulation anomalies from synthetic profiles, over a year, *Ocean Model.*, *20*(1), 1–16, doi:10.1016/j.ocemod.2007.06.001.
Forget, G., H. Mercier, and B. Ferron (2008b), Combining Argo profiles with a general circulation model in the North Atlantic. Part 2: Realistic transports and improved hydrography, between spring 2002 and spring 2003, *Ocean Model.*, *20*(1), 17–34, doi:10.1016/j.ocemod.2007.06.002.
Forget, G., J.-M. Campin, P. Heimbach, C. N. Hill, R. M. Ponte, and C. Wunsch (2015), ECCO version 4: An integrated framework for non-linear inverse modeling and global ocean state estimation, *Geosci. Model Dev.*, *8*(10), 3071–3104, doi:10.5194/gmd-8-3071-2015.
Frajka-Williams, E. (2015), Estimating the Atlantic overturning at 26°N using satellite altimetry and cable measurements, *Geophys. Res. Lett.*, *42*(9), 3458–3464, doi:10.1002/2015GL063220.
Frankcombe, L. M., and H. A. Dijkstra (2009), Coherent multidecadal variability in North Atlantic sea level, *Geophys. Res. Lett.*, *36*, L15604, doi:10.1029/2009GL039455.
Frankcombe, L. M., and H. A. Dijkstra (2011), The role of Atlantic-Arctic exchange in North Atlantic multidecadal climate variability, *Geophys. Res. Lett.*, *38*, L16603, doi:10.1029/2011GL048158.
Frankcombe, L. M., H. A. Dijkstra, and A. von der Heydt (2008), Sub-surface signatures of the Atlantic Multidecadal Oscillation, *Geophys. Res. Lett.*, *35*, L19602, doi:10.1029/2008GL034989.
Frankcombe, L. M., A. von der Heydt, and H. A. Dijkstra (2010), North Atlantic multidecadal climate variability: An investigation of dominant time scales and processes, *J. Clim.*, *23*(13), 3626–3638, doi:10.1175/2010JCLI3471.1.
Frankignoul, C. (1985), Sea surface temperature anomalies, planetary waves, and air-sea feedback in the middle latitudes, *Rev. Geophys.*, *23*(4), 357–390, doi:10.1029/RG023i004p00357.
Frankignoul, C., and K. Hasselmann (1977), Stochastic climate models. Part II: Application to sea-surface temperature anomalies and thermocline variability, *Tellus*, *29*, 289–305, doi:10.1111/j.2153-3490.1977.tb00740.x.
Frankignoul, C., P. Müller, and E. Zorita (1997), A simple model of the decadal response of the ocean to stochastic wind forcing, *J. Phys. Oceanogr.*, *27*(8), 1533–1546, doi:10.1175/1520-0485(1997)027<1533:ASMOTD>2.0.CO;2.
Frankignoul, C., G. D. Coëtlogen, T. Joyce, and S. Dong (2001), Gulf Stream variability and ocean-atmosphere interactions, *J. Phys. Oceanogr.*, *31*, 3516–3529.
Frankignoul, C., J. Deshayes, and R. Curry (2009), The role of salinity in the decadal variability of the North Atlantic meridional overturning circulation, *Clim. Dyn.*, *33*, 777–793, doi:10.1007/s00382-008-0523-2.
Fratantoni, D. M. (2001), North Atlantic surface circulation during the 1990's observed with satellite-tracked drifters, *J. Geophys. Res.*, *106*(C10), 22,067–22,093, doi:10.1029/2000JC000730.
Frierson, D. M. W., Y.-T. Hwang, N. S. Fuckar, R. Seager, S. M. Kang, A. Donohoe, E. A. Maroon, X. Liu, and D. S. Battisti (2013), Contribution of ocean overturning circulation to tropical rainfall peak in the Northern Hemisphere, *Nat. Geosci.*, *6*(11), 940–944, doi:10.1038/ngeo1987.
Fu, L., and B. Qui (2002), Low-frequency variability of the North Pacific ocean the roles of boundary and wind-driven baroclinic Rossby waves, *J. Geophys. Res.*, *107*(C12), 3220, doi:10.1029/2001JC001131.
Fu, Q., C. M. Johanson, J. M. Wallace, and T. Reichler (2006), Enhanced mid-latitude tropospheric warming in satellite measurements, *Science*, *312*(5777), 1179–1179.
Ganachaud, A., and C. Wunsch (2000), Improved estimates of global ocean circulation, heat transport and mixing from hydrographic data, *Nature*, *408*(6811), 453–457.
Ganachaud, A., and C. Wunsch (2003), Large-scale ocean heat and freshwater transports during the World Ocean Circulation Experiment, *J. Clim.*, *16*(4), 696–705, doi:10.1175/1520-0442(2003)016<0696:LSOHAF>2.0.CO;2.
Gary, S. F., M. S. Lozier, C. W. Böning, and A. Biastoch (2011), Deciphering the pathways for the deep limb of the meridional overturning circulation, *Deep Sea Res., Part II*, *58*(17–18), 1781–1797, doi:10.1016/j.dsr2.2010.10.059.
Gary, S. F., M. S. Lozier, A. Biastoch, and C. W. Böning (2012), Reconciling tracer and float observations of the export pathways of Labrador Sea Water, *Geophys. Res. Lett.*, *39*, L24606, doi:10.1029/2012GL053978.
Garzoli, S. L., and M. O. Baringer (2007), Meridional heat transport determined with expandable bathythermograph—Part II: South Atlantic transport, *Deep Sea Res., Part I*, *54*(8), 1402–1420, doi:10.1016/j.dsr.2007.04.013.
Garzoli, S. L., and R. Matano (2011), The South Atlantic and the Atlantic meridional overturning circulation, *Deep Sea Res., Part II*, *58*(17–18), 1837–1847, doi:10.1016/j.dsr2.2010.10.063.
Garzoli, S. L., M. O. Baringer, S. Dong, R. C. Perez, and Q. Yao (2013), South Atlantic meridional fluxes, *Deep Sea Res., Part I*, *71*, 21–32, doi:10.1016/j.dsr.2012.09.003.
Garzoli, S. L., S. Dong, R. Fine, C. S. Meinen, R. C. Perez, C. Schmid, E. van Sebille, and Q. Yao (2015), The fate of the Deep Western Boundary Current in the South Atlantic, *Deep Sea Res., Part I*, *103*, 125–136, doi:10.1016/j.dsr.2015.05.008.

Gent, P. R. (2015), Effects of Southern Hemisphere wind changes on the AMOC from models, *Annu. Rev. Mar. Sci.*, *8*, 79–94, doi:10.1146/annurev-marine-122414-033929.
Gent, P. R., and G. Danabasoglu (2011), Response to increasing Southern Hemisphere winds in CCSM4, *J. Clim.*, *24*(19), 4992–4998, doi:10.1175/JCLI-D-10-05011.1.
Geoffroy, O., D. Saint-Martin, G. Bellon, A. Voldoire, D. J. L. Olivié, and S. Tytéca (2013a), Transient climate response in a two-layer energy-balance model. Part II: Representation of the efficacy of deep-ocean heat uptake and validation for CMIP5 AOGCMs, *J. Clim.*, *26*(6), 1859–1876, doi:10.1175/JCLI-D-12-00196.1.
Geoffroy, O., D. Saint-Martin, D. J. L. Olivié, A. Voldoire, G. Bellon, and S. Tytéca (2013b), Transient climate response in a two-layer energy-balance model. Part I: Analytical solution and parameter calibration using CMIP5 AOGCM experiments, *J. Clim.*, *26*(6), 1841–1857, doi:10.1175/JCLI-D-12-00195.1.
Getzlaff, J., C. W. Böning, C. Eden, and A. Biastoch (2005), Signal propagation related to the North Atlantic overturning, *Geophys. Res. Lett.*, *32*, L09602, doi:10.1029/2004GL021002.
Getzlaff, K., C. W. Böning, and J. Dengg (2006), Lagrangian perspectives of deep water export from the subpolar North Atlantic, *Geophys. Res. Lett.*, *33*, L21S08, doi:10.1029/2006GL026470.
Gnanadesikan, A. (1999), A simple predictive model for the structure of the oceanic pycnocline, *Science*, *283*(5410), 2077–2079.
Gnanadesikan, A., A. M. De Boer, and B. K. Mignone (2007), A simple theory of the pycnocline and overturning revisited, in *Ocean Circulation: Mechanisms and Impacts—Past and Future Changes of Meridional Overturning*, AGU, Washington, D. C., doi:10.1029/173GM04.
Gray, S. T., L. J. Graumlich, J. L. Betancourt, and G. T. Pederson (2004), A tree-ring based reconstruction of the Atlantic Multidecadal Oscillation since 1567 A.D., *Geophys. Res. Lett.*, *31*, L12205, doi:10.1029/2004GL019932.
Greatbach, R., and S. Zhang (1995), An interdecadal oscillation in an idealized ocean basin forced by constant heat flux, *J. Clim.*, *8*, 81–91.
Gregory, J., and M. Webb (2008), Tropospheric adjustment induces a cloud component in CO_2 forcing, *J. Clim.*, *21*(1), 58–71, doi:10.1175/2007JCLI1834.1.
Gregory, J. M. (2000), Vertical heat transports in the ocean and their effect on time-dependent climate change, *Clim. Dyn.*, *16*(7), 501–515, doi:10.1007/s003820000059.
Gregory, J. M. (2010), Long-term effect of volcanic forcing on ocean heat content, *Geophys. Res. Lett.*, *37*, L22701, doi:10.1029/2010GL045507.
Gregory, J. M., O. A. Saenko, and A. J. Weaver (2003), The role of the Atlantic freshwater balance in the hysteresis of the meridional overturning circulation, *Clim. Dyn.*, *21*(7–8), 707–717, doi:10.1007/s00382-003-0359-8.
Gregory, J. M., et al. (2005), A model intercomparison of changes in the Atlantic thermohaline circulation in response to increasing atmospheric CO_2 concentration, *Geophys. Res. Lett.*, *32*, L12703, doi:10.1029/2005GL023209.
Griffies, S., and K. Bryan (1997a), Predictability of North Atlantic multidecadal climate variability, *Science*, *275*(5297), 181–184, doi:10.1126/science.275.5297.181.
Griffies, S. M., and K. Bryan (1997b), A predictability study of simulated North Atlantic multidecadal variability, *Clim. Dyn.*, *13*(7–8), 459–487.
Griffies, S. M., and E. Tziperman (1995), A linear thermohaline oscillator driven by stochastic atmospheric forcing, *J. Clim.*, *8*(10), 2440–2453, doi:10.1175/1520-0442(1995)008<2440:ALTODB>2.0.CO;2.
Grist, J., S. Josey, R. Marsh, S. Good, A. Coward, B. de Cuevas, S. Alderson, A. New, and G. Madec (2010), The roles of surface heat flux and ocean heat transport convergence in determining Atlantic Ocean temperature variability, *Ocean Dyn.*, *60*, 771–790, doi:10.1007/s10236-010-0292-4.
Guemas, V., and D. Salas-Mélia (2008), Simulation of the Atlantic meridional overturning circulation in an atmosphere-ocean global coupled model. Part I: A mechanism governing the variability of ocean convection in a preindustrial experiment, *Clim. Dyn.*, *31*, 29–48, doi:10.1007/s00382-007-0336-8.
Gulev, S. K., M. Latif, N. Keenlyside, W. Park, and K. P. Koltermann (2013), North Atlantic Ocean control on surface heat flux on multidecadal timescales, *Nature*, *499*(7459), 464–467, doi:10.1038/nature12268.
Häkkinen, S. (1999), Variability of the simulated meridional heat transport in the North Atlantic for the period 1951–1993, *J. Geophys. Res.*, *104*(C5), 10,991–11,007, doi:10.1029/1999JC900034.
Häkkinen, S. (2001), Variability in sea surface height: A qualitative measure for the meridional overturning in the North Atlantic, *J. Geophys. Res.*, *106*(C7), 13,837–13,848, doi:10.1029/1999JC000155.
Häkkinen, S., and P. B. Rhines (2004), Decline of Subpolar North Atlantic circulation during the 1990s, *Science*, *304*(5670), 555–559.
Häkkinen, S., and P. B. Rhines (2009), Shifting surface currents in the northern North Atlantic Ocean, *J. Geophys. Res.*, *114*, C04005, doi:10.1029/2008JC004883.
Häkkinen, S., P. B. Rhines, and D. L. Worthen (2011a), Warm and saline events embedded in the meridional circulation of the northern North Atlantic, *J. Geophys. Res.*, *116*, C03006, doi:10.1029/2010JC006275.
Häkkinen, S., P. B. Rhines, and D. L. Worthen (2011b), Atmospheric blocking and Atlantic multidecadal ocean variability, *Science*, *334*(6056), 655–659.
Häkkinen, S., P. B. Rhines, and D. L. Worthen (2013), Northern North Atlantic sea surface height and ocean heat content variability, *J. Geophys. Res.*, *118*, 3670–3678, doi:10.1002/jgrc.20268.
Hall, M. M., and H. L. Bryden (1982), Direct estimates and mechanisms of ocean heat transport, *Deep Sea Res., Part A*, *29*(3), 339–359, doi:10.1016/0198-0149(82)90099-1.
Hallberg, R., and A. Gnanadesikan (2006), The role of eddies in determining the structure and response of the wind-driven Southern Hemisphere overturning: Results from the Modeling Eddies in the Southern Ocean (MESO) project, *J. Phys. Oceanogr.*, *36*(12), 2232–2252, doi:10.1175/JPO2980.1.
Hansen, J., G. Russell, A. Lacis, I. Fung, D. Rind, and P. Stone (1985), Climate response times: Dependence on climate sensitivity and ocean mixing, *Science*, *229*(4716), 857–859.
Hansen, J., M. Sato, and R. Ruedy (1997), Radiative forcing and climate response, *J. Geophys. Res.*, *102*(D6), 6831–6864, doi:10.1029/96JD03436.
Hansen, J., M. Sato, P. Kharecha, and K. von Schuckmann (2011), Earth's energy imbalance and implications, *Atmos. Chem. Phys.*, *11*(24), 13,421–13,449, doi:10.5194/acp-11-13421-2011.
Hasselmann, K. (1976), Stochastic climate models. Part I: Theory, *Tellus*, *6*, 472–485, doi:10.1111/j.2153-3490.1976.tb00696.x.
Hátún, H., A. B. Sando, H. Drange, B. Hansen, and H. Valdimarsson (2005), Influence of the Atlantic subpolar gyre on the thermohaline circulation, *Science*, *309*(5742), 1841–1844.
Hawkins, E., and R. Sutton (2008), Potential predictability of rapid changes in the Atlantic meridional overturning circulation, *Geophys. Res. Lett.*, *35*, L11603, doi:10.1029/2008GL034059.

Hawkins, E., and R. Sutton (2009), Decadal predictability of the Atlantic Ocean in a coupled GCM: Forecast skill and optimal perturbations using linear inverse modeling, *J. Clim.*, *22*(14), 3960–3978, doi:10.1175/2009JCLI2720.1.
Hawkins, E., R. S. Smith, L. C. Allison, J. M. Gregory, T. J. Woollings, H. Pohlmann, and B. de Cuevas (2011), Bistability of the Atlantic overturning circulation in a global climate model and links to ocean freshwater transport, *Geophys. Res. Lett.*, *38*, L10605, doi:10.1029/2011GL047208.
Heimbach, P., C. Wunsch, R. Ponte, G. Forget, C. Hill, and J. Utke (2011), Timescales and regions of the sensitivity of Atlantic meridional volume and heat transport: Toward observing system design, *Deep Sea Res., Part II*, *58*, 1858–1879, doi:10.1016/j.dsr2.2010.10.065.
Held, I. M. (2001), The partitioning of the poleward energy transport between the tropical ocean and atmosphere, *J. Atmos. Sci.*, *58*(8), 943–948, doi:10.1175/1520-0469(2001)058<0943:TPOTPE>2.0.CO;2.
Held, I. M., M. Winton, K. Takahashi, T. Delworth, F. Zeng, and G. K. Vallis (2010), Probing the fast and slow components of global warming by returning abruptly to preindustrial forcing, *J. Clim.*, *23*(9), 2418–2427, doi:10.1175/2009JCLI3466.1.
Hermanson, L., and R. Sutton (2010), Case studies in interannual to decadal climate predictability, *Clim. Dyn.*, *35*(7–8), 1169–1189, doi:10.1007/s00382-009-0672-y.
Hermanson, L., R. Eade, N. H. Robinson, N. J. Dunstone, M. B. Andrews, J. R. Knight, A. A. Scaife, and D. M. Smith (2014), Forecast cooling of the Atlantic subpolar gyre and associated impacts, *Geophys. Res. Lett.*, *41*, 5167–5174, doi:10.1002/2014GL060420.
Hernández-Guerra, A., T. Joyce, E. Fraile-Nuez, and P. Vélez-Belchí (2010), Using Argo data to investigate the Meridional Overturning Circulation in the North Atlantic, *Deep Sea Res., Part I*, *57*, 29–36, doi:10.1016/j.dsr.2009.10.003.
Hirschi, J., and J. Marotzke (2007), Reconstructing the Meridional Overturning Circulation from boundary densities and the zonal wind stress, *J. Phys. Oceanogr.*, *37*(3), 743–763, doi:10.1175/JPO3019.1.
Hirschi, J., J. Baehr, J. Marotzke, J. Stark, S. Cunningham, and J.-O. Beismann (2003), A monitoring design for the Atlantic meridional overturning circulation, *Geophys. Res. Lett.*, *30*(7), 1413, doi:10.1029/2002GL016776.
Hirschi, J., P. Killworth, and J. Blundel (2007), Subannual, seasonal, and interannual variability of the North Atlantic Meridional Overturning Circulation, *J. Phys. Oceanogr.*, *37*(5), 1246–1265.
Hirschi, J. J.-M., P. Killworth, J. Blundel, and D. Cromwell (2009), Sea surface height signals as indicators of ocean meridional mass transports, *J. Phys. Oceanogr.*, *39*, 581–601, doi:10.1175/2008JPO3923.1.
Hirschi, J. J.-M., A. T. Blaker, B. Sinha, A. Coward, B. de Cuevas, S. Alderson, and G. Madec (2013), Chaotic variability of the meridional overturning circulation on subannual to interannual timescales, *Ocean Sci.*, *9*(5), 805–823, doi:10.5194/os-9-805-2013.
Hobbs, W. R., and J. K. Willis (2012), Midlatitude North Atlantic heat transport: A time series based on satellite and drifter data, *J. Geophys. Res.*, *117*(C1), C01008, doi:10.1029/2011JC007039.
Holliday, N. P. (2003), Air-sea interaction and circulation changes in the northeast Atlantic, *J. Geophys. Res.*, *108*(C8), 3259, doi:10.1029/2002JC001344.
Hu, Z.-Z., A. Kumar, B. Huang, W. Wang, J. Zhu, and C. Wen (2013), Prediction skill of monthly SST in the North Atlantic Ocean in NCEP Climate Forecast System version 2, *Clim. Dyn.*, *40*(11–12), 2745–2759, doi:10.1007/s00382-012-1431-z.
Huang, B., Y. Xue, A. Kumar, and D. W. Behringer (2012), AMOC variations in 1979–2008 simulated by NCEP operational ocean data assimilation system, *Clim. Dyn.*, *38*(3–4), 513–525, doi:10.1007/s00382-011-1035-z.
Huck, T., A. Colin de Verdiére, and A. J. Weaver (1999), Interdecadal variability of the thermohaline circulation in box-ocean models forced by fixed surface fluxes, *J. Phys. Oceanogr.*, *29*(5), 865–892, doi:10.1175/1520-0485(1999)029<0865:IVOTTC>2.0.CO;2.
Huisman, S. E., M. den Toom, H. A. Dijkstra, and S. Drijfhout (2010), An indicator of the multiple equilibria regime of the Atlantic Meridional Overturning Circulation, *J. Phys. Oceanogr.*, *40*(3), 551–567, doi:10.1175/2009JPO4215.1.
Isachsen, P. E., J. H. LaCasce, and J. Pedlosky (2007), Rossby wave instability and apparent phase speeds in large ocean basins, *J. Phys. Oceanogr.*, *37*(5), 1177–1191, doi:10.1175/JPO3054.1.
Ivchenko, V. O., D. Sidorenko, S. Danilov, M. Losch, and J. Schröter (2011), Can sea surface height be used to estimate oceanic transport variability?, *Geophys. Res. Lett.*, *38*, L11601, doi:10.1029/2011GL047387.
Jackson, L., and M. Vellinga (2012), Multidecadal to centennial variability of the AMOC: HadCM3 and a perturbed physics ensemble, *J. Clim.*, *26*(7), 2390–2407, doi:10.1175/JCLI-D-11-00601.1.
Jayne, S. R., and J. Marotzke (2001), The dynamics of ocean heat transport variability, *Rev. Geophys.*, *39*(3), 385–411, doi:10.1029/2000RG000084.
Johns, W. E., D. M. Fratantoni, and R. J. Zantopp (1993), Deep western boundary current variability off northeastern Brazil, *Deep Sea Res., Part I*, *40*(2), 293–310, doi:10.1016/0967-0637(93)90005-N.
Johns, W. E., L. M. Beal, M. O. Baringer, J. R. Molina, S. A. Cunningham, T. Kanzow, and D. Rayner (2008), Variability of shallow and deep western boundary currents off the Bahamas during 2004–05: Results from the 26°N RAPID-MOC array, *J. Phys. Oceanogr.*, *38*(3), 605–623, doi:10.1175/2007JPO3791.1.
Johns, W. E., M. O. Baringer, L. M. Beal, S. A. Cunningham, T. Kanzow, H. L. Bryden, J. J. M. Hirschi, J. Marotzke, C. S. Meinen, B. Shaw, and R. Curry (2011), Continuous, array-based estimates of Atlantic Ocean heat transport at 26.5°N, *J. Clim.*, *24*(10), 2429–2449, doi:10.1175/2010JCLI3997.1.
Johnson, H. L., and D. P. Marshall (2002a), Localization of abrupt change in the North Atlantic thermohaline circulation, *Geophys. Res. Lett.*, *29*(6), 1083–1086, doi:10.1029/2001GL014140.
Johnson, H. L., and D. P. Marshall (2002b), A theory for the surface Atlantic response to thermohaline variability, *J. Phys. Oceanogr.*, *32*(4), 1121–1132, doi:10.1175/1520-0485(2002)032<1121:ATFTSA>2.0.CO;2.
Johnson, H. L., D. P. Marshall, and D. A. J. Sproson (2007), Reconciling theories of a mechanically driven meridional overturning circulation with thermohaline forcing and multiple equilibria, *Clim. Dyn.*, *29*(7–8), 821–836, doi:10.1007/s00382-007-0262-9.
Joyce, T. M., and R. Zhang (2010), On the path of the Gulf Stream and the Atlantic Meridional Overturning Circulation, *J. Clim.*, *23*(11), 3146–3154, doi:10.1175/2010JCLI3310.1.
Joyce, T. M., C. Deser, and M. A. Spall (2000), The relation between decadal variability of subtropical mode water and the North Atlantic Oscillation, *J. Clim.*, *13*(14), 2550–2569, doi:10.1175/1520-0442(2000)013<2550:TRBDVO>2.0.CO;2.
Jungclaus, J. H., H. Haak, M. Latif, and U. Mikolajewicz (2005), Arctic–North Atlantic interactions and multidecadal variability of the meridional overturning circulation, *J. Clim.*, *18*(19), 4013–4031, doi:10.1175/JCLI3462.1.
Kalnay, E., et al. (1996), The NCEP/NCAR 40-year reanalysis project, *Bull. Am. Meteorol. Soc.*, *77*(3), 437–471, doi:10.1175/1520-0477(1996)077<0437:TNYRP>2.0.CO;2.
Kang, S. M., I. M. Held, D. M. W. Frierson, and M. Zhao (2008), The response of the ITCZ to extratropical thermal forcing: Idealized slab-ocean experiments with a GCM, *J. Clim.*, *21*(14), 3521–3532, doi:10.1175/2007JCLI2146.1.
Kang, S. M., D. M. W. Frierson, and I. M. Held (2009), The tropical response to extratropical thermal forcing in an idealized GCM: The importance of radiative feedbacks and convective parameterization, *J. Atmos. Sci.*, *66*(9), 2812–2827, doi:10.1175/2009JAS2924.1.

Kang, S. M., R. Seager, D. M. W. Frierson, and X. Liu (2014), Croll revisited: Why is the northern hemisphere warmer than the southern hemisphere?, *Clim. Dyn.*, *44*(5–6), 1457–1472, doi:10.1007/s00382-014-2147-z.
Kanzow, T., U. Send, W. Zenk, A. Chave, and M. Rhein (2006), Monitoring the integrated deep meridional flow in the tropical North Atlantic: Long-term performance of a geostrophic array, *Deep Sea Res., Part I*, *53*(3), 528–546, doi:10.1016/j.dsr.2005.12.007.
Kanzow, T., S. Cunningham, D. Rayner, J. Hirschi, W. Johns, M. Baringer, H. Bryden, L. Beal, C. Meinen, and J. Marotzke (2007), Observed flow compensation associated with the MOC at 26.5°N in the Atlantic, *Science*, *317*, 938–941, doi:10.1126/science.1141304.
Kanzow, T., H. L. Johnson, D. P. Marshall, S. A. Cunningham, J. J. M. Hirschi, A. Mujahid, H. L. Bryden, and W. E. Johns (2009), Basinwide integrated volume transports in an eddy-filled ocean, *J. Phys. Oceanogr.*, *39*(12), 3091–3110, doi:10.1175/2009JPO4185.1.
Kanzow, T., S. A. Cunningham, W. E. Johns, J. J.-M. Hirschi, J. Marotzke, M. O. Baringer, C. S. Meinen, M. P. Chidichimo, C. Atkinson, L. M. Beal, H. L. Bryden, and J. Collins (2010), Seasonal variability of the Atlantic Meridional Overturning Circulation at 26.5°N, *J. Clim.*, *23*(21), 5678–5698, doi:10.1175/2010JCLI3389.1.
Karl, T. R., A. Arguez, B. Huang, J. H. Lawrimore, J. R. McMahon, M. J. Menne, T. C. Peterson, R. S. Vose, and H.-M. Zhang (2015), Possible artifacts of data biases in the recent global surface warming hiatus, *Science*, *348*(6242), 1469–1472.
Karspeck, A., S. Yeager, G. Danabasoglu, and H. Teng (2014), An evaluation of experimental decadal predictions using CCSM4, *Clim. Dyn.*, *44*(3–4), 907–923, doi:10.1007/s00382-014-2212-7.
Karspeck, A. R., et al. (2015), Comparison of the Atlantic meridional overturning circulation between 1960 and 2007 in six ocean reanalysis products, *Clim. Dyn.*,1–26, doi:10.1007/s00382-015-2787-7.
Kaufmann, R. K., H. Kauppi, M. L. Mann, and J. H. Stock (2011), Reconciling anthropogenic climate change with observed temperature 1998–2008, *Proc. Natl. Acad. Sci. U.S.A.*, *108*(29), 11,790–11,793, doi:10.1073/pnas.1102467108.
Kawase, M. (1987), Establishment of deep ocean circulation driven by deep-water production, *J. Phys. Oceanogr.*, *17*(12), 2294–2317, doi:10.1175/1520-0485(1987)017<2294:EODOCD>2.0.CO;2.
Keenlyside, N., M. Latif, J. Jungclaus, L. Kornblueh, and E. Roeckner (2008), Advancing decadal-scale climate prediction in the North Atlantic sector, *Nature*, *453*, 84–88, doi:10.1038/nature06921.
Kerr, R. A. (2000), A North Atlantic climate pacemaker for the centuries, *Science*, *288*(5473), 1984–1985.
Kieke, D., M. Rhein, L. Stramma, W. M. Smethie, D. A. LeBel, and W. Zenk (2006), Changes in the CFC inventories and formation rates of Upper Labrador Sea Water, 1997–2001, *J. Phys. Oceanogr.*, *36*(1), 64–86, doi:10.1175/JPO2814.1.
Kieke, D., M. Rhein, L. Stramma, W. M. Smethie, J. L. Bullister, and D. A. LeBel (2007), Changes in the pool of Labrador Sea Water in the subpolar North Atlantic, *Geophys. Res. Lett.*, *34*, L06605, doi:10.1029/2006GL028959.
Kirtman, B., et al. (2013), Near-term climate change: Projections and predictability, in *Climate Change 2013: The Physical Science Basis. Contribution of Working Group I to the Fifth Assessment Report of the Intergovernmental Panel on Climate Change, chap. Near-term Climate Change: Projections and Predictability*, pp. 953–1028, Cambridge Univ. Press, Cambridge, U. K., and New York.
Klinger, B. A., and C. Cruz (2009), Decadal response of global circulation to Southern Ocean zonal wind stress perturbation, *J. Phys. Oceanogr.*, *39*(8), 1888–1904, doi:10.1175/2009JPO4070.1.
Klinger, B. A., and J. Marotzke (2000), Meridional heat transport by the subtropical cell, *J. Phys. Oceanogr.*, *30*(4), 696–705, doi:10.1175/1520-0485(2000)030<0696:MHTBTS>2.0.CO;2.
Knight, J. R. (2009), The Atlantic Multidecadal Oscillation inferred from the forced climate response in coupled general circulation models, *J. Clim.*, *22*(7), 1610–1625, doi:10.1175/2008JCLI2628.1.
Knight, J. R., R. J. Allan, C. K. Folland, M. Vellinga, and M. E. Mann (2005), A signature of persistent natural thermohaline circulation cycles in observed climate, *Geophys. Res. Lett.*, *32*, L20708, doi:10.1029/2005GL024233.
Knight, J. R., C. K. Folland, and A. A. Scaife (2006), Climate impacts of the Atlantic Multidecadal Oscillation, *Geophys. Res. Lett.*, *33*, L17706, doi:10.1029/2006GL026242.
Kohl, A. (2005), Anomalies of meridional overturning: Mechanisms in the North Atlantic, *J. Phys. Oceanogr.*, *35*(8), 1455–1472, doi:10.1175/JPO2767.1.
Kohl, A., and D. Stammer (2008), Variability of the meridional overturning in the North Atlantic from the 50-year GECCO state estimation, *J. Phys. Oceanogr.*, *38*(9), 1913–1930, doi:10.1175/2008JPO3775.1.
Koltermann, K., A. Sokov, V. Tereschenkov, S. Dobroliubov, K. Lorbacher, and A. Sy (1999), Decadal changes in the thermohaline circulation of the North Atlantic, *Deep Sea Res., Part II*, *46*(1–2), 109–138, doi:10.1016/S0967-0645(98)00115-5.
Kostov, Y., K. C. Armour, and J. Marshall (2014), Impact of the Atlantic meridional overturning circulation on ocean heat storage and transient climate change, *Geophys. Res. Lett.*, *41*, 2108–2116, doi:10.1002/2013GL058998.
Kröger, J., W. A. Müller, and J.-S. von Storch (2012), Impact of different ocean reanalyses on decadal climate prediction, *Clim. Dyn.*, *39*(3–4), 795–810, doi:10.1007/s00382-012-1310-7.
Kuhlbrodt, T., and J. M. Gregory (2012), Ocean heat uptake and its consequences for the magnitude of sea level rise and climate change, *Geophys. Res. Lett.*, *39*, L18608, doi:10.1029/2012GL052952.
Kuhlbrodt, T., S. Titz, U. Feudel, and S. Rahmstorf (2001), A simple model of seasonal open ocean convection, *Ocean Dyn.*, *52*(1), 36–49, doi:10.1007/s10236-001-8175-3.
Kuhlbrodt, T., A. Griesel, M. Montoya, A. Levermann, M. Hofmann, and S. Rahmstorf (2007), On the driving processes of the Atlantic meridional overturning circulation, *Rev. Geophys.*, *45*, RG2001, doi:10.1029/2004RG000166.
Kushner, P. J., I. M. Held, and T. L. Delworth (2001), Southern Hemisphere atmospheric circulation response to global warming, *J. Clim.*, *14*(10), 2238–2249, doi:10.1175/1520-0442(2001)014<0001:SHACRT>2.0.CO;2.
Kushnir, Y. (1994), Interdecadal variations in North Atlantic sea surface temperature and associated atmospheric conditions, *J. Clim.*, *7*(1), 141–157, doi:10.1175/1520-0442(1994)007<0141:IVINAS>2.0.CO;2.
Kwon, Y.-O., and C. Frankignoul (2012), Stochastically-driven multidecadal variability of the Atlantic meridional overturning circulation in CCSM3, *Clim. Dyn.*, *38*(5–6), 859–876, doi:10.1007/s00382-011-1040-2.
Kwon, Y.-O., and C. Frankignoul (2014), Mechanisms of multidecadal Atlantic Meridional Overturning Circulation variability diagnosed in depth versus density space, *J. Clim.*, *27*(24), 9359–9376, doi:10.1175/JCLI-D-14-00228.1.
Kwon, Y.-O., and T. M. Joyce (2013), Northern Hemisphere winter atmospheric transient eddy heat fluxes and the Gulf Stream and Kuroshio-Oyashio extension variability, *J. Clim.*, *26*(24), 9839–9859, doi:10.1175/JCLI-D-12-00647.1.
LaCasce, J. H., and J. Pedlosky (2004), The instability of Rossby basin modes and the oceanic eddy field, *J. Phys. Oceanogr.*, *34*(9), 2027–2041, doi:10.1175/1520-0485(2004)034<2027:TIORBM>2.0.CO;2.
Landerer, F. W., D. N. Wiese, K. Bentel, C. Boening, and M. M. Watkins (2015), North Atlantic meridional overturning circulation variations from GRACE ocean bottom pressure anomalies, *Geophys. Res. Lett.*, *42*, 8114–8121, doi:10.1002/2015GL065730.
Large, W. G., and S. Yeager (2009), The global climatology of an interannually varying air-sea flux data set, *Clim. Dyn.*, *33*, 341–364, doi:10.1007/s00382-008-0441-3.

Latif, M., and N. S. Keenlyside (2011), A perspective on decadal climate variability and predictability, *Deep Sea Res., Part II*, *58*(17–18), 1880–1894, doi:10.1016/j.dsr2.2010.10.066.
Latif, M., E. Roeckner, M. Botzet, M. Esch, H. Haak, S. Hagemann, J. Jungclaus, S. Legutke, S. Marsland, U. Mikolajewicz, and J. Mitchell (2004), Reconstructing, monitoring, and predicting multidecadal-scale changes in the North Atlantic thermohaline circulation with sea surface temperature, *J. Clim.*, *17*(7), 1605–1614, doi:10.1175/1520-0442(2004)017<1605:RMAPMC>2.0.CO;2.
Latif, M., C. Böning, J. Willebrand, A. Biastoch, J. Dengg, N. Keenlyside, U. Schweckendiek, and G. Madec (2006), Is the thermohaline circulation changing?, *J. Clim.*, *19*(18), 4631–4637, doi:10.1175/JCLI3876.1.
Latif, M., C. W. Böning, J. Willebrand, A. Biastoch, F. Alvarez-Garcia, N. Keenlyside, and H. Pohlmann (2007), Decadal to multidecadal variability of the Atlantic MOC: Mechanisms and predictability, in *Ocean Circulation: Mechanisms and Impacts—Past and Future Changes of Meridional Overturning*, edited by A. Schmittner, J. C. H. Chiang, and S. R. Hemming, pp. 149–166, AGU, Washington, D. C., doi:10.1029/173GM11.
Lavender, K. L., R. E. Davis, and W. B. Owens (2000), Mid-depth recirculation observed in the interior Labrador and Irminger seas by direct velocity measurements, *Nature*, *407*(6800), 66–69.
LeBel, D. A., et al. (2008), The formation rate of North Atlantic Deep Water and Eighteen Degree Water calculated from CFC-11 inventories observed during WOCE, *Deep Sea Res., Part I*, *55*(8), 891–910, doi:10.1016/j.dsr.2008.03.009.
Lee, S.-K., and C. Wang (2010), Delayed advective oscillation of the Atlantic thermohaline circulation, *J. Clim.*, *23*(5), 1254–1261, doi:10.1175/2009JCLI3339.1.
Lee, T., and J. Marotzke (1998), Seasonal cycles of meridional overturning and heat transport of the Indian Ocean, *J. Phys. Oceanogr.*, *28*(5), 923–943.
Lenton, T. M., R. J. Myerscough, R. Marsh, V. N. Livina, A. R. Price, and S. J. Cox (2009), Using GENIE to study a tipping point in the climate system, *Philos. Trans. R. Soc. A*, *367*(1890), 871–884.
Levitus, S., J. Antonov, and T. Boyer (2005), Warming of the world ocean, 1955–2003, *Geophys. Res. Lett.*, *32*, L02604, doi:10.1029/2004GL021592.
Liu, W., and Z. Liu (2014), A note on the stability indicator of the Atlantic Meridional Overturning Circulation, *J. Clim.*, *27*(2), 969–975, doi:10.1175/JCLI-D-13-00181.1.
Lohmann, K., H. Drange, and M. Bentsen (2009), Response of the North Atlantic subpolar gyre to persistent North Atlantic oscillation like forcing, *Clim. Dyn.*, *32*(2–3), 273–285, doi:10.1007/s00382-008-0467-6.
Longworth, H. R., and H. L. Bryden (2007), Discovery and quantification of the Atlantic meridional overturning circulation: The importance of 25°N, in *Ocean Circulation: Mechanisms and Impacts—Past and Future Changes of Meridional Overturning, Geophysical Monographs*, vol. 173, edited by H. R. Longworth and H. L. Bryden, pp. 5–18, AGU, Washington, D. C., doi:10.1029/173GM03.
Longworth, H. R., H. L. Bryden, and M. O. Baringer (2011), Historical variability in Atlantic meridional baroclinic transport at 26.5°N from boundary dynamic height observations, *Deep Sea Res., Part II*, *58*(17–18), 1754–1767, doi:10.1016/j.dsr2.2010.10.057.
Lorbacher, K., J. Dengg, C. W. Böning, and A. Biastoch (2010), Regional patterns of sea level change related to interannual variability and multidecadal trends in the Atlantic Meridional Overturning Circulation, *J. Clim.*, *23*(15), 4243–4254, doi:10.1175/2010JCLI3341.1.
Lozier, M. S. (1999), The impact of mid-depth recirculations on the distribution of tracers in the North Atlantic, *Geophys. Res. Lett.*, *26*(2), 219–222, doi:10.1029/1998GL900264.
Lozier, M. S. (2010), Deconstructing the conveyor belt, *Science*, *328*(5985), 1507–1511, doi:10.1126/science.1189250.
Lozier, M. S. (2012), Overturning in the North Atlantic, *Annu. Rev. Mar. Sci.*, *4*, 291–315, doi:10.1146/annurev-marine-120710-100740.
Lozier, M. S., and N. M. Stewart (2008), On the temporally varying northward penetration of Mediterranean Overflow Water and eastward penetration of Labrador Sea Water, *J. Phys. Oceanogr.*, *38*(9), 2097–2103, doi:10.1175/2008JPO3908.1.
Lozier, M. S., L. J. Pratt, A. M. Rogerson, and P. D. Miller (1997), Exchange geometry revealed by float trajectories in the Gulf Stream, *J. Phys. Oceanogr.*, *27*(11), 2327–2341, doi:10.1175/1520-0485(1997)027<2327:EGRBFT>2.0.CO;2.
Lozier, M. S., V. Roussenov, M. S. C. Reed, and R. G. Williams (2010), Opposing decadal changes for the North Atlantic meridional overturning circulation, *Nat. Geosci.*, *3*(10), 728–734, doi:10.1038/ngeo947.
Lozier, M. S., S. F. Gary, and A. S. Bower (2013), Simulated pathways of the overflow waters in the North Atlantic: Subpolar to subtropical export, *Deep Sea Res., Part II*, *85*(0), 147–153, doi:10.1016/j.dsr2.2012.07.037.
Lumpkin, R., and G. C. Johnson (2013), Global ocean surface velocities from drifters: Mean, variance, El Niño-Southern Oscillation response, and seasonal cycle, *J. Geophys. Res.*, *118*, 2992–3006, doi:10.1002/jgrc.20210.
Lumpkin, R., and K. Speer (2003), Large-scale vertical and horizontal circulation in the North Atlantic Ocean, *J. Phys. Oceanogr.*, *33*(9), 1902–1920, doi:10.1175/1520-0485(2003)033<1902:LVAHCI>2.0.CO;2.
Lumpkin, R., and K. Speer (2007), Global ocean meridional overturning, *J. Phys. Oceanogr.*, *37*(10), 2550–2562, doi:10.1175/JPO3130.1.
Lumpkin, R., K. G. Speer, and K. P. Koltermann (2008), Transport across 48°N in the Atlantic Ocean, *J. Phys. Oceanogr.*, *38*(4), 733–752, doi:10.1175/2007JPO3636.1.
Lumpkin, R., S. A. Grodsky, L. Centurioni, M.-H. Rio, J. A. Carton, and D. Lee (2013), Removing spurious low-frequency variability in drifter velocities, *J. Atmos. Oceanic Technol.*, *30*(2), 353–360, doi:10.1175/JTECH-D-12-00139.1.
Mahajan, S., R. Zhang, T. L. Delworth, S. Zhang, A. J. Rosati, and Y.-S. Chang (2011), Predicting Atlantic Meridional Overturning Circulation (AMOC) variations using subsurface and surface fingerprints, *Deep Sea Res., Part II*, *58*(17–18), 1895–1903, doi:10.1016/j.dsr2.2010.10.067.
Maidens, A., A. Arribas, A. A. Scaife, C. MacLachlan, D. Peterson, and J. Knight (2013), The influence of surface forcings on prediction of the North Atlantic Oscillation regime of winter 2010/11, *Mon. Weather Rev.*, *141*(11), 3801–3813, doi:10.1175/MWR-D-13-00033.1.
Manabe, S., and R. J. Stouffer (1988), Two stable equilibria of a coupled ocean-atmosphere model, *J. Clim.*, *1*(9), 841–866, doi:10.1175/1520-0442(1988)001<0841:TSEOAC>2.0.CO;2.
Manabe, S., and R. J. Stouffer (1994), Multiple-century response of a coupled ocean-atmosphere model to an increase of atmospheric carbon dioxide, *J. Clim.*, *7*(1), 5–23, doi:10.1175/1520-0442(1994)007<0005:MCROAC>2.0.CO;2.
Mann, M. E., and K. A. Emanuel (2006), Atlantic hurricane trends linked to climate change, *EOS Trans. AGU*, *87*(24), 233–241, doi:10.1029/2006EO240001.
Mann, M. E., and J. Park (1994), Global-scale modes of surface temperature variability on interannual to century timescales, *J. Geophys. Res.*, *99*(D12), 25,819–25,833, doi:10.1029/94JD02396.
Mann, M. E., J. Park, and R. S. Bradley (1995), Global interdecadal and century-scale climate oscillations during the past five centuries, *Nature*, *378*(6554), 266–270.
Mann, M. E., B. A. Steinman, and S. K. Miller (2014), On forced temperature changes, internal variability, and the AMO, *Geophys. Res. Lett.*, *41*, 3211–3219, doi:10.1002/2014GL059233.
Marotzke, J., and B. A. Klinger (2000), The dynamics of equatorially asymmetric thermohaline circulations, *J. Phys. Oceanogr.*, *30*(5), 955–970.

Marotzke, J., and J. R. Scott (1999), Convective mixing and the thermohaline circulation, *J. Phys. Oceanogr.*, *29*(11), 2962–2970, doi:10.1175/1520-0485(1999)029<2962:CMATTC>2.0.CO;2.
Marsh, R., S. A. Josey, B. A. de Cuevas, L. J. Redbourn, and G. D. Quartly (2008), Mechanisms for recent warming of the North Atlantic: Insights gained with an eddy-permitting model, *J. Geophys. Res.*, *113*, C04031, doi:10.1029/2007JC004096.
Marshall, D. P., and H. L. Johnson (2013), Propagation of meridional circulation anomalies along western and eastern boundaries, *J. Phys. Oceanogr.*, *43*(12), 2699–2717, doi:10.1175/JPO-D-13-0134.1.
Marshall, G. J. (2003), Trends in the Southern Annular Mode from observations and reanalyses, *J. Clim.*, *16*(24), 4134–4143, doi:10.1175/1520-0442(2003)016<4134:TITSAM>2.0.CO;2.
Marshall, J., and A. Plumb (2008), *Atmosphere, Ocean, and Climate Dynamics: An Introductory Text*, Elsevier, Amsterdam.
Marshall, J., and T. Radko (2003), Residual-mean solutions for the Antarctic Circumpolar Current and its associated overturning circulation, *J. Phys. Oceanogr.*, *33*(11), 2341–2354, doi:10.1175/1520-0485(2003)033<2341:RSFTAC>2.0.CO;2.
Marshall, J., and F. Schott (1999), Open-ocean convection: Observations, theory, and models, *Rev. Geophys.*, *37*(1), 1–64, doi:10.1029/98RG02739.
Marshall, J., and K. Speer (2012), Closure of the meridional overturning circulation through Southern Ocean upwelling, *Nat. Geosci.*, *5*(3), 171–180, doi:10.1038/ngeo1391.
Marshall, J., H. Johnson, and J. Goodman (2001a), A study of the interaction of the North Atlantic Oscillation with ocean circulation, *J. Clim.*, *14*(7), 1399–1421, doi:10.1175/1520-0442(2001)014<1399:ASOTIO>2.0.CO;2.
Marshall, J., Y. Kushnir, D. Battisti, P. Chang, A. Czaja, R. Dickson, J. Hurrell, M. McCartney, R. Saravanan, and M. Visbeck (2001b), North Atlantic climate variability: Phenomena, impacts and mechanisms, *Int. J. Climatol.*, *21*, 1863–1898, doi:10.1002/joc.693.
Marshall, J., A. Donohoe, D. Ferreira, and D. McGee (2014a), The ocean's role in setting the mean position of the Inter-Tropical Convergence Zone, *Clim. Dyn.*, *42*(7–8), 1967–1979, doi:10.1007/s00382-013-1767-z.
Marshall, J., K. C. Armour, J. R. Scott, Y. Kostov, U. Hausmann, D. Ferreira, T. G. Shepherd, and C. M. Bitz (2014b), The ocean's role in polar climate change: Asymmetric Arctic and Antarctic responses to greenhouse gas and ozone forcing, *Philos. Trans. R. Soc. A*, *372*(2019), 20130040, doi:10.1098/rsta.2013.0040.
Marshall, J., J. R. Scott, K. C. Armour, J. M. Campin, M. Kelley, and A. Romanou (2014c), The ocean's role in the transient response of climate to abrupt greenhouse gas forcing, *Clim. Dyn.*, *44*, 2287–2299, doi:10.1007/s00382-014-2308-0.
Matei, D., J. Baehr, J. H. Jungclaus, H. Haak, W. A. Müller, and J. Marotzke (2012a), Multiyear prediction of monthly mean Atlantic Meridional Overturning Circulation at 26.5°N, *Science*, *335*(6064), 76–79, doi:10.1126/science.1210299.
Matei, D., H. Pohlmann, J. Jungclaus, W. Müller, H. Haak, and J. Marotzke (2012b), Two tales of initializing decadal climate prediction experiments with the ECHAM5/MPI-OM model, *J. Clim.*, *25*(24), 8502–8523, doi:10.1175/JCLI-D-11-00633.1.
Mauritzen, C., and S. Häkkinen (1999), On the relationship between dense water formation and the "Meridional Overturning Cell" in the North Atlantic Ocean, *Deep Sea Res., Part I*, *46*(5), 877–894, doi:10.1016/S0967-0637(98)00094-6.
McCarthy, G., E. Frajka-Williams, W. E. Johns, M. O. Baringer, C. S. Meinen, H. L. Bryden, D. Rayner, A. Duchez, C. Roberts, and S. A. Cunningham (2012), Observed interannual variability of the Atlantic meridional overturning circulation at 26.5°N, *Geophys. Res. Lett.*, *39*, L19609, doi:10.1029/2012GL052933.
McCarthy, G. D., D. A. Smeed, W. E. Johns, E. Frajka-Williams, B. I. Moat, D. Rayner, M. O. Baringer, C. S. Meinen, J. Collins, and H. L. Bryden (2015), Measuring the Atlantic Meridional Overturning Circulation at 26°N, *Prog. Oceanogr.*, *130*, 91–111, doi:10.1016/j.pocean.2014.10.006.
McDonagh, E. L., and B. A. King (2005), Oceanic fluxes in the South Atlantic, *J. Phys. Oceanogr.*, *35*(1), 109–122, doi:10.1175/JPO-2666.1.
McDonagh, E. L., P. McLeod, B. A. King, H. L. Bryden, and S. T. Valdés (2010), Circulation, heat, and freshwater transport at 36°N in the Atlantic, *J. Phys. Oceanogr.*, *40*(12), 2661–2678, doi:10.1175/2010JPO4176.1.
Medhaug, I., H. R. Langehaug, T. Eldevik, T. Furevik, and M. Bentsen (2012), Mechanisms for decadal scale variability in a simulated Atlantic meridional overturning circulation, *Clim. Dyn.*, *39*(1–2), 77–93, doi:10.1007/s00382-011-1124-z.
Meehl, G. A., et al. (2013), Decadal climate prediction: An update from the trenches, *Bull. Am. Meteorol. Soc.*, *95*, 243–267, doi:10.1175/BAMS-D-12-00241.1.
Meehl, G. A., H. Teng, and J. M. Arblaster (2014), Climate model simulations of the observed early-2000s hiatus of global warming, *Nat. Clim. Change*, *4*(10), 898–902, doi:10.1038/nclimate2357.
Meinen, C. S., M. O. Baringer, and R. F. Garcia (2010), Florida Current transport variability: An analysis of annual and longer-period signals, *Deep Sea Res., Part I*, *57*(7), 835–846, doi:10.1016/j.dsr.2010.04.001.
Meinen, C. S., S. Speich, R. C. Perez, S. Dong, A. R. Piola, S. L. Garzoli, M. O. Baringer, S. Gladyshev, and E. J. D. Campos (2013), Temporal variability of the meridional overturning circulation at 34.5°S: Results from two pilot boundary arrays in the South Atlantic, *J. Geophys. Res.*, *118*(12), 6461–6478, doi:10.1002/2013JC009228.
Mielke, C., E. Frajka-Williams, and J. Baehr (2013), Observed and simulated variability of the AMOC at 26°N and 41°N, *Geophys. Res. Lett.*, *40*, 1159–1164, doi:10.1002/grl.50233.
Mignot, J., and C. Frankignoul (2005), The variability of the Atlantic Meridional Overturning Circulation, the North Atlantic Oscillation, and the El Niño-Southern Oscillation in the Bergen Climate Model, *J. Clim.*, *18*(13), 2361–2375, doi:10.1175/JCLI3405.1.
Monahan, A. H. (2002), Stabilization of climate regimes by noise in a simple model of the thermohaline circulation, *J. Phys. Oceanogr.*, *32*(7), 2072–2085, doi:10.1175/1520-0485(2002)032<2072:SOCRBN>2.0.CO;2.
Msadek, R., and C. Frankignoul (2009), Atlantic multidecadal oceanic variability and its influence on the atmosphere in a climate model, *Clim. Dyn.*, *33*, 45–62, doi:10.1007/s00382-008-0452-0.
Msadek, R., K. W. Dixon, T. L. Delworth, and W. Hurlin (2010), Assessing the predictability of the Atlantic meridional overturning circulation and associated fingerprints, *Geophys. Res. Lett.*, *37*, L19608, doi:10.1029/2010GL044517.
Msadek, R., W. E. Johns, S. G. Yeager, G. Danabasoglu, T. L. Delworth, and A. Rosati (2013), The Atlantic meridional heat transport at 26.5°N and its relationship with the MOC in the RAPID array and the GFDL and NCAR coupled models, *J. Clim.*, *26*, 4335–4356, doi:10.1175/JCLI-D-12-00081.1.
Müller, W. A., J. Baehr, H. Haak, J. H. Jungclaus, J. Kröger, D. Matei, D. Notz, H. Pohlmann, J. S. von Storch, and J. Marotzke (2012), Forecast skill of multi-year seasonal means in the decadal prediction system of the Max Planck Institute for Meteorology, *Geophys. Res. Lett.*, *39*, L22707, doi:10.1029/2012GL053326.
Müller, W. A., H. Pohlmann, F. Sienz, and D. Smith (2014), Decadal climate predictions for the period 1901–2010 with a coupled climate model, *Geophys. Res. Lett.*, *41*, 2100–2107, doi:10.1002/2014GL059259.
Munoz, E., B. Kirtman, and W. Weijer (2011), Varied representation of the Atlantic Meridional Overturning across multidecadal ocean reanalyses, *Deep Sea Res., Part II*, *58*(17–18), 1848–1857, doi:10.1016/j.dsr2.2010.10.064.

Nurser, A. J. G., and R. G. Williams (1990), Cooling Parsons' model of the separated Gulf Stream, *J. Phys. Oceanogr.*, *20*(12), 1974–1979, doi:10.1175/1520-0485(1990)020<1974:CPMOTS>2.0.CO;2.
Ollitrault, M., and A. Colin de Verdiére (2014), The ocean general circulation near 1000-m depth, *J. Phys. Oceanogr.*, *44*(1), 384–409, doi:10.1175/JPO-D-13-030.1.
Ollitrault, M., and J.-P. Rannou (2013), ANDRO: An Argo-based deep displacement dataset, *J. Atmos. Oceanic Technol.*, *30*(4), 759–788, doi:10.1175/JTECH-D-12-00073.1.
Osychny, V., and P. Cornillon (2004), Properties of Rossby waves in the North Atlantic estimated from satellite data, *J. Phys. Oceanogr.*, *34*(1), 61–76, doi:10.1175/1520-0485(2004)034<0061:PORWIT>2.0.CO;2.
Otterå, O. H., M. Bentsen, H. Drange, and L. Suo (2010), External forcing as a metronome for Atlantic multidecadal variability, *Nat. Geosci.*, *3*(10), 688–694.
Palter, J. B. (2014), The role of the Gulf Stream in European climate, *Annu. Rev. Mar. Sci.*, *7*, 113–37, doi:10.1146/annurev-marine-010814-015656.
Palter, J. B., M. S. Lozier, and K. L. Lavender (2008), How does Labrador Sea Water enter the Deep Western Boundary Current?, *J. Phys. Oceanogr.*, *38*(5), 968–983, doi:10.1175/2007JPO3807.1.
Patricola, C. M., P. Chang, and R. Saravanan (2013), Impact of Atlantic SST and high frequency atmospheric variability on the 1993 and 2008 Midwest floods: Regional climate model simulations of extreme climate events, *Clim. Change*, *129*, 397–411, doi:10.1007/s10584-013-0886-1.
Peña Molino, B., and T. M. Joyce (2008), Variability in the slope water and its relation to the Gulf Stream path, *Geophys. Res. Lett.*, *35*, L03606, doi:10.1029/2007GL032183.
Peña Molino, B., T. Joyce, and J. Toole (2011), Recent changes in the Labrador Sea Water within the Deep Western Boundary Current southeast of Cape Cod, *Deep Sea Res., Part I*, *58*, 1019–1030, doi:10.1016/j.dsr.2011.07.006.
Peña Molino, B., T. M. Joyce, and J. M. Toole (2012), Variability in the Deep Western Boundary Current: Local versus remote forcing, *J. Geophys. Res.*, *117*, C12022, doi:10.1029/2012JC008369.
Pedro, J. B., T. D. van Ommen, S. O. Rasmussen, V. I. Morgan, J. Chappellaz, A. D. Moy, V. Masson-Delmotte, and M. Delmotte (2011), The last deglaciation: Timing the bipolar seesaw, *Clim. Past*, *7*(2), 671–683, doi:10.5194/cp-7-671-2011.
Pickart, R. S., and M. A. Spall (2007), Impact of labrador sea convection on the North Atlantic meridional overturning circulation, *J. Phys. Oceanogr.*, *37*(9), 2207–2227, doi:10.1175/JPO3178.1.
Piecuch, C. G., and R. M. Ponte (2012), Importance of circulation changes to Atlantic heat storage rates, *J. Clim.*, *25*(1), 350–362, doi:10.1175/JCLI-D-11-00123.1.
Pohlmann, H., M. Botzet, M. Latif, A. Roesch, M. Wild, and P. Tschuck (2004), Estimating the decadal predictability of a coupled AOGCM, *J. Clim.*, *17*, 4463–4472.
Pohlmann, H., F. Sienz, and M. Latif (2006), Influence of the multidecadal Atlantic Meridional Overturning Circulation variability on European climate, *J. Clim.*, *19*(23), 6062–6067, doi:10.1175/JCLI3941.1.
Pohlmann, H., J. H. Jungclaus, A. Köhl, D. Stammer, and J. Marotzke (2009), Initializing decadal climate predictions with the GECCO oceanic synthesis: Effects on the North Atlantic, *J. Clim.*, *22*(14), 3926–3938, doi:10.1175/2009JCLI2535.1.
Pohlmann, H., D. M. Smith, M. A. Balmaseda, N. S. Keenlyside, S. Masina, D. Matei, W. A. Müller, and P. Rogel (2013), Predictability of the mid-latitude Atlantic meridional overturning circulation in a multi-model system, *Clim. Dyn.*, *41*(3–4), 775–785, doi:10.1007/s00382-013-1663-6.
Polo, I., J. Robson, R. Sutton, and M. A. Balmaseda (2014), The importance of wind and buoyancy forcing for the boundary density variations and the geostrophic component of the AMOC at 26°N, *J. Phys. Oceanogr.*, *44*(9), 2387–2408, doi:10.1175/JPO-D-13-0264.1.
Qiu, B. (2002), Large-scale variability in the midlatitude subtropical and subpolar North Pacific Ocean: Observations and causes, *J. Phys. Oceanogr.*, *32*(1), 353–375, doi:10.1175/1520-0485(2002)032<0353:LSVITM>2.0.CO;2.
Qiu, B., and S. Chen (2006), Decadal variability in the large-scale sea surface height field of the South Pacific Ocean: Observations and causes, *J. Phys. Oceanogr.*, *36*, 1751–1762.
Quadfasel, D., and R. Käse (2007), Present-day manifestation of the Nordic Seas overflows, in *Ocean Circulation: Mechanisms and Impacts—Past and Future Changes of Meridional Overturning*, edited by A. Schmittner, J. C. H. Chiang, and S. R. Hemming, pp. 75–89, AGU, Washington, D. C., doi:10.1029/173GM07.
Rahmstorf, S. (1995), Bifurcations of the Atlantic thermohaline circulation in response to changes in the hydrological cycle, *Nature*, *378*(6553), 145–149.
Rahmstorf, S. (1996), On the freshwater forcing and transport of the Atlantic thermohaline circulation, *Clim. Dyn.*, *12*(12), 799–811, doi:10.1007/s003820050144.
Rahmstorf, S. (1999), Decadal variability of the thermohaline ocean circulation, in *Beyond El Niño*, edited by A. Navarra, pp. 309–331, Springer, Berlin.
Rahmstorf, S. (2002), Ocean circulation and climate during the past 120,000 years, *Nature*, *419*(6903), 207–214.
Rahmstorf, S., et al. (2005), Thermohaline circulation hysteresis: A model intercomparison, *Geophys. Res. Lett.*, *32*, L23605, doi:10.1029/2005GL023655.
Rahmstorf, S., J. E. Box, G. Feulner, M. E. Mann, A. Robinson, S. Rutherford, and E. J. Schaffernicht (2015), Exceptional twentieth-century slowdown in Atlantic Ocean overturning circulation, *Nat. Clim. Change*, *5*(5), 475–480, doi:10.1038/nclimate2554.
Raper, S. C. B., J. M. Gregory, and R. J. Stouffer (2002), The role of climate sensitivity and ocean heat uptake on AOGCM transient temperature response, *J. Clim.*, *15*(1), 124–130, doi:10.1175/1520-0442(2002)015<0124:TROCSA>2.0.CO;2.
Rayner, D., et al. (2011), Monitoring the Atlantic meridional overturning circulation, *Deep Sea Res., Part II*, *58*(17–18), 1744–1753, doi:10.1016/j.dsr2.2010.10.056.
Rayner, N. A., D. E. Parker, E. B. Horton, C. K. Folland, L. V. Alexander, D. P. Rowell, E. C. Kent, and A. Kaplan (2003), Global analyses of sea surface temperature, sea ice, and night marine air temperature since the late nineteenth century, *J. Geophys. Res.*, *108*(D14), 4407, doi:10.1029/2002JD002670.
Reynolds, R. W., and T. M. Smith (1994), Improved global sea surface temperature analyses using optimum interpolation, *J. Clim.*, *7*(6), 929–948, doi:10.1175/1520-0442(1994)007<0929:IGSSTA>2.0.CO;2.
Rhein, M. (1994), The deep western boundary current: Tracers and velocities, *Deep Sea Res., Part I*, *41*(2), 263–281, doi:10.1016/0967-0637(94)90003-5.
Rhein, M., J. Fischer, W. M. Smethie, D. Smythe-Wright, R. F. Weiss, C. Mertens, D. H. Min, U. Fleischmann, and A. Putzka (2002), Labrador Sea Water: Pathways, CFC inventory, and formation rates, *J. Phys. Oceanogr.*, *32*(2), 648–665, doi:10.1175/1520-0485(2002)032<0648:LSWPCI>2.0.CO;2.

Rhein, M., D. Kieke, S. Hüttl-Kabus, A. Roessler, C. Mertens, R. Meissner, B. Klein, C. W. Böning, and I. Yashayaev (2011), Deep water formation, the subpolar gyre, and the meridional overturning circulation in the subpolar North Atlantic, *Deep Sea Res., Part II*, *58*(17–18), 1819–1832, doi:10.1016/j.dsr2.2010.10.061.

Rhein, M., D. Kieke, and R. Steinfeldt (2015), Advection of North Atlantic Deep Water from the Labrador Sea to the Southern Hemisphere, *J. Geophys. Res. Oceans*, *120*, 2471–2487, doi:10.1002/2014JC010605.

Rhines, P., S. Häkkinen, and S. A. Josey (2008), Is Oceanic Heat Transport Significant in the Climate System?, in *Arctic-Subarctic Ocean Fluxes*, pp. 87–109, Springer, Netherlands, doi:10.1007/978-1-4020-6774-7_5.

Roberts, C. D., F. K. Garry, and L. C. Jackson (2013a), A multimodel study of sea surface temperature and subsurface density fingerprints of the Atlantic Meridional Overturning Circulation, *J. Clim.*, *26*(22), 9155–9174, doi:10.1175/JCLI-D-12-00762.1.

Roberts, C. D., J. Waters, K. A. Peterson, M. D. Palmer, G. D. McCarthy, E. Frajka-Williams, K. Haines, D. J. Lea, M. J. Martin, D. Storkey, E. W. Blockley, and H. Zuo (2013b), Atmosphere drives recent interannual variability of the Atlantic meridional overturning circulation at 26.5°N, *Geophys. Res. Lett.*, *40*, 5164–5170, doi:10.1002/grl.50930.

Roberts, C. D., L. Jackson, and D. McNeall (2014), Is the 2004–2012 reduction of the Atlantic meridional overturning circulation significant?, *Geophys. Res. Lett.*, *41*, 3204–3210, doi:10.1002/2014GL059473.

Robson, J., R. Sutton, K. Lohmann, D. Smith, and M. D. Palmer (2012), Causes of the rapid warming of the North Atlantic Ocean in the mid-1990s, *J. Clim.*, *25*(12), 4116–4134, doi:10.1175/JCLI-D-11-00443.1.

Roemmich, D., and C. Wunsch (1985), Two trans-Atlantic sections: Meridional circulation and heat flux in the subtropical North Atlantic Ocean, *Deep Sea Res. Part A*, *32*, 619–664, doi:10.1016/0198-0149(85)90070-6.

Rossby, T. (1996), The North Atlantic Current and surrounding waters: At the crossroads, *Rev. Geophys.*, *34*(4), 463–481, doi:10.1029/96RG02214.

Rossby, T. (1999), On gyre interactions, *Deep Sea Res., Part II*, *46*(1–2), 139–164, doi:10.1016/S0967-0645(98)00095-2.

Rugenstein, M. A. A., M. Winton, R. J. Stouffer, S. M. Griffies, and R. Hallberg (2013), Northern high-latitude heat budget decomposition and transient warming, *J. Clim.*, *26*(2), 609–621, doi:10.1175/JCLI-D-11-00695.1.

Rypina, I. I., L. J. Pratt, and M. S. Lozier (2011), Near-surface transport pathways in the North Atlantic Ocean: Looking for throughput from the subtropical to the subpolar gyre, *J. Phys. Oceanogr.*, *41*(5), 911–925, doi:10.1175/2011JPO4498.1.

Saenko, O. A., and W. J. Merryfield (2006), Vertical partition of ocean heat transport in isothermal coordinates, *Geophys. Res. Lett.*, *33*, L01606, doi:10.1029/2005GL024902.

Sandström, J. W. (1908), Dynamische versuche mit meerwasser, *Ann. Hydrogr. Mar. Meteorol.*, *36*, 6–23.

Saravanan, R., and J. C. McWilliams (1998), Advective ocean-atmosphere interaction: An analytical stochastic model with implications for decadal variability, *J. Clim.*, *11*(2), 165–188, doi:10.1175/1520-0442(1998)011<0165:AOAIAA>2.0.CO;2.

Sasaki, Y. N., and N. Schneider (2011), Interannual to decadal Gulf Stream variability in an eddy-resolving ocean model, *Ocean Model.*, *39*(3–4), 209–219, doi:10.1016/j.ocemod.2011.04.004.

Sato, O. T., and T. Rossby (2000), Seasonal and low-frequency variability of the meridional heat flux at 36°N in the North Atlantic, *J. Phys. Oceanogr.*, *30*(3), 606–621.

Scaife, A. A., D. Copsey, C. Gordon, C. Harris, T. Hinton, S. Keeley, A. O'Neill, M. Roberts, and K. Williams (2011), Improved Atlantic winter blocking in a climate model, *Geophys. Res. Lett.*, *38*, L23703, doi:10.1029/2011GL049573.

Scaife, A. A., et al. (2014), Skillful long-range prediction of European and North American winters, *Geophys. Res. Lett.*, *41*, 2514–2519, doi:10.1002/2014GL059637.

Schaeffer, M., F. M. Selten, J. D. Opsteegh, and H. Goosse (2002), Intrinsic limits to predictability of abrupt regional climate change in IPCC SRES scenarios, *Geophys. Res. Lett.*, *29*(16), 1767, doi:10.1029/2002GL015254.

Schiller, A. (1995), The mean circulation of the Atlantic Ocean north of 30°S determined with the adjoint method applied to an ocean general circulation model, *J. Mar. Res.*, *53*(3), 453–497, doi:10.1357/0022240953213188.

Schiller, A., U. Mikolajewicz, and R. Voss (1997), The stability of the North Atlantic thermohaline circulation in a coupled ocean-atmosphere general circulation model, *Clim. Dyn.*, *13*(5), 325–347, doi:10.1007/s003820050169.

Schlax, M. G., D. B. Chelton, and M. H. Freilich (2001), Sampling errors in wind fields constructed from single and tandem scatterometer datasets, *J. Atmos. Oceanic Technol.*, *18*(6), 1014–1036, doi:10.1175/1520-0426(2001)018<1014:SEIWFC>2.0.CO;2.

Schlesinger, M. E., and N. Ramankutty (1994), An oscillation in the global climate system of period 65–70 years, *Nature*, *367*(6465), 723–726.

Schloesser, F., R. Furue, J. P. McCreary Jr., and A. Timmermann (2012), Dynamics of the Atlantic meridional overturning circulation. Part 1: Buoyancy-forced response, *Prog. Oceanogr.*, *101*(1), 33–62, doi:10.1016/j.pocean.2012.01.002.

Schmith, T., S. Yang, E. Gleeson, and T. Semmler (2014), How much have variations in the meridional overturning circulation contributed to sea surface temperature trends since 1850? A study with the EC-Earth global climate model, *J. Clim.*, *27*, 6343–6357, doi:10.1175/JCLI-D-13-00651.1.

Schneider, E. K., and M. Fan (2012), Observed decadal North Atlantic tripole SST variability. Part II: Diagnosis of mechanisms, *J. Atmos. Sci.*, *69*(1), 51–64, doi:10.1175/JAS-D-11-019.1.

Schneider, N., and A. Miller (2001), Predicting western North Pacific Ocean climate, *J. Clim.*, *14*, 3997–4002.

Schott, F., J. Fischer, J. Reppin, and U. Send (1993), On mean and seasonal currents and transports at the western boundary of the equatorial Atlantic, *J. Geophys. Res.*, *98*(C8), 14,353–14,368, doi:10.1029/93JC01287.

Schott, F. A., and P. Brandt (2007), Circulation and deep water export of the subpolar North Atlantic during the 1990's, in *Ocean Circulation: Mechanisms and Impacts—Past and Future Changes of Meridional Overturning*, edited by A. Schmittner, J. C. H. Chiang, and S. R. Hemming, pp. 91–118, AGU, Washington, D. C., doi:10.1029/173GM08.

Schott, F. A., R. Zantopp, L. Stramma, M. Dengler, J. Fischer, and M. Wibaux (2004), Circulation and deep-water export at the western exit of the subpolar North Atlantic, *J. Phys. Oceanogr.*, *34*(4), 817–843, doi:10.1175/1520-0485(2004)034<0817:CADEAT>2.0.CO;2.

Schott, F. A., J. Fischer, M. Wibaux, M. Dengler, and R. Zantopp (2006), Variability of the Deep Western Boundary Current east of the Grand Banks, *Geophys. Res. Lett.*, *33*, L21S07, doi:10.1029/2006GL026563.

Seager, R., Y. Kushnir, M. Visbeck, N. Naik, J. Miller, G. Krahmann, and H. Cullen (2000), Causes of Atlantic Ocean climate variability between 1958 and 1998, *J. Clim.*, *13*(16), 2845–2862, doi:10.1175/1520-0442(2000)013<2845:COAOCV>2.0.CO;2.

Seager, R., D. S. Battisti, J. Yin, N. Gordon, N. Naik, A. C. Clement, and M. A. Cane (2002), Is the Gulf Stream responsible for Europe's mild winters?, *Q. J. R. Meteorol. Soc.*, *128*(586), 2563–2586, doi:10.1256/qj.01.128.

Send, U., M. Lankhorst, and T. Kanzow (2011), Observation of decadal change in the Atlantic meridional overturning circulation using 10 years of continuous transport data, *Geophys. Res. Lett.*, *38*, L24606, doi:10.1029/2011GL049801.

Sévellec, F., and A. V. Fedorov (2012), The leading, interdecadal eigenmode of the Atlantic Meridional Overturning Circulation in a realistic ocean model, *J. Clim.*, *26*(7), 2160–2183, doi:10.1175/JCLI-D-11-00023.1.

Shaffrey, L., and R. Sutton (2006), Bjerknes compensation and the decadal variability of the energy transports in a coupled climate model, *J. Clim.*, *19*(7), 1167–1181, doi:10.1175/JCLI3652.1.
Shoosmith, D., M. Baringer, and W. E. Johns (2005), A continuous record of Florida Current temperature transport at 27°N, *Geophys. Res. Lett.*, *32*, L23603, doi:10.1029/2005GL024075.
Sinha, B., B. Topliss, A. T. Blaker, and J.-M. Hirschi (2013), A numerical model study of the effects of interannual time scale wave propagation on the predictability of the Atlantic meridional overturning circulation, *J. Geophys. Res. Oceans*, *1*, 131–146, doi:10.1029/2012JC008334.
Skinner, L. C., H. Elderfield, and M. Hall (2007), Phasing of millennial climate events and Northeast Atlantic deep-water temperature change since 50 Ka Bp, in *Ocean Circulation: Mechanisms and Impacts—Past and Future Changes of Meridional Overturning*, edited by A. Schmittner, J. C. H. Chiang, and S. R. Hemming, pp. 197–208, AGU, Washington, D. C., doi:10.1029/173GM14.
Smeed, D. A., et al. (2014), Observed decline of the Atlantic Meridional Overturning Circulation 2004 to 2012, *Ocean Sci.*, *10*(1), 29–38, doi:10.5194/os-10-29-2014.
Smethie, W. M., and R. A. Fine (2001), Rates of North Atlantic Deep Water formation calculated from chlorofluorocarbon inventories, *Deep Sea Res., Part I*, *48*(1), 189–215, doi:10.1016/S0967-0637(00)00048-0.
Smethie, W. M., R. A. Fine, A. Putzka, and E. P. Jones (2000), Tracing the flow of North Atlantic Deep Water using chlorofluorocarbons, *J. Geophys. Res.*, *105*(C6), 14,297–14,323, doi:10.1029/1999JC900274.
Smethie, W. M., D. A. Lebel, R. A. Fine, M. Rhein, and D. Kieke (2007), Strength and variability of the deep limb of the North Atlantic meridional overturning circulation from chlorofluorocarbon inventories, in *Ocean Circulation: Mechanisms and Impacts—Past and Future Changes of Meridional Overturning*, edited by A. Schmittner, J. C. H. Chiang, and S. R. Hemming, pp. 119–130, AGU, Washington, D. C., doi:10.1029/173GM09.
Smith, D. M., S. Cusack, A. W. Colman, C. K. Folland, G. R. Harris, and J. M. Murphy (2007), Improved surface temperature prediction for the coming decade from a global climate model, *Science*, *317*(5839), 796–799, doi:10.1126/science.1139540.
Smith, T. M., P. A. Arkin, L. Ren, and S. S. P. Shen (2012), Improved reconstruction of global precipitation since 1900, *J. Atmos. Oceanic Technol.*, *29*(10), 1505–1517, doi:10.1175/JTECH-D-12-00001.1.
Solomon, A., et al. (2011), Distinguishing the roles of natural and anthropogenically forced decadal climate variability, *Bull. Am. Meteorol. Soc.*, *92*(2), 141–156, doi:10.1175/2010BAMS2962.1.
Solomon, S., D. Qin, M. Manning, Z. Chen, M. Marquis, K. B. Averyt, M. Tignor, and H. L. Miller (Eds.) (2007), *Climate Change 2007: The Physical Science Basis. Contribution of Working Group I to the Fourth Assessment Report of the Intergovernmental Panel on Climate Change.*, Cambridge Univ. Press, Cambridge, U. K., and New York.
Solomon, S., K. H. Rosenlof, R. W. Portmann, J. S. Daniel, S. M. Davis, T. J. Sanford, and G.-K. Plattner (2010), Contributions of stratospheric water vapor to decadal changes in the rate of global warming, *Science*, *327*(5970), 1219–1223, doi:10.1126/science.1182488.
Spall, M. A. (1996), Dynamics of the Gulf Stream/Deep Western Boundary Current crossover. Part I: Entrainment and recirculation, *J. Phys. Oceanogr.*, *26*(10), 2152–2168, doi:10.1175/1520-0485(1996)026<2152:DOTGSW>2.0.CO;2.
Spall, M. A. (2004), Boundary currents and watermass transformation in marginal seas, *J. Phys. Oceanogr.*, *34*(5), 1197–1213, doi:10.1175/1520-0485(2004)034<1197:BCAWTI>2.0.CO;2.
Spall, M. A., and R. S. Pickart (2001), Where does dense water sink? A subpolar gyre example, *J. Phys. Oceanogr.*, *31*(3), 810–826, doi:10.1175/1520-0485(2001)031<0810:WDDWSA>2.0.CO;2.
Spence, P., O. A. Saenko, M. Eby, and A. J. Weaver (2009), The Southern Ocean overturning: Parameterized versus permitted eddies, *J. Phys. Oceanogr.*, *39*(7), 1634–1651, doi:10.1175/2009JPO4120.1.
Spooner, P. T., H. L. Johnson, and T. J. Woollings (2013), Influence of the Southern Annular Mode on projected weakening of the Atlantic Meridional Overturning Circulation, *J. Clim.*, *26*(20), 8017–8036, doi:10.1175/JCLI-D-12-00663.1.
Srokosz, M., M. Baringer, H. Bryden, S. Cunningham, T. Delworth, S. Lozier, J. Marotzke, and R. Sutton (2012), Past, present, and future changes in the Atlantic Meridional Overturning Circulation, *Bull. Am. Meteorol. Soc.*, *93*(11), 1663–1676, doi:10.1175/BAMS-D-11-00151.1.
Srokosz, M. A., and H. L. Bryden (2015), Observing the Atlantic Meridional Overturning Circulation yields a decade of inevitable surprises, *Science*, *348*(6241), 1255575, doi:10.1126/science.1255575.
Steinman, B. A., M. E. Mann, and S. K. Miller (2015), Atlantic and Pacific multidecadal oscillations and Northern Hemisphere temperatures, *Science*, *347*(6225), 988–991.
Stenchikov, G., T. L. Delworth, V. Ramaswamy, R. J. Stouffer, A. Wittenberg, and F. Zeng (2009), Volcanic signals in oceans, *J. Geophys. Res.*, *114*, D16104, doi:10.1029/2008JD011673.
Stocker, T. F. (1998), The seesaw effect, *Science*, *282*(5386), 61–62, doi:10.1126/science.282.5386.61.
Stommel, H. (1958), The abyssal circulation, *Deep Sea Res.*, *5*(1), 80–82, doi:10.1016/S0146-6291(58)80014-4.
Stommel, H. (1961), Thermohaline convection with two stable regimes of flow, *Tellus*, *13*(2), 224–230, doi:10.1111/j.2153-3490.1961.tb00079.x.
Stouffer, R. J. (2004), Time scales of climate response, *J. Clim.*, *17*(1), 209–217, doi:10.1175/1520-0442(2004)017<0209:TSOCR>2.0.CO;2.
Stouffer, R. J., et al. (2006), Investigating the causes of the response of the thermohaline circulation to past and future climate changes, *J. Clim.*, *19*(8), 1365–1387, doi:10.1175/JCLI3689.1.
Stramma, L., and M. England (1999), On the water masses and mean circulation of the South Atlantic Ocean, *J. Geophys. Res.*, *104*(C9), 20,863–20,883, doi:10.1029/1999JC900139.
Straneo, F. (2006), On the connection between dense water formation, overturning, and poleward heat transport in a convective basin, *J. Phys. Oceanogr.*, *36*(9), 1822–1840, doi:10.1175/JPO2932.1.
Sturges, W., and B. G. Hong (1995), Wind forcing of the Atlantic thermocline along 32°N at low frequencies, *J. Phys. Oceanogr.*, *25*(7), 1706–1715, doi:10.1175/1520-0485(1995)025<1706:WFOTAT>2.0.CO;2.
Sturges, W., B. G. Hong, and A. J. Clarke (1998), Decadal wind forcing of the North Atlantic subtropical gyre, *J. Phys. Oceanogr.*, *28*(4), 659–668, doi:10.1175/1520-0485(1998)028<0659:DWFOTN>2.0.CO;2.
Sutton, R. T., and M. R. Allen (1997), Decadal predictability of North Atlantic sea surface temperature and climate, *Nature*, *388*(6642), 563–567, doi:10.1038/41523.
Sutton, R. T., and D. L. R. Hodson (2005), Atlantic Ocean forcing of North American and European summer climate, *Science*, *309*(5731), 115–118, doi:10.1126/science.1109496.
Svendsen, L., S. Hetzinger, N. Keenlyside, and Y. Gao (2014), Marine-based multiproxy reconstruction of Atlantic multidecadal variability, *Geophys. Res. Lett.*, *41*, 1295–1300, doi:10.1002/2013GL059076.
Szuts, Z. B., J. R. Blundell, M. P. Chidichimo, and J. Marotzke (2102), A vertical-mode decomposition to investigate low-frequency internal motion across the Atlantic at 26°N, *Ocean Sci.*, *8*, 345–367, doi:10.5194/os-8-345-2012.
Talley, L. D. (1999), Some aspects of ocean heat transport by the shallow, intermediate and deep overturning circulations, in *Mechanisms of Global Climate Change at Millennial Time Scales, Geophys. Monogr.*, vol. 112, pp. 1–22, AGU, Washington, D. C.

Talley, L. D. (2003), Shallow, intermediate, and deep overturning components of the global heat budget, *J. Phys. Oceanogr.*, *33*(3), 530–560, doi:10.1175/1520-0485(2003)033<0530:SIADOC>2.0.CO;2.
Talley, L. D. (2008), Freshwater transport estimates and the global overturning circulation: Shallow, deep and throughflow components, *Prog. Oceanogr.*, *78*(4), 257–303, doi:10.1016/j.pocean.2008.05.001.
Talley, L. D., J. L. Reid, and P. E. Robbins (2003), Data-based meridional overturning streamfunctions for the global ocean, *J. Clim.*, *16*(19), 3213–3226, doi:10.1175/1520-0442(2003)016<3213:DMOSFT>2.0.CO;2.
Taws, S. L., R. Marsh, N. C. Wells, and J. Hirschi (2011), Re-emerging ocean temperature anomalies in late-2010 associated with a repeat negative NAO, *Geophys. Res. Lett.*, *38*, L20601, doi:10.1029/2011GL048978.
te Raa, L., J. Gerrits, and H. A. Dijkstra (2004), Identification of the mechanism of interdecadal variability in the North Atlantic Ocean, *J. Phys. Oceanogr.*, *34*(12), 2792–2807, doi:10.1175/JPO2655.1.
te Raa, L. A., and H. A. Dijkstra (2002), Instability of the thermohaline ocean circulation on interdecadal timescales, *J. Phys. Oceanogr.*, *32*(1), 138–160.
Terray, L. (2012), Evidence for multiple drivers of North Atlantic multi-decadal climate variability, *Geophys. Res. Lett.*, *39*, L19712, doi:10.1029/2012GL053046.
Tett, S. F. B., T. J. Sherwin, A. Shravat, and O. Browne (2014), How much has the North Atlantic Ocean overturning circulation changed in the last 50 years?, *J. Clim.*, *27*, 6325–6342, doi:10.1175/JCLI-D-12-00095.1.
Thompson, D. W. J., and S. Solomon (2002), Interpretation of recent Southern Hemisphere climate change, *Science*, *296*(5569), 895–899.
Thompson, D. W. J., J. M. Wallace, J. J. Kennedy, and P. D. Jones (2010), An abrupt drop in Northern Hemisphere sea surface temperature around 1970, *Nature*, *467*(7314), 444–447.
Thompson, J. D., and W. J. Schmitz (1989), A limited-area model of the Gulf Stream: Design, initial experiments, and model-data intercomparison, *J. Phys. Oceanogr.*, *19*(6), 791–814.
Thorpe, R. B., J. M. Gregory, T. C. Johns, R. A. Wood, and J. F. B. Mitchell (2001), Mechanisms determining the Atlantic thermohaline circulation response to greenhouse gas forcing in a non-flux-adjusted coupled climate model, *J. Clim.*, *14*(14), 3102–3116, doi:10.1175/1520-0442(2001)014<3102:MDTATC>2.0.CO;2.
Tiedje, B., A. Köhl, and J. Baehr (2012), Potential predictability of the North Atlantic heat transport based on an oceanic state estimate, *J. Clim.*, *25*, 8475–8486, doi:10.1175/JCLI-D-11-00606.1.
Ting, M., Y. Kushnir, R. Seager, and C. Li (2009), Forced and internal twentieth-century SST trends in the North Atlantic, *J. Clim.*, *22*(6), 1469–1481, doi:10.1175/2008JCLI2561.1.
Ting, M., Y. Kushnir, R. Seager, and C. Li (2011), Robust features of Atlantic multi-decadal variability and its climate impacts, *Geophys. Res. Lett.*, *38*, L17705, doi:10.1029/2011GL048712.
Toggweiler, J. R., and B. Samuels (1995), Effect of Drake Passage on the global thermohaline circulation, *Deep Sea Res., Part I*, *42*(4), 477–500, doi:10.1016/0967-0637(95)00012-U.
Toole, J., R. Curry, T. Joyce, M. McCartney, and B. Peña-Molino (2011), Transport of the North Atlantic Deep Western Boundary Current about 39°N, 70°W: 2004–2008, *Deep Sea Res., Part II*, *58*, 1768–1780.
Trenberth, K. E., and J. M. Caron (2001), Estimates of meridional atmosphere and ocean heat transports, *J. Clim.*, *14*(16), 3433–3443, doi:10.1175/1520-0442(2001)014<3433:EOMAAO>2.0.CO;2.
Trenberth, K. E., and J. T. Fasullo (2013), An apparent hiatus in global warming?, *Earth's Future*, *1*(1), 19–32, doi:10.1002/2013EF000165.
Trenberth, K. E., and D. J. Shea (2006), Atlantic hurricanes and natural variability in 2005, *Geophys. Res. Lett.*, *33*, L12704, doi:10.1029/2006GL026894.
Trenberth, K. E., J. T. Fasullo, and M. A. Balmaseda (2014), Earth's energy imbalance, *J. Clim.*, *27*(9), 3129–3144, doi:10.1175/JCLI-D-13-00294.1.
Tulloch, R., and J. Marshall (2012), Diagnosis of variability and predictability in the NCAR CCSM3 and GFDL CM2.1 coupled climate models, *J. Clim.*, *25*(12), 4067–4080, doi:10.1175/JCLI-D-11-00460.1.
Tung, K.-K., and J. Zhou (2013), Using data to attribute episodes of warming and cooling in instrumental records, *Proc. Natl. Acad. Sci. U.S.A.*, *110*(6), 2058–2063, doi:10.1073/pnas.1212471110.
Tziperman, E., L. Zanna, and C. Penland (2008), Nonnormal thermohaline circulation dynamics in a coupled ocean-atmosphere GCM, *J. Phys. Oceanogr.*, *38*, 588–604.
Vage, K., R. S. Pickart, V. Thierry, G. Reverdin, C. M. Lee, B. Petrie, T. A. Agnew, A. Wong, and M. H. Ribergaard (2009), Surprising return of deep convection to the subpolar North Atlantic Ocean in winter 2007–2008, *Nat. Geosci.*, *2*(1), 67–72.
Valdivieso, M., K. Haines, H. Zuo, and D. Lea (2014), Freshwater and heat transports from global ocean synthesis, *J. Geophys. Res. Oceans*, *119*, 394–409, doi:10.1002/2013JC009357.
van der Swaluw, E., S. S. Drijfhout, and W. Hazeleger (2007), Bjerknes compensation at high northern latitudes: The ocean forcing the atmosphere, *J. Clim.*, *20*(24), 6023–6032, doi:10.1175/2007JCLI1562.1.
van Sebille, E., M. O. Baringer, W. E. Johns, C. S. Meinen, L. M. Beal, M. F. de Jong, and H. M. van Aken (2011), Propagation pathways of classical Labrador Sea Water from its source region to 26°N, *J. Geophys. Res.*, *116*, C12027, doi:10.1029/2011JC007171.
Vecchi, G. A., et al. (2012), Comment on "Multiyear prediction of monthly mean Atlantic Meridional Overturning Circulation at 26.5°N", *Science*, *338*(6107), 604–604.
Vellinga, M., and R. Wood (2002), Global climatic impacts of a collapse of the Atlantic thermohaline circulation, *Clim. Change*, *54*(3), 251–267, doi:10.1023/A:1016168827653.
Vellinga, M., and P. Wu (2004), Low-latitude freshwater influence on centennial variability of the Atlantic thermohaline circulation, *J. Clim.*, *17*(23), 4498–4511, doi:10.1175/3219.1.
Visbeck, M. (2007), Power of pull, *Nature*, *447*(7143), 383, doi:10.1038/447383a.
Voigt, A., B. Stevens, J. Bader, and T. Mauritsen (2013), The observed hemispheric symmetry in reflected shortwave irradiance, *J. Clim.*, *26*(2), 468–477, doi:10.1175/JCLI-D-12-00132.1.
Wang, W., A. Köhl, and D. Stammer (2010), Estimates of global ocean volume transports during 1960 through 2001, *Geophys. Res. Lett.*, *37*, L15601, doi:10.1029/2010GL043949.
Warren, B. A. (1983), Why is no deep water formed in the North Pacific?, *J. Mar. Res.*, *41*, 327–347, doi:10.1357/002224083788520207.
Watts, D. R. (Ed.) (1991), Equatorward currents in temperatures 1.8–6.0°C on the continental slope in the Mid-Atlantic Bight, in *Deep Convection and Deep Water Formation in the Oceans*, pp. 183–196, Elsevier, Amsterdam.
Weaver, A. J., M. Eby, M. Kienast, and O. A. Saenko (2007), Response of the Atlantic meridional overturning circulation to increasing atmospheric CO_2: Sensitivity to mean climate state, *Geophys. Res. Lett.*, *34*, L05708, doi:10.1029/2006GL028756.
Weaver, A. J., et al. (2012), Stability of the Atlantic meridional overturning circulation: A model intercomparison, *Geophys. Res. Lett.*, *39*, L20709, doi:10.1029/2012GL053763.

Wei, W., G. Lohmann, and M. Dima (2012), Distinct modes of internal variability in the global Meridional Overturning Circulation associated with the Southern Hemisphere westerly winds, *J. Phys. Oceanogr.*, *42*(5), 785–801, doi:10.1175/JPO-D-11-038.1.
Weijer, W., W. P. M. de Ruijter, H. A. Dijkstra, and P. J. van Leeuwen (1999), Impact of interbasin exchange on the Atlantic overturning circulation, *J. Phys. Oceanogr.*, *29*(9), 2266–2284, doi:10.1175/1520-0485(1999)029<2266:IOIEOT>2.0.CO;2.
Welander, P. (1967), On the oscillatory instability of a differentially heated fluid loop, *J. Fluid Mech.*, *29*, 17–30, doi:10.1017/S0022112067000606.
Welander, P. (1986), Thermohaline effects in the ocean circulation and related simple models, in *Large-Scale Transport Processes in Oceans and Atmosphere*, edited by P. Welander, pp. 163–200, Springer, Netherlands.
Williams, R. G., V. Roussenov, D. Smith, and M. S. Lozier (2014), Decadal evolution of ocean thermal anomalies in the North Atlantic: The effects of Ekman, overturning, and horizontal transport, *J. Clim.*, *27*(2), 698–719, doi:10.1175/JCLI-D-12-00234.1.
Willis, J. (2010), Can in situ floats and satellite altimeters detect long-term changes in the Atlantic Ocean overturning?, *Geophys. Res. Lett.*, *37*, L06602, doi:10.1029/2010GL042372.
Winton, M., K. Takahashi, and I. M. Held (2010), Importance of ocean heat uptake efficacy to transient climate change, *J. Clim.*, *23*(9), 2333–2344, doi:10.1175/2009JCLI3139.1.
Winton, M., S. M. Griffies, B. L. Samuels, J. L. Sarmiento, and T. L. Frölicher (2013), Connecting changing ocean circulation with changing climate, *J. Clim.*, *26*(7), 2268–2278, doi:10.1175/JCLI-D-12-00296.1.
Wolfe, C. L., and P. Cessi (2010), What sets the strength of the middepth stratification and overturning circulation in eddying ocean models?, *J. Phys. Oceanogr.*, *40*(7), 1520–1538, doi:10.1175/2010JPO4393.1.
Wolfe, C. L., and P. Cessi (2014), Salt feedback in the adiabatic overturning circulation, *J. Phys. Oceanogr.*, *44*(4), 1175–1194, doi:10.1175/JPO-D-13-0154.1.
Woollings, T., J. M. Gregory, J. G. Pinto, M. Reyers, and D. J. Brayshaw (2012), Response of the North Atlantic storm track to climate changes shaped by ocean-atmosphere coupling, *Nat. Geosci.*, *5*, 313–317, doi:10.1038/NGEO1438.
Wouters, B., S. Drijfhout, and W. Hazeleger (2012), Interdecadal North Atlantic meridional overturning circulation variability in EC-EARTH, *Clim. Dyn.*, *39*(11), 2695–2712, doi:10.1007/s00382-012-1366-4.
Wunsch, C. (2002), What is the thermohaline circulation?, *Science*, *298*(5596), 1179–1181.
Wunsch, C. (2005), The total meridional heat flux and its oceanic and atmospheric partition, *J. Clim.*, *18*(21), 4374–4380, doi:10.1175/JCLI3539.1.
Wunsch, C. (2008), Mass and volume transport variability in an eddy-filled ocean, *Nat. Geosci.*, *1*(3), 165–168.
Wunsch, C. (2013), Covariances and linear predictability of the Atlantic Ocean, *Deep Sea Res., Part II*, *85*(0), 228–243, doi:10.1016/j.dsr2.2012.07.015.
Wunsch, C., and R. Ferrari (2004), Vertical mixing, energy, and the general circulation off the oceans, *Annu. Rev. Fluid Mech.*, *36*(1), 281–314.
Wunsch, C., and P. Heimbach (2006), Estimated decadal changes in the North Atlantic Meridional Overturning Circulation and heat flux 1993–2004, *J. Phys. Oceanogr.*, *36*(11), 2012–2024, doi:10.1175/JPO2957.1.
Wunsch, C., and P. Heimbach (2009), The global zonally integrated ocean circulation, 1992–2006: Seasonal and decadal variability, *J. Phys. Oceanogr.*, *39*(2), 351–368, doi:10.1175/2008JPO4012.1.
Wunsch, C., and P. Heimbach (2013a), Dynamically and kinematically consistent global ocean circulation and ice state estimates, in *Ocean Circulation and Climate: Observing and Modelling the Global Ocean*, edited by G. Siedler et al., 2nd ed., pp. 553–579, Elsevier, Oxford, U. K.
Wunsch, C., and P. Heimbach (2013b), Two decades of the Atlantic Meridional Overturning Circulation: Anatomy, variations, extremes, prediction, and overcoming its limitations, *J. Clim.*, *26*(18), 7167–7186, doi:10.1175/JCLI-D-12-00478.1.
Wunsch, C., R. M. Ponte, and P. Heimbach (2007), Decadal trends in sea level patterns: 1993–2004, *J. Clim.*, *20*(24), 5889–5911, doi:10.1175/2007JCLI1840.1.
Wunsch, C., P. Heimbach, R. M. Ponte, and I. Fukumori (2009), The global general circulation of the ocean estimated by the ECCO consortium, *Oceanography*, *22*(2), 88–103, doi:10.5670/oceanog.2009.41.
Xu, X., H. E. Hurlburt, W. J. Schmitz, R. Zantopp, J. Fischer, and P. J. Hogan (2013), On the currents and transports connected with the Atlantic meridional overturning circulation in the subpolar North Atlantic, *J. Geophys. Res. Oceans*, *118*, 502–516, doi:10.1002/jgrc.20065.
Xu, X., E. P. Chassignet, W. E. Johns, W. J. Schmitz, and E. J. Metzger (2014), Intraseasonal to interannual variability of the Atlantic meridional overturning circulation from eddy-resolving simulations and observations, *J. Geophys. Res. Oceans*, *119*, 5140–5159, doi:10.1002/2014JC009994.
Yamamoto, A., J. B. Palter, M. S. Lozier, M. S. Bourqui, and S. J. Leadbetter (2015), Ocean versus atmosphere control on western European wintertime temperature variability, *Clim. Dyn.*, *45*(11–12), 3593–3607, doi:10.1007/s00382-015-2558-5.
Yashayaev, I. (2007), Hydrographic changes in the Labrador Sea, 1960–2005, *Prog. Oceanogr.*, *73*(3–4), 242–276, doi:10.1016/j.pocean.2007.04.015.
Yashayaev, I., and J. W. Loder (2009), Enhanced production of Labrador Sea Water in 2008, *Geophys. Res. Lett.*, *36*, L01606, doi:10.1029/2008GL036162.
Yeager, S., and G. Danabasoglu (2014), The origins of late-twentieth-century variations in the large-scale North Atlantic circulation, *J. Clim.*, *27*(9), 3222–3247, doi:10.1175/JCLI-D-13-00125.1.
Yeager, S., A. Karspeck, G. Danabasoglu, J. Tribbia, and H. Teng (2012), A decadal prediction case study: Late twentieth-century North Atlantic Ocean heat content, *J. Clim.*, *25*(15), 5173–5189, doi:10.1175/JCLI-D-11-00595.1.
Yin, J., M. E. Schlesinger, N. G. Andronova, S. Malyshev, and B. Li (2006), Is a shutdown of the thermohaline circulation irreversible?, *J. Geophys. Res.*, *111*, D12104, doi:10.1029/2005JD006562.
Zanna, L. (2012), Forecast skill and predictability of observed Atlantic sea surface temperatures, *J. Clim.*, *25*(14), 5047–5056, doi:10.1175/JCLI-D-11-00539.1.
Zanna, L., P. Heimbach, A. M. Moore, and E. Tziperman (2011), Optimal excitation of interannual Atlantic Meridional Overturning Circulation variability, *J. Clim.*, *24*(2), 413–427, doi:10.1175/2010JCLI3610.1.
Zanna, L., P. Heimbach, A. Moore, and E. Tziperman (2012), Upper ocean singular vectors of the North Atlantic climate with implications for linear predictability and variability, *Q. J. R. Meteorol. Soc.*, *138*(663), 500–513, doi:10.1002/qj.937.
Zaucker, F., and W. S. Broecker (1992), The influence of atmospheric moisture transport on the fresh water balance of the Atlantic drainage basin: General circulation model simulations and observations, *J. Geophys. Res.*, *97*(D3), 2765–2773, doi:10.1029/91JD01699.
Zhai, X., and L. Sheldon (2012), On the North Atlantic Ocean heat content change between 1955–70 and 1980–95, *J. Clim.*, *25*(10), 3619–3628, doi:10.1175/JCLI-D-11-00187.1.
Zhang, L., and C. Wang (2013), Multidecadal North Atlantic sea surface temperature and Atlantic meridional overturning circulation variability in CMIP5 historical simulations, *J. Geophys. Res. Oceans*, *118*, 5772–5791, doi:10.1002/jgrc.20390.

Zhang, R. (2007), Anticorrelated multidecadal variations between surface and subsurface tropical North Atlantic, *Geophys. Res. Lett.*, *34*, L12713, doi:10.1029/2007GL030225.
Zhang, R. (2008), Coherent surface-subsurface fingerprint of the Atlantic meridional overturning circulation, *Geophys. Res. Lett.*, *35*, L20705, doi:10.1029/2008GL035463.
Zhang, R. (2010a), Latitudinal dependence of Atlantic Meridional Overturning Circulation (AMOC) variations, *Geophys. Res. Lett.*, *37*, L16703, doi:10.1029/2010GL044474.
Zhang, R. (2010b), Northward intensification of anthropogenically forced changes in the Atlantic Meridional Overturning Circulation (AMOC), *Geophys. Res. Lett.*, *37*, L24603, doi:10.1029/2010GL045054.
Zhang, R. (2010c), Sensitivity of climate change induced by the weakening of the Atlantic Meridional Overturning Circulation to cloud feedback, *J. Clim.*, *23*(2), 378–389, doi:10.1175/2009JCLI3118.1.
Zhang, R., and T. L. Delworth (2005), Simulated tropical response to a substantial weakening of the Atlantic thermohaline circulation, *J. Clim.*, *18*(12), 1853–1860, doi:10.1175/JCLI3460.1.
Zhang, R., and T. L. Delworth (2006), Impact of Atlantic multidecadal oscillations on India/Sahel rainfall and Atlantic hurricanes, *Geophys. Res. Lett.*, *33*, L17712, doi:10.1029/2006GL026267.
Zhang, R., and G. K. Vallis (2007), The role of bottom vortex stretching on the path of the North Atlantic Western Boundary Current and on the Northern Recirculation Gyre, *J. Phys. Oceanogr.*, *37*(8), 2053–2080, doi:10.1175/JPO3102.1.
Zhang, R., T. L. Delworth, and I. M. Held (2007), Can the Atlantic Ocean drive the observed multidecadal variability in Northern Hemisphere mean temperature?, *Geophys. Res. Lett.*, *34*, L02709, doi:10.1029/2006GL028683.
Zhang, R., T. L. Delworth, A. Rosati, W. G. Anderson, K. W. Dixon, H.-C. Lee, and F. Zeng (2011), Sensitivity of the North Atlantic Ocean circulation to an abrupt change in the Nordic Sea overflow in a high resolution global coupled climate model, *J. Geophys. Res.*, *116*, C12024, doi:10.1029/2011JC007240.
Zhang, R., et al. (2013), Have aerosols caused the observed Atlantic multidecadal variability?, *J. Atmos. Sci.*, *70*(4), 1135–1144, doi:10.1175/JAS-D-12-0331.1.
Zhang, S., and A. Rosati (2010), An inflated ensemble filter for ocean data assimilation with a biased coupled GCM, *Mon. Weather Rev.*, *138*(10), 3905–3931, doi:10.1175/2010MWR3326.1.
Zhao, J., and W. Johns (2014), Wind-forced interannual variability of the Atlantic meridional overturning circulation at 26.5°N, *J. Geophys. Res. Oceans*, *119*, 2403–2419, doi:10.1002/2013JC009407.
Zhu, X., and J. Jungclaus (2008), Interdecadal variability of the meridional overturning circulation as an ocean internal mode, *Clim. Dyn.*, *31*, 731–741, doi:10.1007/s00382-008-0383-9.

Erratum

The title of the originally published version of this article was "Observations, inferences, and mechanisms of Atlantic Meridional Overturning Circulation variability: A review." The title has since been corrected to read "Observations, inferences, and mechanisms of the Atlantic Meridional Overturning Circulation: a review". This version may be considered the authoritative version of record.